CODEN:LUTEDX/(TEIE-5547)/1-74/(2025)

Industrial Electrical Engineering and Automation

Fault Detection Techniques for Process Parameter Monitoring in Dairy Milk and Cream Fat In-Line Standardization: A Comparative Analysis

Jacob Anjou
Alexandra Wallin

Division of Industrial Electrical Engineering and Automation
Faculty of Engineering, Lund University

Fault Detection Techniques for Process Parameter Monitoring in Dairy Milk and Cream Fat In-Line Standardization: A Comparative Analysis

Jacob Anjou & Alexandra Wallin

June, 2025

Division for Industrial Electrical Engineering and Automation
LTH, Faculty of Engineering, Lund University
Supervisor: Erik Ottosson
Examiner: Ulf Jeppsson

Division of Industrial Electrical Engineering and Automation
Faculty of Engineering
Lund University
Lund 2025

Abstract

Detecting and recognizing when there is a deviation in process behavior is a crucial aspect of industrial automation. This study investigates one such deviation, a volume discrepancy accidentally introduced during the commissioning of a Tetra Pak Standardization Unit (TPSU). The analysis aims to develop theory for a future implementation with the purpose of detecting this deviation by evaluating principal component analysis-based (PCA-based) detection methods and frequency spectrum analysis (FSA). The comparison focuses on the accuracy, validity, reliability, and feasibility of the detection methods. Results demonstrate that FSA is the most promising method and two approaches to implementation are proposed, evaluating the strengths and limitations of each approach. This work acts as a guide and framework for Tetra Pak to use during a potential future implementation and provides insights into necessary future work.

Acknowledgements

This Master's thesis was completed in the summer of 2025 and is the finalization of 5 years of study at the Faculty of Engineering (LTH) at Lund University. We, the authors, Alexandra Wallin and Jacob Anjou, have contributed equally to the project in terms of research and writing.

We, as authors, would like to express our gratitude to the people who made this thesis possible.

First and foremost, a sincere thank you to Patrik Önnheim at Tetra Pak for offering us the Master thesis opportunity. Patrik has over 10 years of knowledge of the Standardization Unit, and his dedication, guidance, and passion have been invaluable throughout the project.

Furthermore, we extend our gratitude to Erik Ottosson, our LTH supervisor at the Division of Industrial Electrical Engineering and Automation (IEA), for his dedicated support and academic guidance. Lastly, we thank Ulf Jeppsson, our examiner at LTH.

Contents

List of Abbreviations

TPSU Tetra Pak® Standardization Unit

PLC Programmable Logic Controller

PCA Principal Component Analysis

PC Principal Components

FFT Fast Fourier Transform

FSA Frequency Spectrum Analysis

TIA Portal Totally Integrated Automation Portal

LD Ladder Diagram

FBD Function Block Diagrams

ST Structured Text

PROFINET Process Field Network

CPU Central Processing Unit

HMI Human Machine Interface

IEC International Electrotechnical Commission

TS Total Solids

SNF Solids-Non-Fat

QA Quality Assurance

UI User Interface

1 Introduction

1.1 Background

To develop and maintain an efficient and consistent refinement process, understanding of occurrences of issues is crucial to allow for optimization and quick resolutions of faults. Many industrial processes track efficiency in the form of margins around a set workpoint, which creates an interval within which the results of these processes are expected to be confined.

To further optimize these processes, it is essential to narrow this interval, which could result in a reduced amount of resources needed for production. To accomplish this, the identification of the occurrences of issues, their origin, and possible solutions is a key concept. One of these processes is the in-line standardization of milk and cream at Tetra Pak.

Tetra Pak was founded 1951 in Sweden by Ruben Rausing and Holger Crafoord. Today, they are a world leading food processing and packaging solution company. They are delivering solutions to customers and suppliers in more than 160 countries around the world. Tetra Pak is divided into two divisions, processing and packaging. The processing division handles dairy, cheese, ice cream, beverage, New Food, powder and plant-based. The main office is located in Lund, where they develop automated solutions for dairy milk and cream fat standardization. [1]

Furthermore, to standardize cream and milk fat content and other components of milk such as protein, Total-solids, etc., in-line in the milk process in the dairy industry, the Tetra Pak® Standardization Unit (TPSU) can be used. The TPSU is acknowledged worldwide with a class leading performance in control precision (fat, protein, etc.). It is, together with its predecessor, installed in 1000 dairy processing lines around the world. The process begins with the processing of raw milk in a centrifugal separator, which separates the raw milk into a light phase and a heavy phase. [2] The output of this machine is normally cream with 40% fat and milk with 0.02-0.08% fat, however milk for direct consumption is produced with different fat levels, such as 0.5 %, 1.5 % and 3 %. Therefore, some of the separated cream is remixed with the separated skim milk to standardize the milk fat content within the desired level, which is the task of the TPSU.

Governmental food authorities mandate that the fat content in milk must strictly exceed the fat content of the labeled packaging. As a result, many producers opt to produce milk with a fat content of +0.15 percentage units above the working setpoint for the standardized milk fat content. TPSU offers greater efficiency, allowing producers to reduce fat content to +0.015 percentage units above the same working setpoint [3].

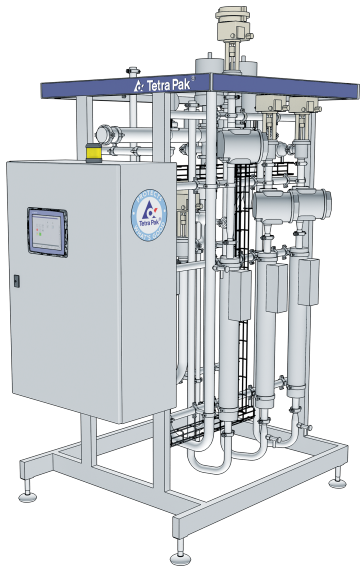

Figure 1: Tetra Pak Standardization Unit

1.2 Aim of Research

A common issue is that the performance of the process is not fully optimized, which could be due to lack of skills during commissioning, poor maintenance of the equipment, or issues in the surrounding process.

In the system today, there are some statistical analysis tools that are used for visualization available to the user. The system is monitored in discrete events, i.e. it creates an alarm when process parameters exceed a limit setpoint during a certain time. For example, when the standardized fat content is too high or when the density is too low. To maintain efficient production and produce products of high quality for the customer, monitoring of performance is crucial to provide feedback to the machine operator to minimize the effects of any malfunctions or deviating events.

The challenges are in identifying the occurrence of an issue, to help streamline the process and enable the possibility of optimization. The identification of these issues focuses mainly on their origin, whether they are due to, e.g. limitations in the hardware of the Programmable Logic Controller (PLC), or due to lack of information about the process in the available data. The latter, corresponding to a number of difficulties, one of which is a discrepancy between the actual volume parameter and the monitor volume parameter, causes disturbances and leads to an increment of the integral time of the system, resulting in a slower response. By detecting these issues at an early stage, production can resume quickly and maintain an efficient working setpoint.

The purpose of the research is to understand how a process can be better monitored and controlled, to maximize the profit for the customer, and to improve the machine. More specifically, it will aim to investigate whether it is possible to identify a volume parameter deviation, through statistical and mathematical methods, for the process to maintain within its own limitation and thus make it more stable. The methods will also be evaluated to determine which is the most suitable for identification of the issue and, moreover, establish a foundation for a future software implementation.

To conduct an initial comparison of different statistical methods, "Pattern recognition and machine learning" by Bishop, C.M. (2006) will be used as the literature of reference [4]. The comparison will mainly focus on the benefits and drawbacks of the statistical methods, as well as the applicability to the process. Furthermore, to fully understand the process during the initial stages of the project, Dairy Processing Handbook by Tetra Pak was provided by Tetra Pak to help identify key characteristics and process parameters [3].

1.3 Objectives

The objective of the Master's thesis project is to find and/or develop theory that is suited to analyze data in the application in terms of system performance and performance indicators when there is a present volume discrepancy in the system to reduce human error. Furthermore, the theory should serve as a foundation for future software implementations.

1.4 Limitations

There are some limitations in this project. The project is limited to direct in-line fat standardization of separated cream and milk without external/additional ingredients. The available real-world data provided from Tetra Pak is limited and therefore adds some additionally restrictions to the research. Data is only available in a confined time period from two different machines, where only the measured process parameters are known. Therefore, the study will have to be based solely on these available datasets and their respective recipes and measurements.

In addition to this, Tetra Pak provides hardware, and software with the capability to simulate the production in a sufficiently realistic way. However, similarly to the majority of simulations, this software might not fully represent the real process, and can thus be considered a limitation.

2 Process setup

This section describes the principle of standardization and the physical process.

2.1 The Chemistry of Cow Milk

The principal constituents of milk are water, fat, proteins, lactose (milk sugar) and minerals (salts). The average composition of the main components of cow milk can be seen in Table 1. Milk fat exists as small globules or droplets dispersed in the milk serum, and milk fat is liquid above 37° C. Together, fat, proteins, lactose and minerals are labeled as total solids (TS), and solid-non-fat (SNF) is defined as the total solids minus the fat. The density of milk and cream is determined by the amount of different constituents in the solution and the temperature.

Component	**Average composition (%)**
Moisture	87.5
Fat	3.9
Proteins	3.4
Lactose	4.8
Minerals (Ash)	0.8

Table 1: Average composition (%) of cow milk constituents

2.2 Principle of Standardization and Calculation for Blending of Products

Standardization involves the process of making something conform to a certain standard, in this case adjustment of the fat content of milk by addition of cream or skim milk to obtain a desired output fat level. Whole milk is therefore first separated into cream and skim milk, thereafter a certain amount of fat content from the separated cream is remixed into the skim milk to achieve the given setpoint value. This relation is described in Equations 1 and 2. From the equations, it is then possible to calculate the amounts of A and B needed to obtain the desired quantity (X) of C. [3]

$A =$ Cream fat content, %
$B =$ Skim milk fat content, %
$C =$ Fat content of the end product, %
$X =$ Desired quantity of C (end product)

$$X\frac{C-B}{(C-B)+(A-C)} = \text{Amount [kg] of A} \tag{1}$$

$$X\frac{A-C}{(C-B)+(A-C)} = \text{Amount [kg] of B} \tag{2}$$

The general process of standardizing, together with example values for calculation, is described in Figure 2.

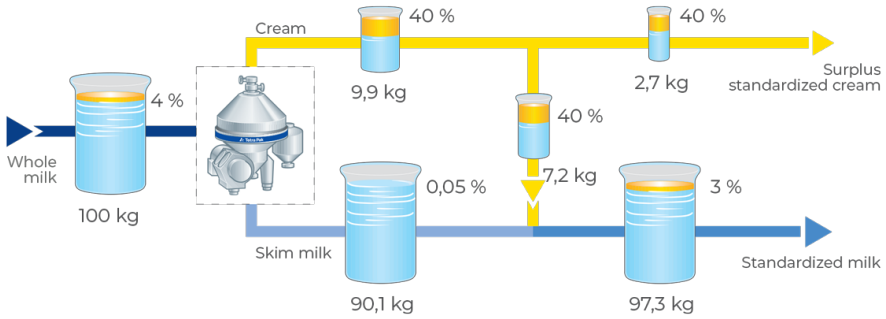

Figure 2: Principle of fat standardization. The process begins with 100 kg of whole milk with 4% fat, the recipe is 3% standardized milk and surplus cream with 40% fat. Separation of 100 kg milk yields 90.1 kg of skim milk with 0.05% fat and 9.9 kg of cream with 40% fat. The amount of 40% cream that must be added to the skim milk is 7.2 kg. In the end, this gives a total of 97.3 kg of 3% milk, leaving 9.9 - 7.2 = 2.7 kg surplus 40% cream. [3]

2.3 Process Overview and Process Flow

The complete process for hot milk standardization (>40° C) used for this Master's Thesis is explained in this section.

Raw milk is stored in large tanks, where laboratory measurements are made on sample data to determine fat content, protein and SNF or TS. This is called Quality Assurance (QA). After this, the whole milk is heated to 40-65° in a pasteurizer or a thermizer, and the warm whole milk is then transported to a separator. This Master's thesis will consider only the use of a hermetic separator. The separator uses centrifugal forces to separate the cream from the raw milk. At the separator outlet, there are pumps for skim milk and cream, which add pressure. In addition, there is a flow regulating valve in the separated cream and a valve to maintain constant pressure on the skim milk. The cream leaves the separator with a setpoint between 20-60 % fat content and the skimmed milk contains around 0.02-0.08 % fat. Lastly, TPSU is used to regulate the mass flow of cream back to skim milk, to achieve the desired setpoint of fat level, with standardized surplus cream and standardized milk as the two end products. [3]

Throughout the two pipes connected to the separator, there are several sensors and two regulators. In the pipe connected to the cream outlet, there is a temperature transmitter and a massflow transmitter, then regulator 1 is used to calculate and control the mass flow of separated cream, and regulator 2 is used to control the remixing in the system. In the pipe transporting skim milk, there is a flow transmitter and a valve that maintain constant skim milk back pressure to the separator. Lastly, in the remixing pipe there is a flow transmitter. The transmitters are used to take measurements and collect data from the system. An in-depth description of the system is shown in Figure 3. [3]

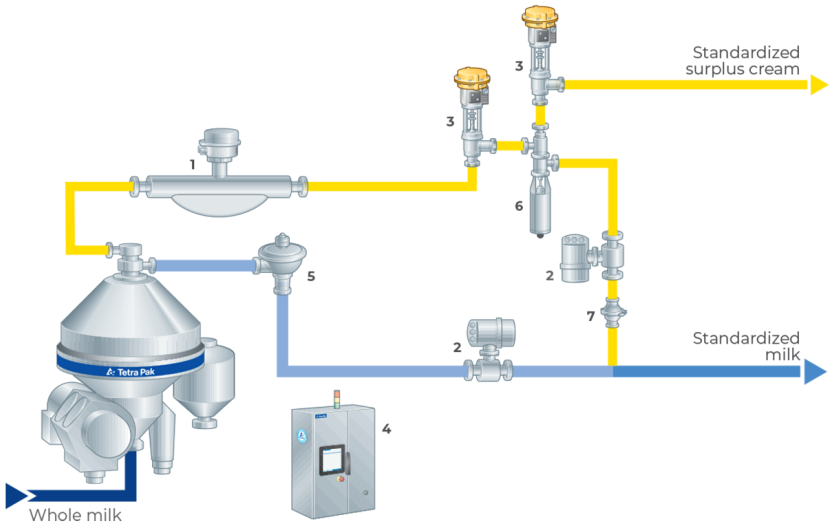

Figure 3: Complete process overview for automatic, direct standardization of milk and cream. 1. Mass flow transmitter. 2. Flow transmitter. 3. Control Valve. 4. Control Panel. 5. Constant-pressure valve. 6. Change-over valve. 7. Check Valve. [3]

2.4 Process Parameters

The process utilizes both flow and mass flow transmitters to measure flow, mass flow, and densities. The most relevant process parameters are shown in Table 2. However, it should be noted that this table does not display all the relevant parameters for this apparatus.

Symbol		Description
Q	=	Flow [m^3/s]
Q_c	=	Flow of cream [m^3/s]
Q_s	=	Flow of skim milk [m^3/s]
Q_r	=	Flow of of raw milk [m^3/s]
Q_{add}	=	Flow of cream in mixing pipe [m^3/s]
μ	=	Rate of mass flow [kg/s]
μ_c	=	Rate of mass flow of cream [kg/s]
μ_s	=	Rate of mass flow of skim milk [kg/s]
μ_r	=	Rate of mass flow of raw milk [kg/s]
μ_{add}	=	Rate of mass flow in mixing pipe [kg/s]
ρ	=	Density of cream [kg/m^3]
C_f	=	Concentration of fat [%]
$C_{c,f}$	=	Concentration of fat in cream [%]
$C_{s,f}$	=	Concentration of fat in skim milk [%]
$C_{r,f}$	=	Concentration of fat in raw milk [%]

Table 2: Overview of some important variables used in the process model.

The process parameters translate to different simulation tags, which can be seen in Appendix B.

2.5 Equations of Equilibrium

The characteristics of the system can be described using the mass flow equations. Given the concentration and flow, the mass flow can be calculated using

$$\mu = Q \cdot C_f \tag{3}$$

where Q is the flow, μ is the rate of mass flow and C is the fat concentration at the point of analysis. The mass flow is calculated as the volume flow times the density. The incoming mass flow of raw milk entering the system will always be equal to the mass flow of cream and skim milk according to the equation of continuity. [3] This gives

$$\mu_r = \mu_c + \mu_s \tag{4}$$

Combining eq. 3 and eq. 4, the equation of equilibrium can be obtained, where $Q_r = (Q_s + Q_c)$.

$$Q_r \cdot C_{r,f} = Q_c \cdot C_{cf} + Q_s \cdot C_{sf} \tag{5}$$

2.6 Cascade Control of the Process

To remain in proximity to the setpoint, the process uses cascade control to control the separated cream fat content. The system consists of two regulators that are connected in series. These regulators indirectly control the flow dynamics of the system to meet the desired characteristics of the end product. The first regulator determines the flow of cream, while the second regulator determines the flow of cream that is added to the skim milk at the mixing point. The setpoint for the first regulator is the percentage of cream fat, and the process value is the concentration of cream fat. [3]

The cascade control has two modes, one inactive state at startup and one active during production. At startup the concentration of fat in the raw milk $C_{r,f}$ is a fixed parameter measured from a laboratory sample. When cascade control is active during production, this value is calculated with equation (5).

2.7 Volume Deviation Definition

There are different volumes in the process, but for the purpose of this study, the volume is defined as the total volume of the hermetic separator outlet in addition to the volume in the separated cream outlet pipe. This volume is typically around 10-30 l and is fixed manually during machine commissioning.

The volume deviation, often referred to as the volume error or volume discrepancy, originates from a calibration error where the monitored value used by the PLC does not match the actual volume of the process. This results in the first regulator in Figure 2 performing calculations using the wrong volume, which in turn results in a regulator problem and induced oscillations.

3 Deviation analysis

In industrial processes, a high performing system is crucial. A frequently used technique utilized for this is fault detection. Fault detection is based on the identification of abnormal process behavior and deviations to avoid risks of poor performance or process failure.

3.1 Deviations

Deviations in the process behavior can occur in various ways. There are both human-caused deviations and natural deviations caused by the process. However, both types of deviation are important to detect and distinguish, so that the problem is addressed appropriately.

One common deviation is the previously mentioned volume deviation. The problem is introduced manually during machine commissioning, typically there is a lack of knowledge of the actual volume or it is measured wrong, and therefore the monitored value is configured poorly. This deviation causes instability, and therefore oscillations will appear in the process, which are monitored visually in the user interface (UI). For maintenance personnel or service engineers, when commissioning the unit, a typical solution is to increase the integral time of regulator 1 which in turn will result in a slower and more inefficient system. Slow control will, moreover, make the system unresponsive to disturbances, resulting in the wrong process value for a long time. To be able to deliver world-class performance with minimal resource waste, the volume discrepancy needs to be resolved early in the process. This deviation will be the target of detection.

3.2 Data Collection

Data is collected from m different features, measured during a finite, predefined time period with ΔT time interval separating the different measurements. Each measurement is an individual sample in the dataset. The data is then stored and represented by m features and n number of measurements. Consider the collected data arranged in an $n \times m$ matrix ($\mathbf{X}$) as follows:

$$\mathbf{X} = \begin{pmatrix} x_{11} & x_{12} & \cdots & x_{1j} & \cdots & x_{1m} \\ \vdots & \vdots & & \vdots & & \vdots \\ x_{i1} & x_{i2} & \cdots & x_{ij} & \cdots & x_{im} \\ \vdots & \vdots & & \vdots & & \vdots \\ x_{n1} & x_{n2} & \cdots & x_{nj} & \cdots & x_{nm} \end{pmatrix} = \begin{pmatrix} \mathbf{v}_1 \mid \mathbf{v}_2 \mid \cdots \mid \mathbf{v}_j \mid \cdots \mid \mathbf{v}_m \end{pmatrix} \tag{6}$$

where each row vector (x_i) represents measurements of all features at a specific time instant. Similarly, each column vector (v_j) represents all measurements of a feature in a certain time interval. The matrix contains measurements with different units and magnitudes, hence pre-processing of the data is of necessity.

3.3 Data Pre-Processing

To make the evaluation yield as much as possible, the datasets require pre-processing. Many methods used for statistical analysis require standardization of the data, since the different variables in the dataset are of different magnitudes and units. Different scales can inhibit the use of statistical methods that need quantitative data to perform calculations of quantitative measures such as (co)variance. To resolve this issue, autoscaling is used. The standardization of data is described in equation (7), where a standardized feature z is calculated by removing the mean μ from a sample x and scaling it to unit variance with a factor σ. [4]

$$z = \frac{(x - \mu)}{\sigma} \tag{7}$$

Following this section, the scaled data is denoted as x_{ij} instead of z for simplicity. Furthermore, it is important to note that a more comprehensive pre-processing of data is usually performed. However, the data is simulated and does not contain outliers or missing values. Therefore autoscaling is considered sufficient.

3.4 Principal Component Analysis (PCA)

Principal Component Analysis (PCA) is a technique to reduce dimensionality in complex datasets. The method transforms high-dimensional data into a lower-dimensional space while maintaining a maximized variance. PCA is frequently used to explore, visualize, and analyze data in industrial processes. PCA is defined as the orthogonal projection of data into a lower-dimensional linear space. [5] The variables are transformed and de-correlated into vectors in a principal subspace, while the variance of the projected data is maximized.

Given the scaled data matrix $\mathbf{X}$ in equation (6), the covariance matrix $\mathbf{C_x}$ is defined as a $m \times m$ square symmetric matrix, where m is the number of dimensions:

$$\mathbf{C_X} \equiv \frac{1}{n-1}\mathbf{X}^\top\mathbf{X} = \frac{1}{n-1}\begin{pmatrix} v_1^\top v_1 & v_1^\top v_2 & \dots & v_1^\top v_j & \dots & v_1^\top v_m \\ \vdots & \vdots & \dots & \vdots & \dots & \vdots \\ v_j^\top v_1 & v_j^\top v_2 & \dots & v_j^\top v_j & \dots & v_j^\top v_m \\ \vdots & \vdots & \dots & \vdots & \dots & \vdots \\ v_m^\top v_1 & v_m^\top v_2 & \dots & v_m^\top v_j & \dots & v_m^\top v_m \end{pmatrix} \tag{8}$$

The matrix measures the degree of linear relationship between all pairs of features. The values correspond to the covariance between the pairs of variables. [6]

$$\sigma^2_{v_j,v_k} = \frac{1}{n-1}\mathbf{v_j^T v_k} = \frac{1}{n-1}\sum_{i=1}^{n} x_{ij}x_{ik} \tag{9}$$

A positive value indicates correlation, a zero value indicates no correlation, and a negative value indicates inverse correlation. Furthermore, the variance of a given variable is defined as the average of the squared differences from the mean and is described in eq. 10, where the square root of the variance is the standard deviation.

$$\sigma^2_{v_j} = \frac{1}{n-1}\mathbf{v_j^T v_j} = \frac{1}{n-1}\sum_{i=1}^{n} x_{ij}^2 \tag{10}$$

Subsequently, the variance of each individual variable is given by the values on the diagonal of the covariance matrix. The aim is to arrange the data along the directions of maximal variance, therefore the original data has to be transformed into different orthonormal basis. The covariance matrix is symmetric, hence it has m real eigenvalues λ_j, equivalently it also has m orthonormal eigenvectors p_j. Together, these form a basis in the m-dimensional space. The transformation matrix $\mathbf{P}$ is chosen as follows:

$$\mathbf{P} = (\mathbf{p_1} \mid \mathbf{p_2} \mid \dots \mid \mathbf{p_j} \mid \dots \mid \mathbf{p_m}) \tag{11}$$

This matrix has zero covariance, and consequently the row vectors are not correlated with their respective variances given by the eigenvalues of the covariance matrix $\mathbf{C_x}$ of the original data. The eigenvectors represent the direction of the axes where the most variance is captured, respectively, the eigenvalues represent the amount of variance captured in each eigenvector. Moreover, the eigenvalues are then ordered in descending order, with the first eigenvector accounting for the highest amount of variance captured, thus being the most significant, the second principal component, orthogonal to the first, accounting for the second largest variance, and this pattern continues for the subsequent components. The eigenvectors are also referred to as principal components. [6]

Since the eigenvalues are ordered by importance, it is possible to reduce the dimensionality of the dataset $\mathbf{X}$ by choosing a limited number r of principal components. There exist various methods on how to choose a suitable number of principal components, one of them is to choose the amount of eigenvalues that account for a cumulated variance explanation above 90%. [7]

The reduced transformation matrix $\mathbf{P}$ has the dimensions $m \times r$ and is defined according to equation (12):

$$\mathbf{P} = (\mathbf{p_1} \mid \mathbf{p_2} \mid \cdots \mid \mathbf{p_r}) \tag{12}$$

The new vector is used to reorient the data from the original axes to those represented by the principal component by transposing the original dataset with the transpose of the reduced matrix. $\mathbf{X}$ can then be written as:

$$\mathbf{T} = \mathbf{XP} \tag{13}$$

$$\mathbf{X} = \hat{\mathbf{X}} + \tilde{\mathbf{X}} \tag{14}$$

$$\hat{\mathbf{X}} = \mathbf{X}(\mathbf{P}\mathbf{P}^{\mathrm{T}}) \tag{15}$$

$$\tilde{\mathbf{X}} = \mathbf{X}(\mathbf{I} - \mathbf{P}\mathbf{P}^{\mathrm{T}}) \tag{16}$$

where $\hat{\mathbf{X}}$ is the projection of the data matrix $\mathbf{X}$ onto the selected r principal components and $\tilde{\mathbf{X}}$ is the projection onto the residual left components.

Principal components in a 3D-space

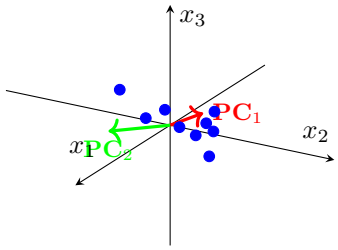

3.5 Data Requirements for PCA

The collected data need to be two-dimensional, multivariate and contain high redundancy, to be able to reduce the dimensions in a meaningful way [5]. It is also assumed that there is a linear relationship between the variables, this means that the data requires a linear relationship with at least 30 % of the original variables m that are correlating with a value X of $|X| = 0.45$ or higher [8]. Moreover, the data need to be free from outliers and there need to be a sufficient number of available measurements. Generally, a sample size of at least five to ten times the number of variables is recommended to perform PCA [9].

Furthermore, each sample for an individual value is expected to be independent of the other samples. This means that there should not be any autocorrelation between the data samples. Nevertheless, industrial processes generally differ from this rule. Most industrial processes contain a high amount of autocorrelation, but PCA is still possible since it is used to create a standard space based on historical data during good operation and, with this standard model, identify abnormalities. In other words, the PCA model learns slow changes in the process resulting in deviations, creating abnormal residues, being possible to detect. [10] [11] To help with this deviation analysis, Hotellings T^2 and Q residuals is used, and explained more down below.

3.6 Hotelling's T^2

While PCA helps to analyze complex systems efficiently, it is rarely used on its own. To complement PCA, Hotelling's T^2 distribution is used to further analyze and visualize deviations in process behavior. Hotelling's T^2 values describe a measure of the variance captured within the PCA-model for each sampled value.

Mathematically, Hotelling's T^2 value is a weighted sum of squares and is described in the PCA transformed space in equation (17)

$$T_i^2 = t_i \mathbf{P}\mathbf{L}t_i^T\mathbf{P}^T \tag{17}$$

In this equation t_i represents a vector of the scores of the principal components for the i-th observation and $\mathbf{L}$ is a diagonal matrix where each element is $1/\lambda_j$ where λ_j are the eigenvalues of the covariance matrix. The $\mathbf{P}$ matrix is the transformation matrix.

3.7 Q residuals

To complement Hotelling's T^2 statistics, the Q residuals describe the extent to which each sample conforms to the established PCA model. It is a residual between the sample and the corresponding projection with the chosen number of principal components. The Q statistics take into account the residuals that appear because the principal components retained cannot reproduce the original data to a full extent [5]. The Q statistic of the i-th observation vector x_i is defined in equation (18).

$$Q_i = x_i(\mathbf{I} - \mathbf{P}\mathbf{P}^T)x_i^T \tag{18}$$

The $\mathbf{P}$ matrix is the same transformation matrix used in (17). The Q distribution is, together with Hotelling's T^2 distribution, used in fault detection [6], when a predetermined threshold separates deviations from the normal process behavior.

3.8 Frequency Spectrum Analysis

Spectrum analysis is a commonly used method within frequency domain analysis. A signal in the time domain *x(t)* can contain different frequencies, and to understand what different frequencies are present in the signal, frequency spectrum analysis is used. Different frequencies can be represented by the sinusoidal signal in equation (19). A is the amplitude, f_0 is the frequency in Hz and t is the time. A lower frequency f_0 is equal to a slower component. [12]

$$x(t) = A \cdot \sin(2\pi f_0 t) \tag{19}$$

This technique then utilizes the transformation of time series data into discrete frequency components using the Discrete Fourier Transform (DFT). The computation of the DFT is described in (20), where x_n is the value of the signal at the n:th sampling point, k is the index of the current frequency component and N is the total number of samples. [12]

$$X_k = \sum_{n=0}^{N-1} x_n \cdot e^{-i\pi \frac{2kn}{N}} \tag{20}$$

X_k then represents how intense a contribution from a certain frequency in the signal is. Hence, the frequency spectrum displays which signals are present and the amplitude for each frequency component. If a certain distortion is made up of a specific frequency, it is possible to utilize the spectrum diagram to detect the noise. [13]

3.9 Nyquist-Shannon Sampling Theorem

For a signal to be completely determined by its sampled counterpart, it must be sampled at a rate of minimum twice the highest existing frequency in the signal. This highest existing frequency is defined as the Nyquist frequency. [12]

$$f_n \frac{f_s}{2} \tag{21}$$

3.10 Low-Pass Filter

A low-pass filter is a filter that allows signals with a frequency smaller than the cutoff frequency to pass and attenuates any frequencies higher than the cutoff frequency. These filters are popular when trying to avoid anti-aliasing and conform to the Nyquist-Shannon sampling theorem described in 3.9. [14] [15]

3.11 Band-Pass Filter

A band-pass filter is a filter that passes signals in a selected frequency band and attenuates any frequencies outside of this band. Band-pass filters can be used to isolate certain frequencies during frequency spectrum analysis to highlight the desired characteristics of the signal. [15]

4 Available data

Two data logs are available from two different companies. These logs contain production data spanning multiple weeks operating in different recipes. However, the datasets are not labeled and require analysis of trends to determine which recipes were active and when the system operated in production. Furthermore, two datasets, one from each company, are extracted and used as a reference target during the tuning of the simulation. From this section and onward these companies and their respective datasets will be referred to as A and B, and datasets A and B.

All datasets are extracted in a similar manner from the log files, using a developed Python script. The sampling interval, sampling frequency, and date of production are entered as inputs. For both datasets, a time period of 15 minutes is used, with a sampling frequency of 1 Hz. The datasets differ in terms of recipe and process dynamics, which is explained further in later sections. However, for now it is sufficient to describe the datasets in terms of their recipes. Dataset A operates at a cream fat concentration of 38% and includes a setpoint drop to 37%. This dataset has a temperature of 40 degrees and a product fat concentration of 0.5%. Dataset B operates at a cream fat concentration of 40% and a temperature of 49 degrees. The product fat concentration is 1.4%. This dataset does not include a setpoint change.

5 Simulation Software

This section gives a more in-depth description of the used simulation software, the PLC and the virtual machines. The simulation software is first described in a block diagram, to get general a comprehension of how it works. The different programs are then described further.

5.1 Simulation Software

The simulation utilizes the same PLC-logic as the real-world process, but there are some differences. The simulation replaces sensor data with simulated parameters. These parameters are created during a process that introduces three things:

1. Lag
2. Delay
3. Noise

The simulation can therefore be described as in Figure 4. The variables cream temperature and raw milk flow are the main process parameters that are manually adjusted when tuning the simulation. When declaring these values, a max amplitude and a max control signal are given. These control signals are normalized into a span between 0 and 100 % and correspond to the strength of the variable, which varies linearly with the control signal. If a control signal of 100 % is sent to the simulation, the corresponding simulated parameter takes the max amplitude. These parameters, along with a few others, are the simulation correspondents of sensor data in the real process and are simulated with added lag, delay, and noise. Lag is modeled as a first-order filter, which captures the finite response times often exhibited by sensors. Delay adds a pure time delay to represent delays in the process, and noise is added to model random disturbances. The simulated parameters are sent as sensor inputs to the PLC. There is also a feedback loop from the PLC to the simulation, which essentially describes the control signals sent from the PLC to the simulation, which affects how the simulated sensor data should change in reaction to the controllers. These control signals are the position of the two valves in the process regulators, describing the behavior of the system and affecting the simulated parameters.

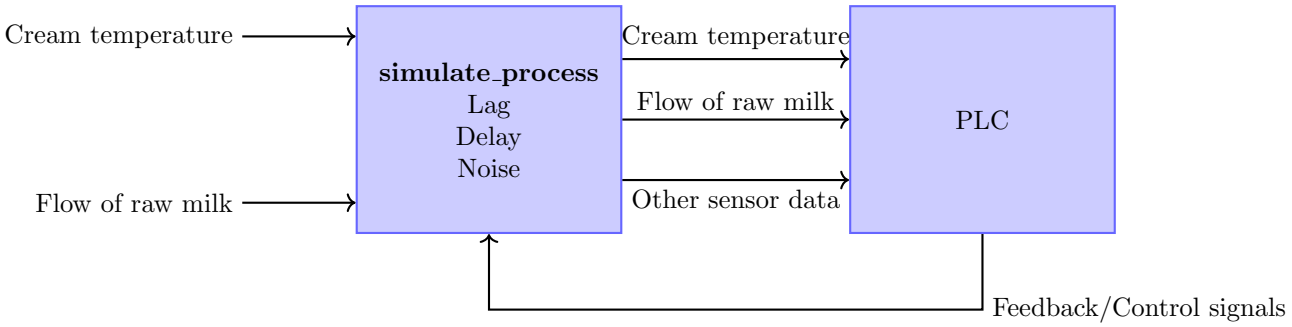

Figure 4: Block diagram describing the simulation software. Parameters are simulated with the addition of lag, delay and noise which then acts as sensor inputs to the PLC. The PLC sends the control signals of the regulators as feedback back to the simulation, which affects the next iteration of sensor data being simulated.

5.1.1 Totally Integrated Automation Portal v18 (TIA Portal)

The Totally Integrated Automation Portal (TIA Portal) from Siemens enables access to a range of digitalized automation services. It is used to program, configure and visualize automation systems. The available PLC programming languages are Ladder Diagram (LD), Function Block Diagram (FBD), and Structured Text (ST), according to the standard IEC 6113-3 [16]. In this thesis, only ST and FBD have been used to tune the simulation. [17] The TIA Portal is connected to the PLC, (CPU 1516-3 PN/DP), which communicates with the HMI. An example view of TIA Portal can be seen in Figure 5, where the PLC modules and PROFINET devices are found to the right. The PLC programming

is found in the middle bottom window and the tags are found in the middle upper window. The TIA portal is used to introduce and enhance disturbances, and random noise.

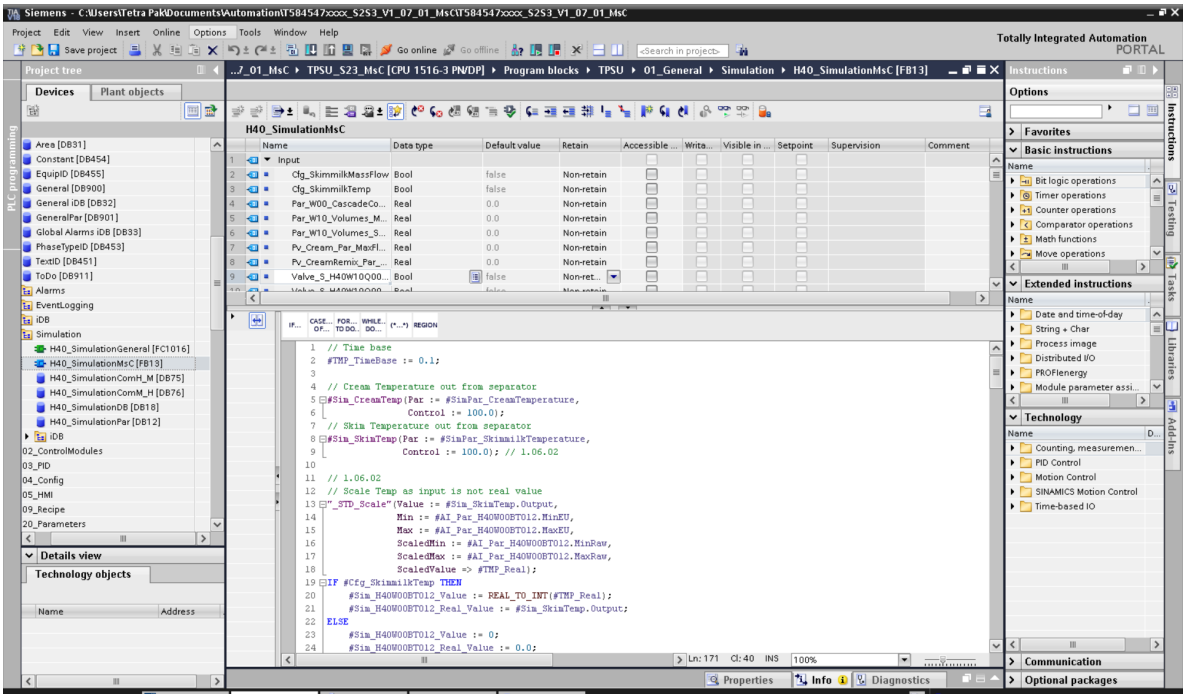

Figure 5: Example view of the TIA Portal

5.1.2 Aveva InTouch HMI 2023

Aveva InTouch HMI is a HMI visualization software used to supervise, control and visualize industrial processes in real time. For the purpose of this project, Aveva Intouch HMI 2023 is used to monitor and change the integral time T_i. [18]

The process overview for the standardization unit is visualized in Figure 6. The process overview allows to track the process values in real time.

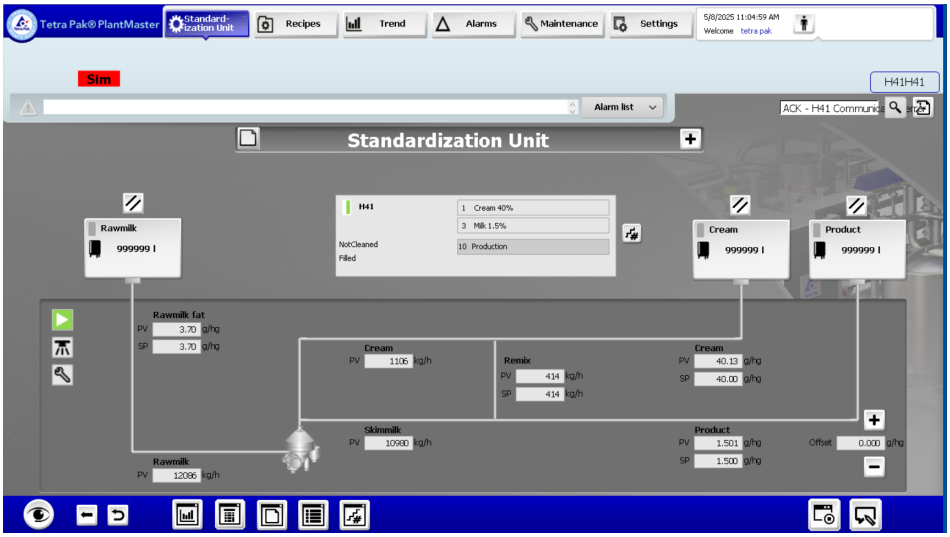

Figure 6: Overview of the process in the HMI with real time updates of the process values.

Furthermore, it is possible to manually change the recipe configuration in the process. This is shown in Figure 7. All types of combinations can be configured, and custom recipes may be created.

A recipe change is also the phase during which the setpoint change is performed.

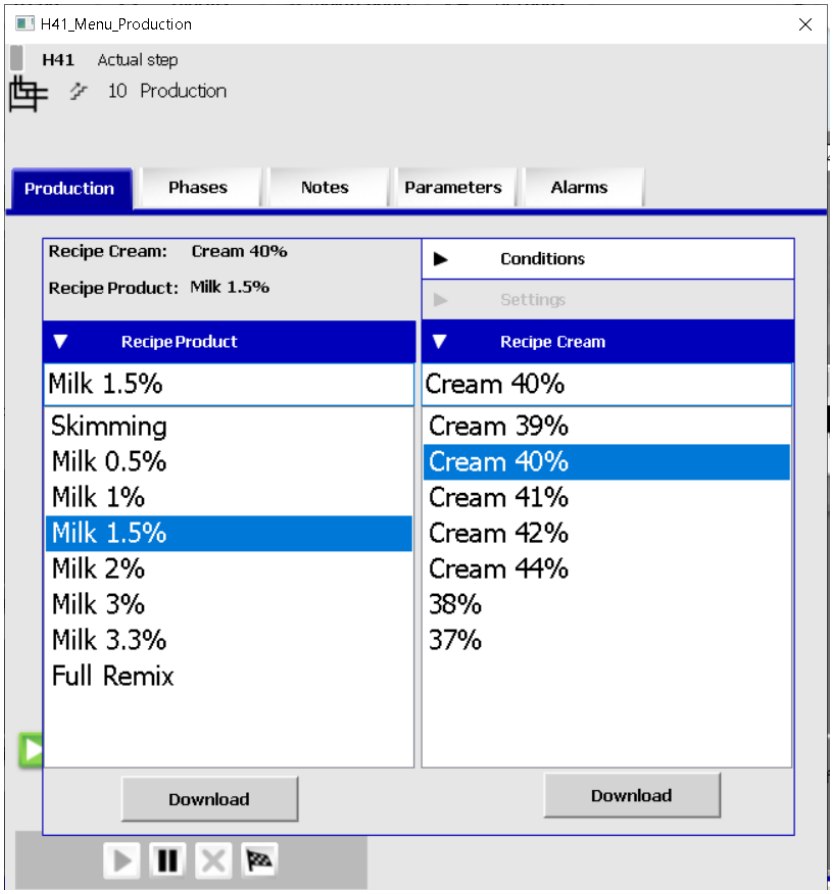

Figure 7: Recipe configuration used to introduce a setpoint change for the regulators.

Then it is possible to monitor, in real time, the outputs through a trend window, with up to eight chosen tags, as seen in Figure 8. The trend monitor in the UI tracks the different values for the system, and at this stage, oscillatory behavior can be identified by maintenance staff or service engineers, prompting an adjustment wherein the integral time is increased in an attempt to address the instability.

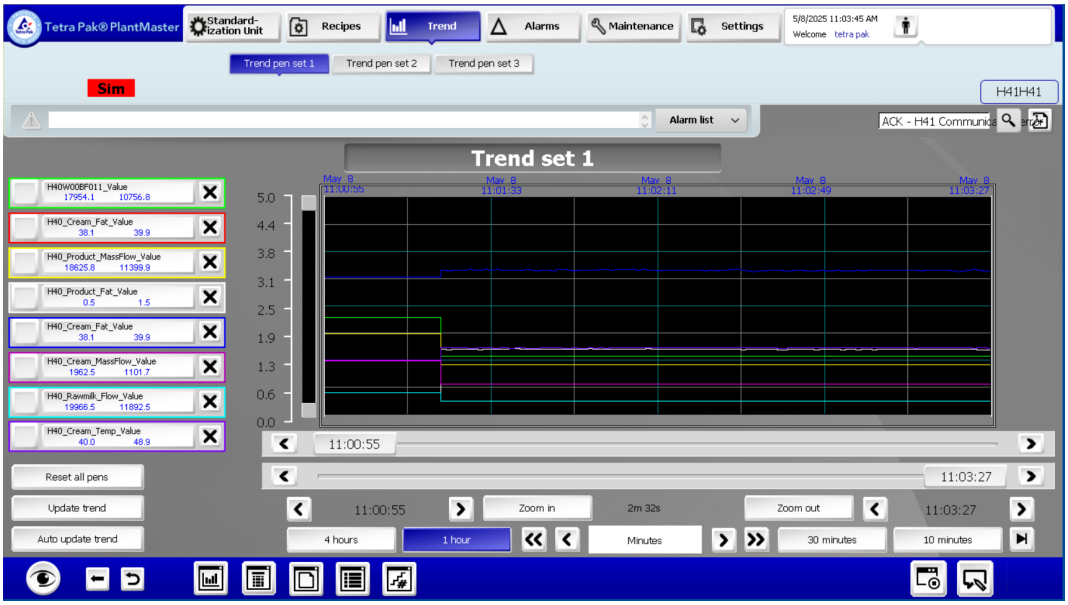

Figure 8: Trend monitor in the UI of some chosen tags, to track the performance of the system.

Another, earlier version of Aveva InTouch (Aveva InTouch 2017) is used for monitoring data from Company B, but the configuration is the same.

5.2 Python

To analyze the data statistically, Microsoft Visual Studio and Python are utilized. There is no purpose of the research to further describe this software and the code here; thus, for the interested reader, the complete code is found in the appendix A.

5.3 Simulation Tags

As mentioned earlier in Section 2.4, the process parameters translate into a number of simulation tags. For all the performed simulations from Company A the collected datasets include 57 tags and for Company B the collected dataset includes 32 tags. These parameters consist of setpoints, calculations and measurements from the control circuit, mentioned in 2.3. All the included parameters vary dynamically with noise and changes in the system. An explanation of the seven most crucial parameters, also used later to tune and monitor the simulation software, is included in Table 3. The complete list of simulation tags for data retrieval from the logs of both companies is found in Appendix B.

Tag	Description
H40_Rawmilk_Fat_Value	Fat content in the incoming raw milk
H40_Cream_Fat_Value	Fat content in the separated cream stream
H40_Product_MassFlow_Value	Mass flow rate of the final milk product
H40_Product_Fat_Value	Fat content in the final milk product
H40_Cream_MassFlow_Value	Mass flow rate of the cream stream
H40_Rawmilk_Flow_Value	Flow rate of the incoming raw milk
H40_Cream_Temp_Value	Temperature of the cream stream

Table 3: Simulation tags and corresponding descriptions.

However, some originally measured simulation tags are not included in the statistical analysis, since they only represent incrementing values such as amount of cream produced over time, which only contributes with an offset that might hide the desired process parameter variance. The exact number of tags that can be collected depend on what software is used, and differs between the datasets collected from Company A and Company B.

6 Method

This section presents the performed method for the aim of the project. The method roughly follows the structure seen in Figure 9.

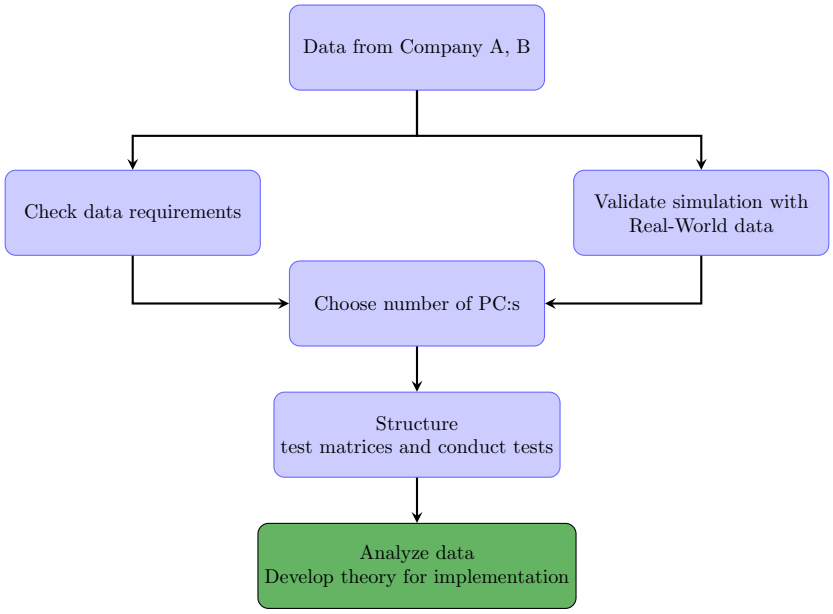

Figure 9: Simplified work flow of the methodology

6.1 Data Requirements

For Principal Component Analysis to be efficient, a number of criteria must be met in accordance with Section 3.5. To determine whether these criteria can be met, the datasets are evaluated according to a few principles.

1. Amount of correlation in the dataset
2. How much variance that is explained by the first few PC:s
3. Autocorrelation

Furthermore, to reduce the risk of overfitting in PCA, that is, fitting to noise rather than structure, 10 observations per variable are taken with a sample interval of 1 second [9].

6.2 Simulation Validation

Due to the fact that the method is structured around the data acquired from simulations, the precision of the simulation is crucial. To determine whether the macroscopical behavior of the process is inherently similar between the simulation and the physical process, the data collected during simulation is compared with real-world data acquired from Company A.

To be able to obtain an accurate comparison, the process parameters of the simulation during steady-state operation are tuned to roughly match the same parameters in the dataset from Company A. This tuning is mainly achieved by changing seven relevant parameters during simulations.

1. Raw milk fat
2. Product mass flow
3. Product fat
4. Cream fat

5. Cream temperature
6. Raw milk flow
7. Cream mass flow

To be able to perform this validation and compare the data from Company A with simulated data gathered from a system without introduced errors, it is assumed that the data from Company A do not contain any significant volume error. This assumption is made after conducting an analysis on the seven parameters mentioned above specifically looking for indications of a present volume error. The most important indication for this purpose is oscillatory behavior.

Furthermore, the simulation is compared to the real process during operation in two modes.

1. Steady-state operation
2. Setpoint change

Steady-state operation is defined as a flow process in which the conditions of the process are constant or remain within a small interval of the process setpoints at all times. During operation, there are no manual changes to the setpoints of the process. To complement steady-state operation and describe behavior that occurs between steady-states, setpoint changes are introduced. There are several ways of introducing these changes, such as switching the recipe or manually changing the setpoint of regulator 1, but for this comparison, the sole method of choice will be switching the recipe. The exact setpoint change included in the data to validate the simulation is a decrease in the cream fat concentration from 38 % to 37%, similar to the setpoint change introduced in test matrix 1 which will be introduced in more detail in Section 6.5.

6.3 Choosing the Number of Principal Components

To retain as much variation as possible while still eliminating redundancy in the data, a scree plot is used to visualize the amount of variance captured in each component. Referring to Section 3.4, the number of principal components will be determined by the amount of variance captured. Hence, the scree plot in Figure 10 will be used to determine the minimum number of principal components that captures the desired variance of the data, for which a good target is 85-90% [7]. The scree plot shows the how much variance is explained by each principal component. In this case, a captured variance over 90% corresponds to three principal components for the data acquired from Company A and Company B. However, for their simulated counterparts, there is a slight variation across the different test cases regarding whether three or four PCs explain more than 90% of the variance, hence 4 PCs will be used forward. The datasets described above as the simulated counterparts of the real-world data will be explained further in the next section, but for now it is sufficient to know that they are referred to as Reference data 1 and Reference data 2.

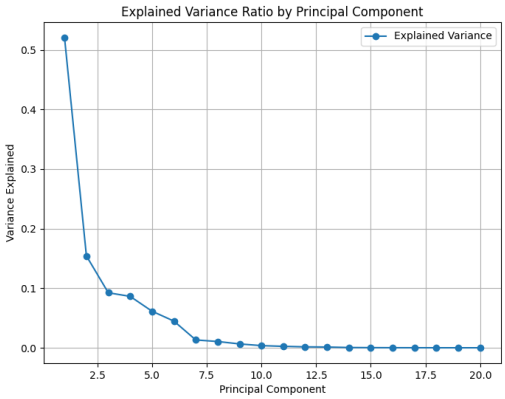

Figure 10: Scree plot for the Reference Data 1 to determine number of principal components. Here, 4 principal components corresponds to over 90% cumulated variance and will therefore be used onwards.

6.4 Structure of Tests

To be able to detect a difference in behavior due to the volume discrepancy or the increased integral time that this error usually results in, the study is comparative. To be certain that the datasets analyzed during these comparisons are plausible to encounter in an industrial context, and therefore have relevant configuration, the simulations will be tuned to resemble the data acquired from Company A and B.

To perform this comparison, a baseline is required. In all tests, this will be inherently the same: a simulation of a process without an introduced volume discrepancy or increased integral time. This applies to all test iterations. As mentioned above, these baseline tests will be denoted as Reference Data 1 for test matrix 1 and Reference Data 2 for test matrix 2.

For these tests, some predefined values are relevant. The volume discrepancy, ΔV, is a difference between the real volume of the process and the volume used by the PLC module during operation. Table 4 describes the different values used during the different tests influenced by the data from Company A, where a volume value of 12 and an integral time of 3 s represent a system without introduced errors or slow process behavior. Table 5 describes the same, but for tests influenced by the data of Company B.

Volume (l)	ΔV	T_i **(s)**
12	0	3, 5, 7.5
16	4	3, 5, 7.5, 10
20	8	3, 5, 7.5, 10
22	10	3, 5, 7.5, 10

Table 4: Volume and integral time values used during simulation for test set 1

Volume (l)	ΔV	T_i **(s)**
12	0	5, 7.5
14	2	5, 7.5, 12.5
16	4	5, 7.5, 12.5, 17.5
18	6	5, 7.5, 12.5, 17.5

Table 5: Volume and integral time values used during simulation for test set 2

To better resemble real-world conditions, where a volume deviation in high likelihood is masked by slower process dynamics due to an increased integral time, this integral time is varied to simulate these scenarios and evaluate the possibility of detecting the volume deviation in a system that is subject to a latent deviation rather than an obvious deviation.

For all tests performed, the volume error is assumed to be positive, which means that no values less than 12 l will be used to represent a volume error. This will be done to conduct efficient tests, the primary attribute of the volume deviation being the size of the discrepancy. Based on prior knowledge shared by Tetra Pak, changing the sign of the volume deviation does not affect the resulting behavior. To put this into numbers, a volume configured 4 l too large is comparable to a volume configured 4 l too small.

To achieve the best possible comparison between the reference data and the test data with the purpose of detecting either of these introduced characteristics, the dataset used will include a setpoint change. This setpoint change is introduced roughly at the same sample in each dataset, approximately at the midpoint of the sampling interval. The size of the setpoint change for each test matrix is explained in more detail in Section 6.5. A setpoint change is applied to observe the system's stabilizing behavior upon returning to the reference value, enabling differentiation of the dynamic responses. The setpoint change introduced refers to a change of setpoint of the first regulator in the cascade control system, i.e. the controller regulating the fat concentration of the cream. This value can be accessed and manipulated by changing recipes. Furthermore, the PCA-model is constructed on the reference dataset, that is, the dataset containing no introduced errors or slow dynamics. For each simulation, the

test dataset is projected onto the same principal components. The following enumerated list describes each test after each simulation is performed and the datasets are collected.

1. PCA-model is constructed on the reference dataset.
2. The test dataset is projected onto the PCA model retained from the reference dataset.
3. Dimensionality reduction is visualized with score plots.
4. Hotelling's T^2, Q residuals, and frequency analysis are computed on the principal components.

To evaluate the different methods of identification in a system during steady-state operation, a number of datasets that do not contain setpoint changes are gathered as a complement. These steady-state simulations are based on the same settings used during the tuning of test matrix 1.

The data is sampled with a one second interval, during a time period of 15 minutes resulting in approximately 900 individual data samples.

6.5 Test Matrices

To streamline the simulation stage, a test matrix is created. This matrix describes each test, the integral time of the first regulator, and the magnitude of the volume deviation which is the main focus of detection. Since two iterations of tests are performed, in which the simulation is configured to resemble the datasets from both companies, two test matrices are created.

Test	ΔV (l)	T_i (s)
Reference test 1	0	3
Test 2	4	3
Test 3	8	3
Test 4	0	5
Test 5	4	5
Test 6	8	5
Test 7	10	5
Test 8	0	7.5
Test 9	4	7.5
Test 10	8	7.5
Test 11	10	7.5
Test 12	0	10
Test 13	4	10
Test 14	8	10
Test 15	10	10

Table 6: Test matrix 1, tuned to resemble data from Company A

Test	ΔV (l)	T_i (s)
Reference test 2	0	3
Test 2	2	5
Test 3	0	7.5
Test 4	2	7.5
Test 5	4	7.5
Test 6	6	7.5
Test 7	0	12.5
Test 8	2	12.5
Test 9	4	12.5
Test 10	6	12.5
Test 11	0	17.5
Test 12	2	17.5
Test 13	4	17.5
Test 14	6	17.5
Test 15	8	17.5

Table 7: Test matrix 2, tuned to resemble data from Company B

The datasets collected from both companies are different in terms of many variables, which affect the behavior of the process. Tuning the simulation to resemble the data from Company B resulted in the system being prone to instability at smaller volume deviations than when the simulation was tuned to resemble the data from Company A. To account for this and still analyze a stable system, smaller volume increments and larger increments of integral time are used in Text matrix 2. The setpoint change introduced in all datasets differs slightly between the two test matrices. For the tests in Table 6 the setpoint of the first regulator is initially at 38 percent, and becomes 37 percent during the change. For the tests in Table 7 in a similar manner, the setpoint drops from 40 percent to 39 percent.

6.6 Analysis of Data

The results obtained from the analysis of the different datasets, described in Section 6.4, are used to establish theory on the possibility of implementing a method with the purpose of detecting this volume deviation. This analysis takes into account several aspects.

1. How efficiently the different methods detect the volume deviation.
2. Accuracy, false positives, and true negatives during detection.
3. Limitations of the different methods.

7 Results and Discussion

7.1 Data Requirements Evaluated

Following the criteria mentioned in Section 3.5 some evaluations were performed to ensure that the data meet these specifications and are applicable to PCA.

Firstly, analyzing the trends of the seven manually tuned parameters, no indication of a significant volume error is present in the data from Company A. Therefore, the assumption that the dataset from Company A does not include a volume error can be made, and a validating comparison between the simulation and the real-world data can be made.

For each dataset, the correlation matrix was calculated and used to determine the correlation of each pair of variables. For the real-world dataset, the average correlation above or below a preset threshold of 0.45 was 39 percent. The same value for a simulated dataset is 42 percent. Hence, this is enough to perform an accurate analysis. [8]

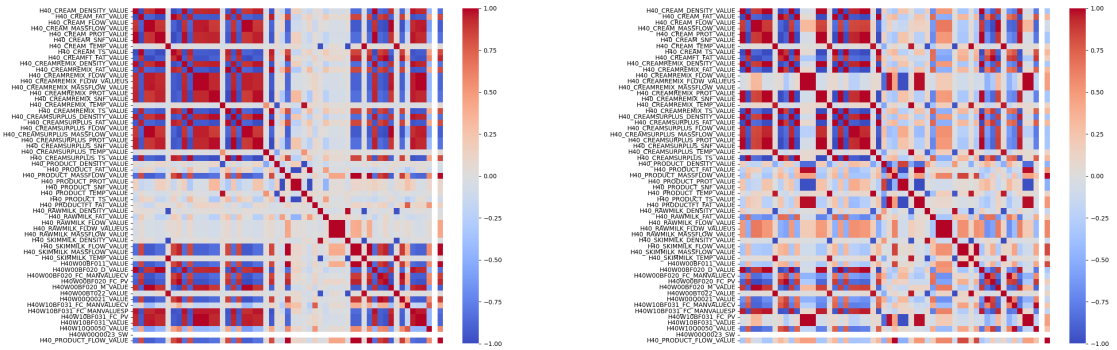

(a) Simulated data from Reference Data 1

(b) Real-world data from Company A

Figure 11: Correlation matrix of the simulated data from Reference Data 1 and the real-world data from Company A. Strong colors of red and blue indicates an enhanced linear relationship. Grey indicates no present linear relationship.

For all datasets, around 90 percent of variation can be explained by the first 3-4 PC:s. This includes both the real-world datasets and their simulated counterparts, which shows that efficient dimensionality reduction is possible within the data. The fact that both the process data from the companies and the simulated process data exhibit roughly the same amount of explained variance in the first 3-4 components also validates the claim that the simulation is, in this case, representative of the real process. [5].

Since it is an industrial process, the samples are not independent of each other and autocorrelation is therefore present in the dataset. Nevertheless, PCA is still considered applicable because PCA in this case is used as pattern recognition and deviation recognition. [10] [11]

Moreover, it is worth reminding the reader that the data is simulated. Hence, there are no outliers or missing data that need to be taken into account.

7.2 Validating the Simulation

Figures 12 and 13 describe steady-state operation, as well as a setpoint change for the dataset that compares the simulation with the data received from Company A.

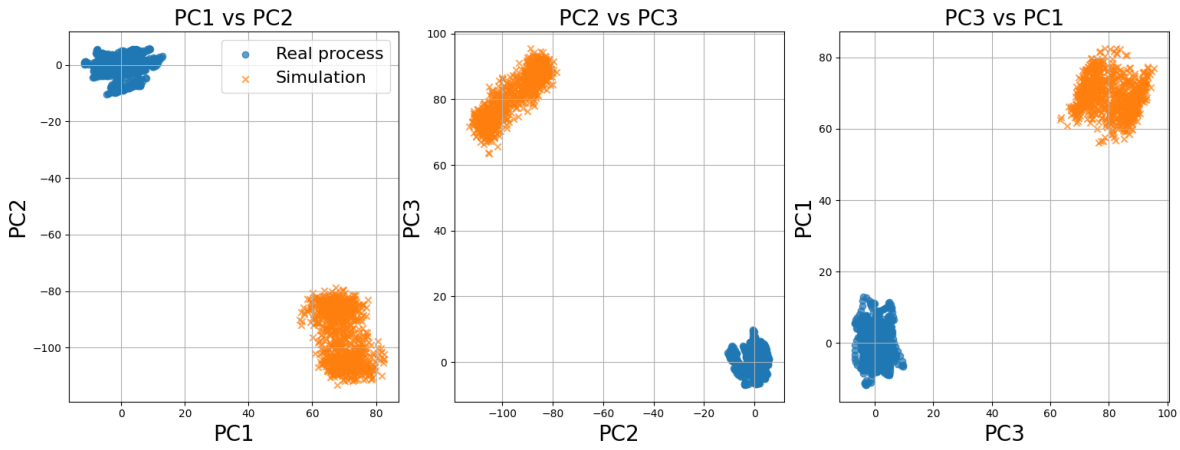

Figure 12: Score plot showing a comparison between data acquired from Company A and data from simulation with resembling process dynamics during steady-state operation.

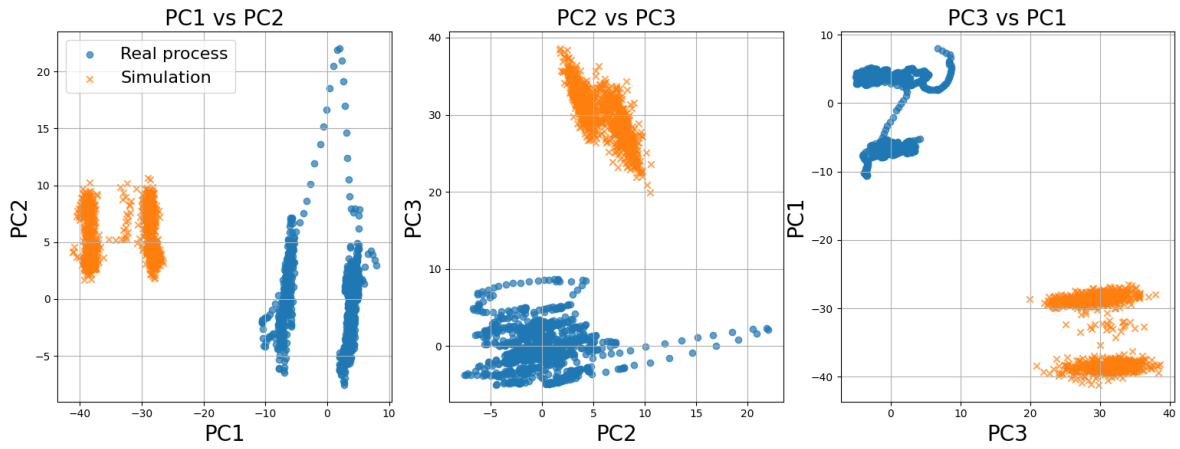

Figure 13: Score plot showing a comparison between data acquired from Company A and data from simulation with resembling process dynamics including a setpoint change where the cream fat concentration dropped from 38 % to 37%.

It is clear from Figures 12 and 13 that macroscopical behavior is inherently the same between simulation and real-world process. A rough estimation of the size of the clusters indicates that the overlying structure of the process is captured in a similar manner for both the real-world data(blue) and simulated data(orange). The real-world data exhibit non-linear characteristics, while the simulated data exhibit linear relationships, which could indicate that the simulation is simplified to some degree. [19] In addition to this, the data points are separated in the PCA space by a distance. This phenomenon can be explained in several ways, such as variables not being completely equal throughout each and every sample for both datasets, that is, the simulation not being tuned so that each and every component of the process aligns in a perfect manner with the same data from the actual process. Despite this, since the primary objective is to analyze the macroscopical behavior of the system and capture the effects of volume error on process dynamics as a whole rather than monitor small changes in the values of features, the simulation is deemed accurate enough to represent the real-world process.

7.3 Principal Component Analysis

This section presents plots relevant to the Principal Component Analysis performed. The dimensionality reductions are presented as score plots, where the three components that retain most of the variance are plotted against each other. The order of the score plots follows the structure described in

the test matrices in Section 6.5. First, the results from the simulation tuned to resemble the data from Company A are presented, and thereafter the results from the simulation tuned to resemble the data from Company B are presented, and lastly the results from the steady-state analysis are presented. The fourth PC did not provide any additional information, hence, it is not included in the presented results.

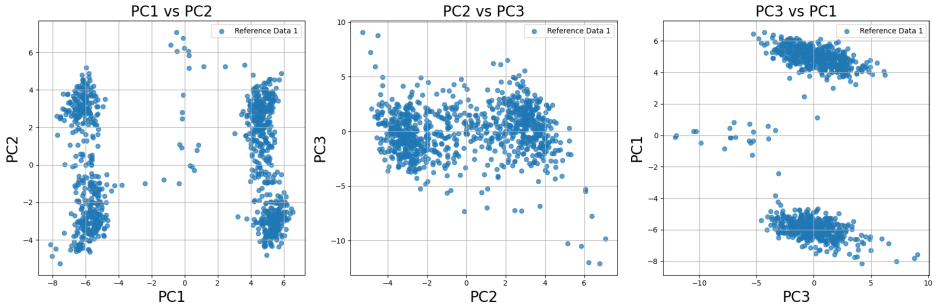

(a) Reference test 1

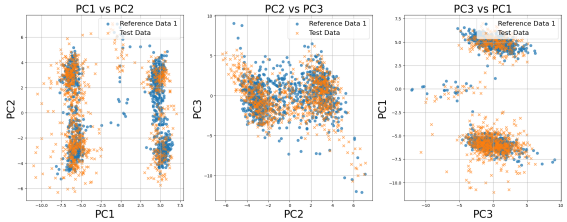

(b) $\Delta V = 4l$

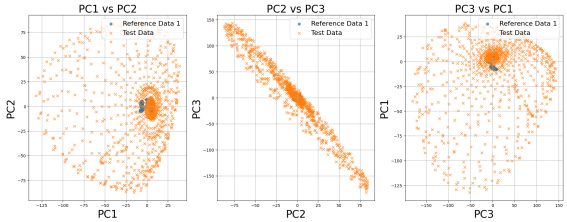

(c) $\Delta V = 8l$.

Figure 14: Score plot showing the different principal components for $T_i = 3\ s$ for (a) The Reference test, (b) Test 2 in comparison with Reference test 1, and (c) Test 3 in comparison with Reference test 1. Furthermore, (c) shows a system becoming unstable due to the volume deviation being too large.

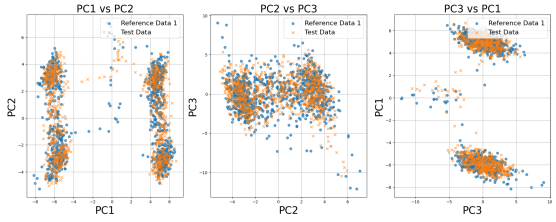

(a) $\Delta V = 0l$

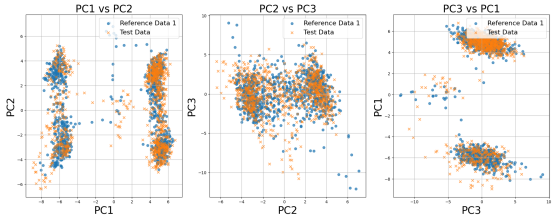

(b) $\Delta V = 4l$

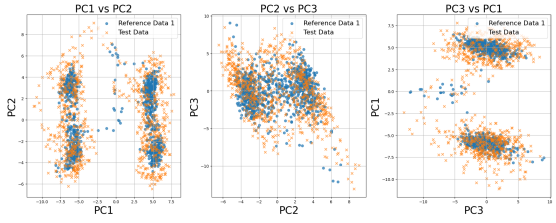

(c) $\Delta V = 8l$

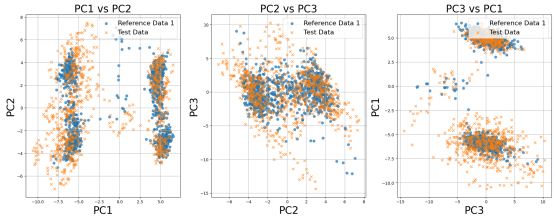

(d) $\Delta V = 10l$

Figure 15: Score plot showing the first three principal components for $T_i = 5\ s$ for (a) Test 4 in comparison with Reference test 1, (b) Test 5 in comparison with Reference test 1, (c) Test 6 in comparison with Reference test 1, and (d) Test 7 in comparison with Reference test 1.

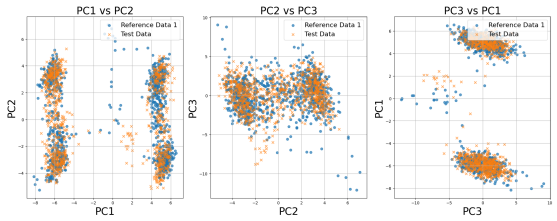

(a) $\Delta V = 0l$

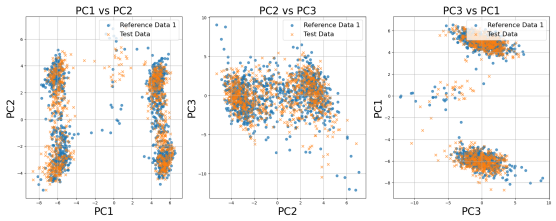

(b) $\Delta V = 4l$

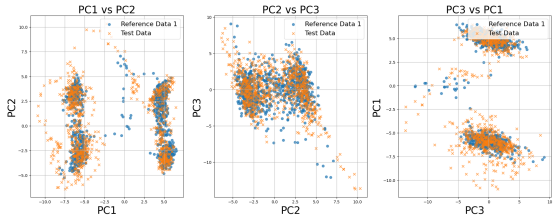

(c) $\Delta V = 8l$

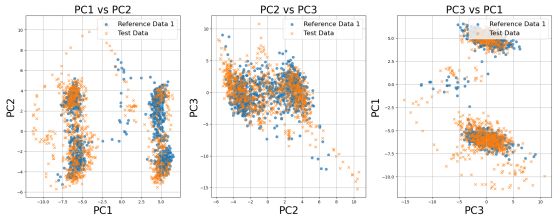

(d) $\Delta V = 10l$

Figure 16: Score plot showing the first three principal components for $T_i = 7.5\ s$ for (a) Test 8 in comparison with Reference test 1 , (b) Test 9 in comparison with Reference test 1, (c) Test 10 in comparison with Reference test 1, and (d) Test 11 in comparison with Reference test 1.

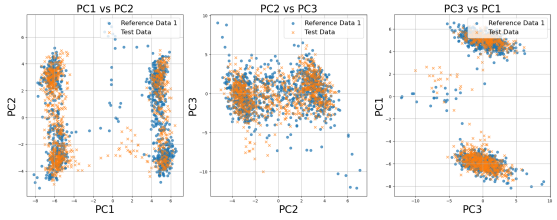

(a) $\Delta V = 0l$

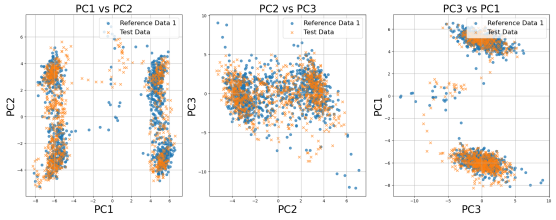

(b) $\Delta V = 4l$

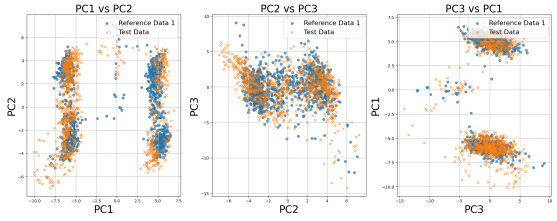

(c) $\Delta V = 8l$

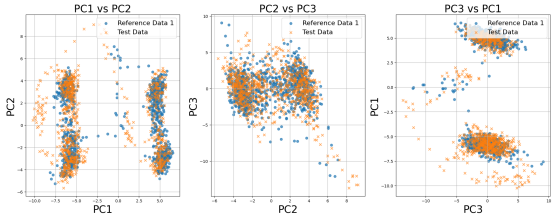

(d) $\Delta V = 10l$

Figure 17: Score plot showing the first three principal components for $T_i = 10\ s$ for (a) Test 12 in comparison with Reference test 1, (b) Test 13 in comparison with Reference test 1, (c) Test 14 in comparison with Reference test 1, and (d) Test 15 in comparison with Reference test 1.

Looking at the graphs, it is possible to identify a consequent trend from the different components. To start with, the reference test in Figure 14a depicts two very narrow formations. Having a further look, these formations tend to expand, i.e. the variance increases with a greater volume deviation. It is very clear, compared to Figure 14b or Figure 15c, that a greater variance occurs between these formations. However, it is harder to distinguish a greater variance in smaller volume deviations and higher integral time. Looking at Figure 15b, Figure 16b and Figure 17b, there are hardly any differences in the shape of the formations. Test 3, i.e. Figure 14c, depicts a system where T_i is too low to compensate for a larger volume deviation combined with a setpoint change and thus the system starts to oscillate uncontrollably.

Changing focus, the second graph in the reference test in Figure 14a, i.e. PC2 plotted against PC3, depicts a somewhat collected cloud, but there are two more concentrated collections. PC3 plotted

against PC1 in Figure 14a presents a similar behavior, except for an increase in the distance between the clusters of data points. The same pattern can be seen in these two subspaces, as for the first subspace, that an increasing volume discrepancy consequently leads to a larger spread in the variance. However, a volume discrepancy of $\Delta V = 4l$ is still difficult to differentiate. From these plots, it is therefore possible to distinguish and conclude that a volume deviation leads to a change in the PC subspaces.

Test matrix 2, or the simulation tuned to resemble the data from Company B, is presented below.

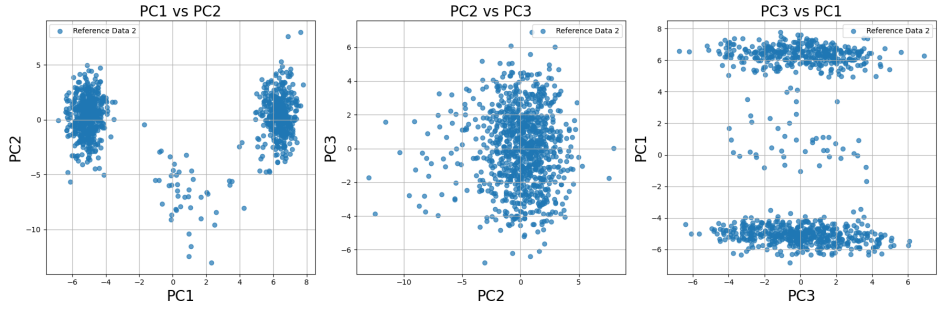

Figure 18: Reference test 2: $\Delta V = 0$ l, $T_i = 3$ s

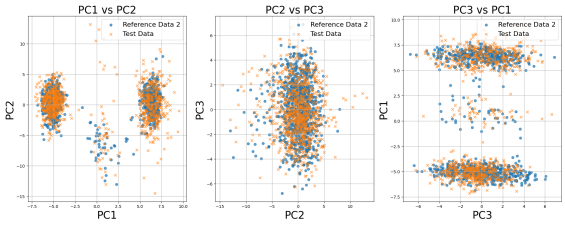

Figure 19: Score plot showing a comparison between Test 2 and Reference test 2. $\Delta V = 2$ l, $T_i = 5$ s

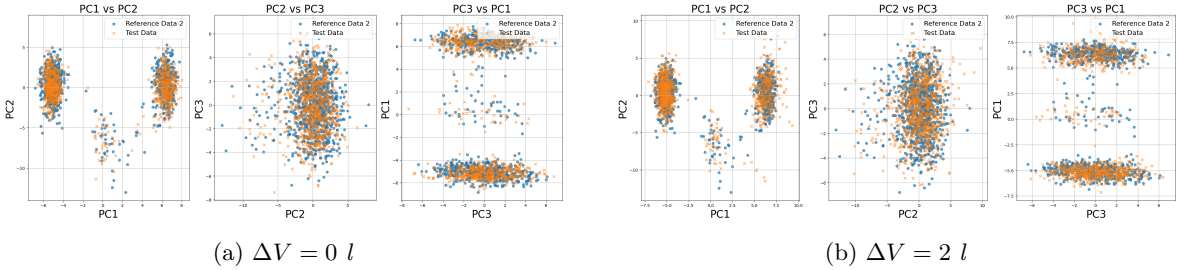

(a) $\Delta V = 0$ l

(b) $\Delta V = 2$ l

(c) $\Delta V = 4$ l

(d) $\Delta V = 6$ l

Figure 20: Score plot showing the three first principal components for $T_i = 7.5$ s for (a) Test 3 in comparison with Reference test 2, (b) Test 4 in comparison with Reference test 2, (c) Test 5 in comparison with Reference test 2, and (d) Test 6 in comparison with Reference test 2. Furthermore, (d) shows a system becoming unstable due to the volume deviation being too large.

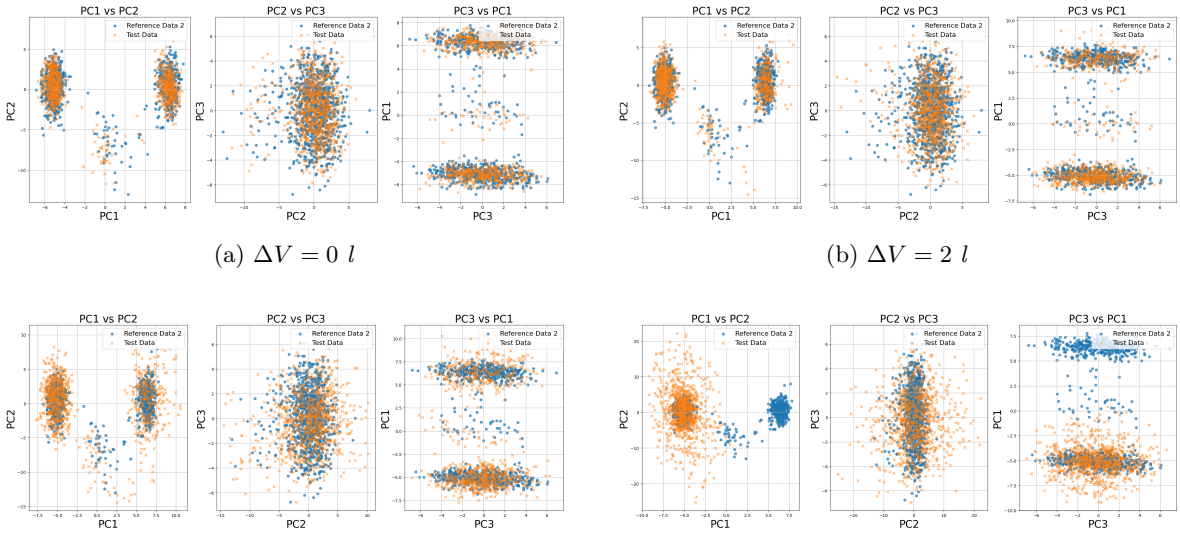

(a) $\Delta V = 0\ l$ (b) $\Delta V = 2\ l$

(c) $\Delta V = 4\ l$ (d) $\Delta V = 6\ l$

Figure 21: Score plot showing the three first principal components for $T_i = 12.5\ s$ for (a) Test 7 in comparison to Reference test 2, (b) Test 8 in comparison with Reference test 2, (c) Test 9 in comparison with Reference test 2, and (d) Test 10 in comparison with Reference test 2. Furthermore, (d) shows a system becoming unstable instantly due to the volume deviation being too large. For this test no setpoint change was introduced due to the aforementioned circumstance.

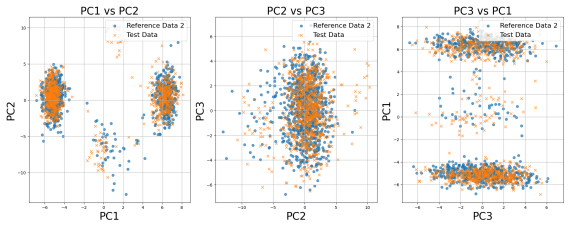

(a) $\Delta V = 0$ l

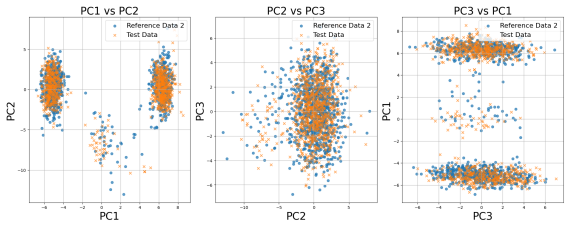

(b) $\Delta V = 2$ l

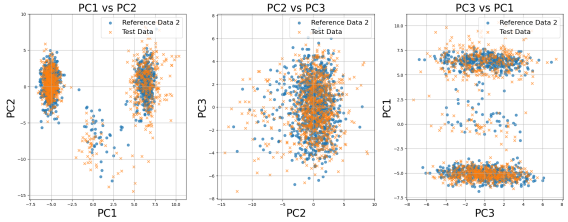

(c) $\Delta V = 4$ l

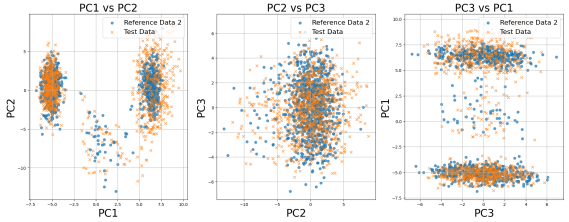

(d) $\Delta V = 6$ l

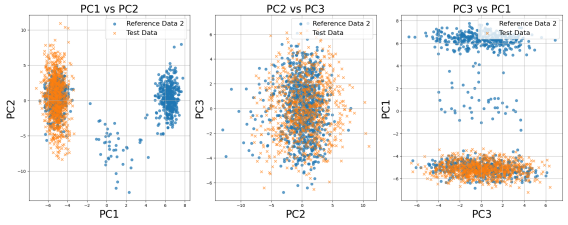

(e) $\Delta V = 8$ l

Figure 22: Score plot showing the three first principal components for $T_i = 17.5$ s for (a) Test 11 in comparison to Reference test 2, (b) Test 12 in comparison with Reference test 2, (c) Test 13 in comparison with Reference test 2, (d) Test 14 in comparison with Reference test 2, and (e) Test 15 in comparison with Reference test 2. Furthermore, (e) shows a system becoming unstable instantly due to the volume deviation being too large. For this test no setpoint change was introduced due to the aforementioned circumstance.

The result from Test Matrix 2 indicates a similar behavior as the previous test matrix. A larger volume deviation together with an increased integral time is reflected with a wider spread in the variance, in accordance with the test results obtained from Test Matrix 1, although the clouds in the PCA subspaces look a little bit different due to another recipe configuration. The flow of raw milk is significantly lower in Test Matrix 2, resulting in more tests becoming unstable faster, as seen in Figure 20d, and sometimes it is not even possible to initiate a setpoint change, which can be seen in Figure 21d. It is still difficult to notice a small volume deviation.

Finally, the steady-state results are presented below.

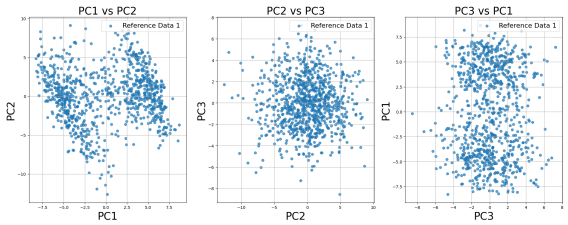

(a) Reference Data 1, $\Delta V = 0$ l, $T_i = 3$ s

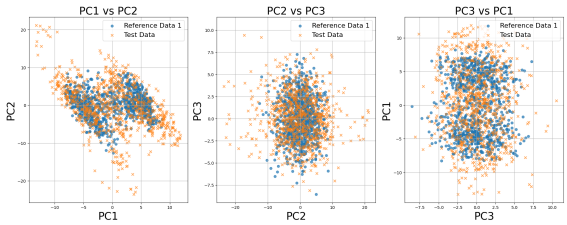

(b) Test 7: $\Delta V = 10$ l, $T_i = 5$ s

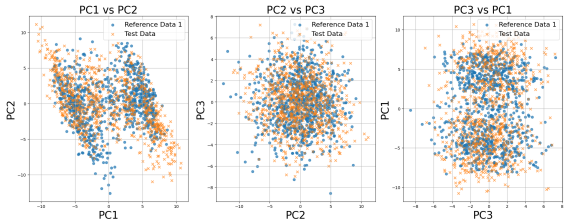

(c) Test 11: $\Delta V = 10$ l, $T_i = 7.5$ s

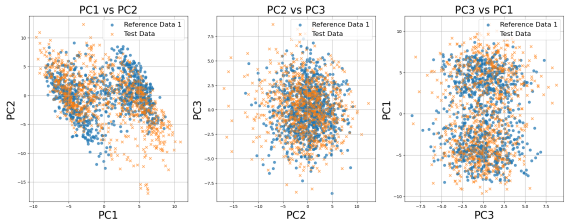

(d) Test 15: $\Delta V = 10$ l, $T_i = 15$ s

Figure 23: Score plot showing the three first principal components during steady-state operation for (a) Reference Data 1, (b) Test 7 in comparison with Reference Data 1, (c) Test 11 in comparison with Reference Data 1, and (d) Test 15 in comparison with Reference Data 1.

It is possible to notice a difference in the amount of variance when the volume error is introduced. This difference is greater at low integral time T_i. The difference in variance decreases as the integral time T_i increases, but a difference is still possible to notice.

7.4 Residuals

The residuals are presented almost analogously to the figures in the above section. The results of the data made to resemble Company A are presented. However, the data made to resemble Company B is included in Appendix D. The focus here is to study the magnitude and duration of the peak following the setpoint change. Since Hotelling's T^2 did not yield any meaningful results, no effort was made to develop a corresponding threshold.

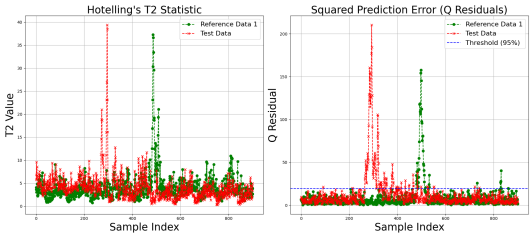

(a) $\Delta V = 4$ l

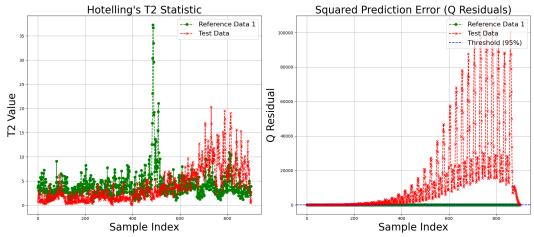

(b) $\Delta V = 8$ l

Figure 24: Figures showing Hotellings T^2 (left) and Q residuals (right) for $T_i = 3$ s for(a) Test 2 in comparison with Reference test 1 and (b) Test 3 in comparison with Reference test 1. Furthermore, (b) shows a system becoming unstable due to a large volume error.

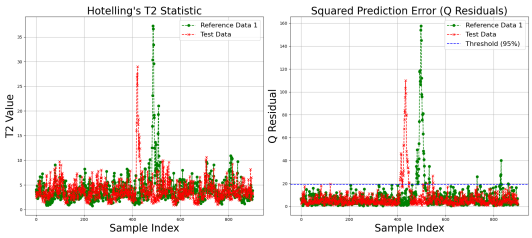

(a) $\Delta V = 0$ l

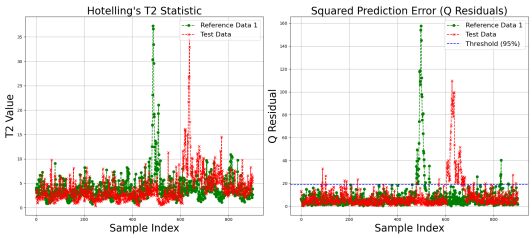

(b) $\Delta V = 4$ l

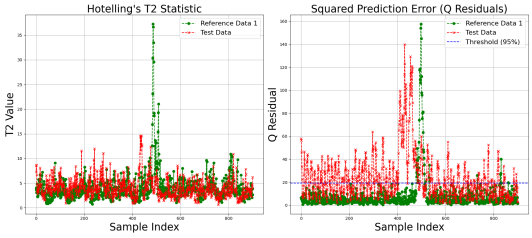

(c) $\Delta V = 8$ l

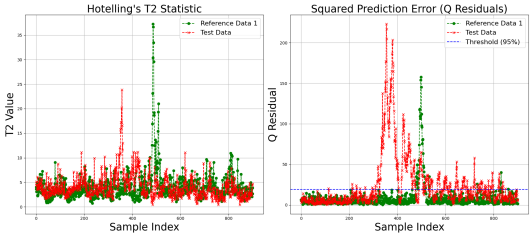

(d) $\Delta V = 10$ l

Figure 25: Figures showing Hotellings T^2 (left) and Q residuals (right) for $T_i = 5$ s for (a) Test 4 in comparison with Reference test 1, (b) Test 5 in comparison with Reference test 1, (c) Test 6 in comparison with Reference test 1 and, (d) Test 7 in comparison with Reference test 1.

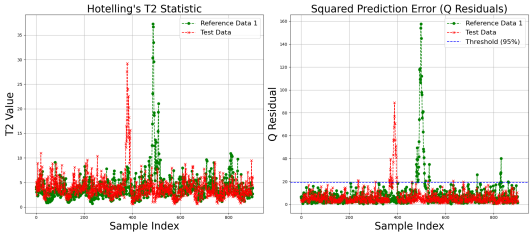

(a) $\Delta V = 0$ l

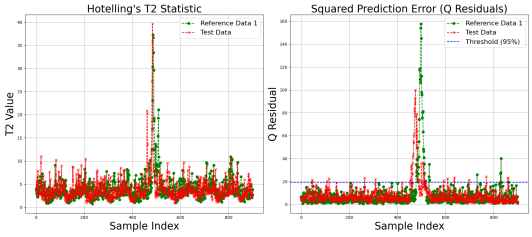

(b) $\Delta V = 4$ l

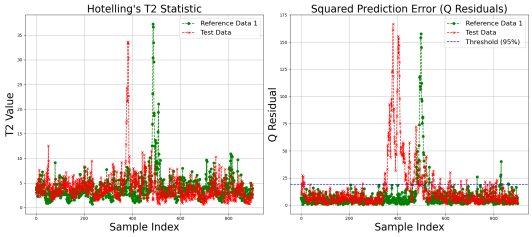

(c) $\Delta V = 8$ l

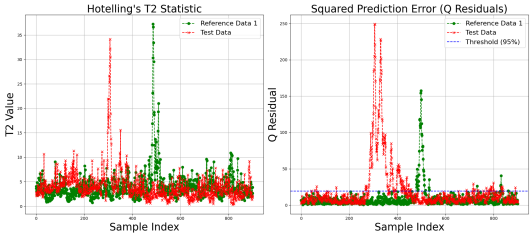

(d) $\Delta V = 10$ l

Figure 26: Figures showing Hotellings T^2 (left) and Q residuals (right) for $T_i = 7.5$ s for (a) Test 8 in comparison with Reference test 1, (b) Test 9 in comparison with Reference test 1, (c) Test 10 in comparison with Reference test 1 and, (d) Test 11 in comparison with Reference test 1.

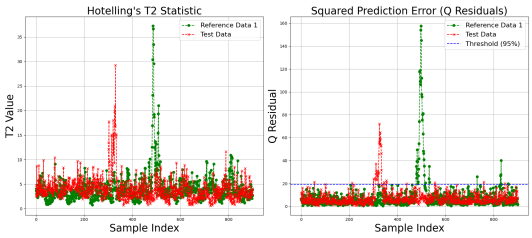

(a) $\Delta V = 0$ l

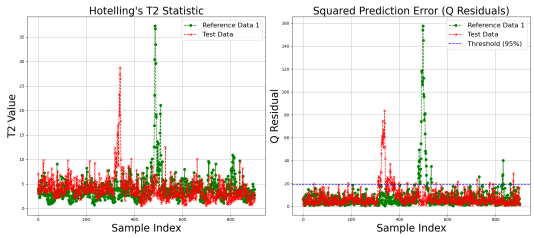

(b) $\Delta V = 4$ l

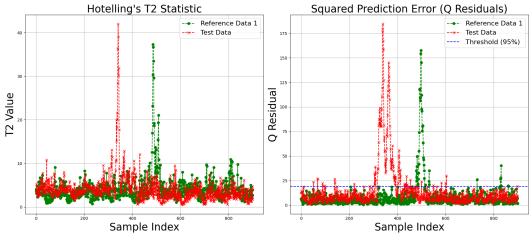

(c) $\Delta V = 8$ l

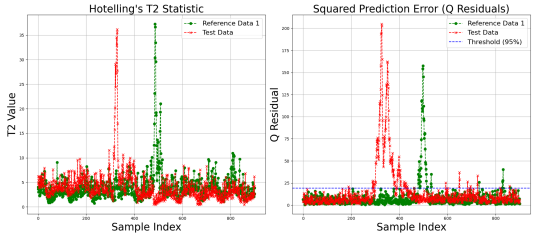

(d) $\Delta V = 10$ l

Figure 27: Figures showing Hotellings T^2 (left) and Q residuals (right) for $T_i = 10$ s for (a) Test 12 in comparison with Reference test 1, (b) Test 13 in comparison with Reference test 1, (c) Test 14 in comparison with Reference test 1 and, (d) Test 15 in comparison with Reference test 1.

All the residuals in Hotelling's T^2 depict a clear deviation by the time the setpoint is changed, similarly the setpoint change clearly violates the chosen threshold in the Q residuals. The time when the setpoint change is introduced can vary slightly, and therefore there is sometimes a shift displacement of the peaks in the reference dataset and the test datasets.

Although the peak is very obvious, Hotelling's T^2 does not conclude any observable trend. Looking at Figure 24a, the test peak is larger than the reference peak, contradictory, in Figure 25b with the same volume deviation of $\Delta V = 4l$, the peak is marginally smaller than the reference peak. Furthermore, the peak in 25c, for the test data with an even higher volume discrepancy, is barely noticeable. Continuing to look at the rest of the results from the other integral times, the peaks have very irregular distributions.

However, the Q residuals present a more obvious trend. Initially, a higher T_i shrinks the peak, but as the volume deviation increases, the peak also follows in magnitude, and it also depicts a wider horizontal distribution. In Figures 26b and 26d, there is a clear difference in magnitude and broadness. The pattern is the same for the other test sets. However, it is still hard to distinguish a lower volume deviation.

It is worth mentioning again that residuals only show discrepancy between the reference values and the test values, but do not show what is really wrong. These peaks could therefore, in theory, be any type of sudden and large deviation in the system.

In conclusion, it is not possible to notice a certain pattern among the T^2:s, but the Q residuals show a more promising trend.

From the plots, no consistent results regarding Hotellings T^2 can be presented. The peaks vary in magnitude randomly and do not follow any specific pattern. Regarding the Q residuals, there seems to be a more noticeable pattern, in most cases the peak is increasing in magnitude with an increasing volume deviation. Instability and oscillations are still very visible in the Q residuals.

The results of the steady-state operation comparison are presented below.

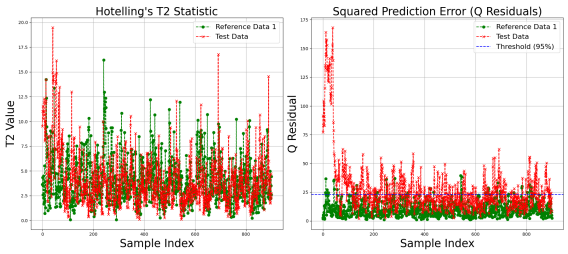

(a) Test 5: $\Delta V = 10$ l, $T_i = 5$ s

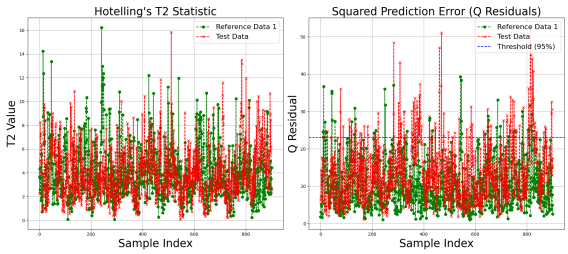

(b) Test 11: $\Delta V = 10$ l, $T_i = 7.5$ s

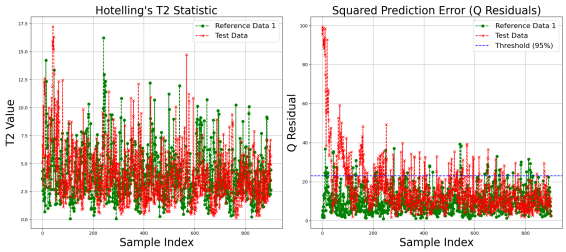

(c) Test 15: $\Delta V = 10$ l, $T_i = 10$ s

Figure 28: Figures showing Hotellings T^2 (left) and Q residuals (right) during steady-state operation for (a) Test 7 in comparison with Reference test 1, (b) Test 11 in comparison with Reference test 1, (c) Test 15 in comparison with Reference test 1.

For the steady-state plots, no clear results are visible in neither the Hotelling's T^2, nor the Q residuals. The variations and deviations in both the reference data and the test data appear to follow the same pattern.

7.5 Frequency Spectrum Analysis

This section presents results of the frequency spectrum analysis. The results are presented in the same manner as in section 7.3, that is, first the reference test is displayed in 29a and the other tests will follow, presented in increasing integral time and volume deviation.

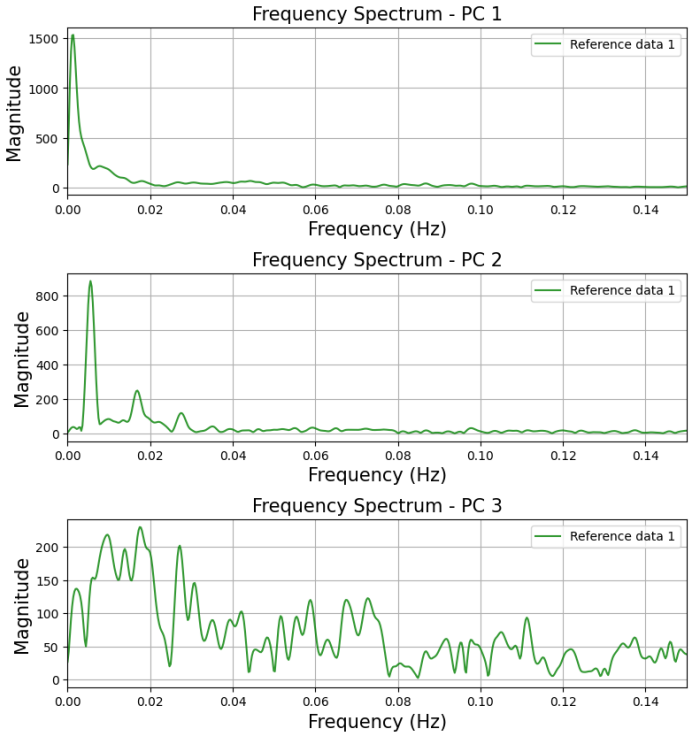

(a) Reference test 1

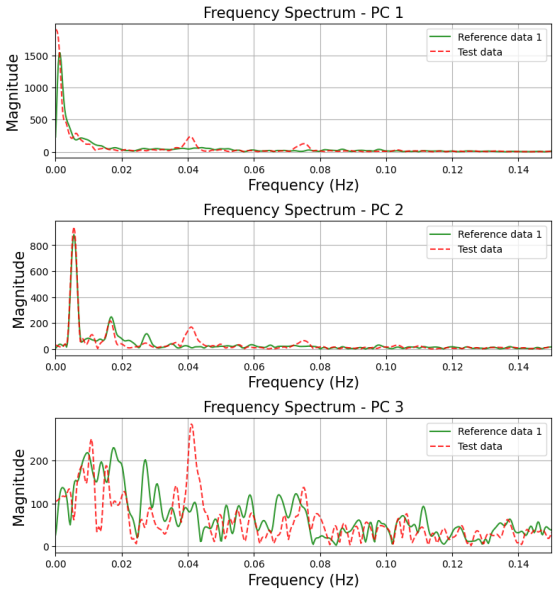

(b) $\Delta V = 4\ l$

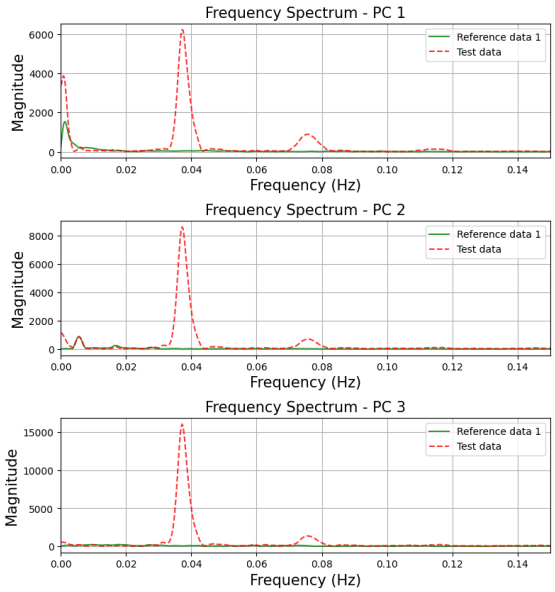

(c) $\Delta V = 8\ l$

Figure 29: Plots showing frequency analyses on the three first principal components for $T_i = 3\ s$ for (a) Reference test 1, (b) Test 2 in comparison to Reference test 1 and, (c) Test 3 in comparison to Reference test 1. Furthermore, (c) show a system unstable due to a large volume error.

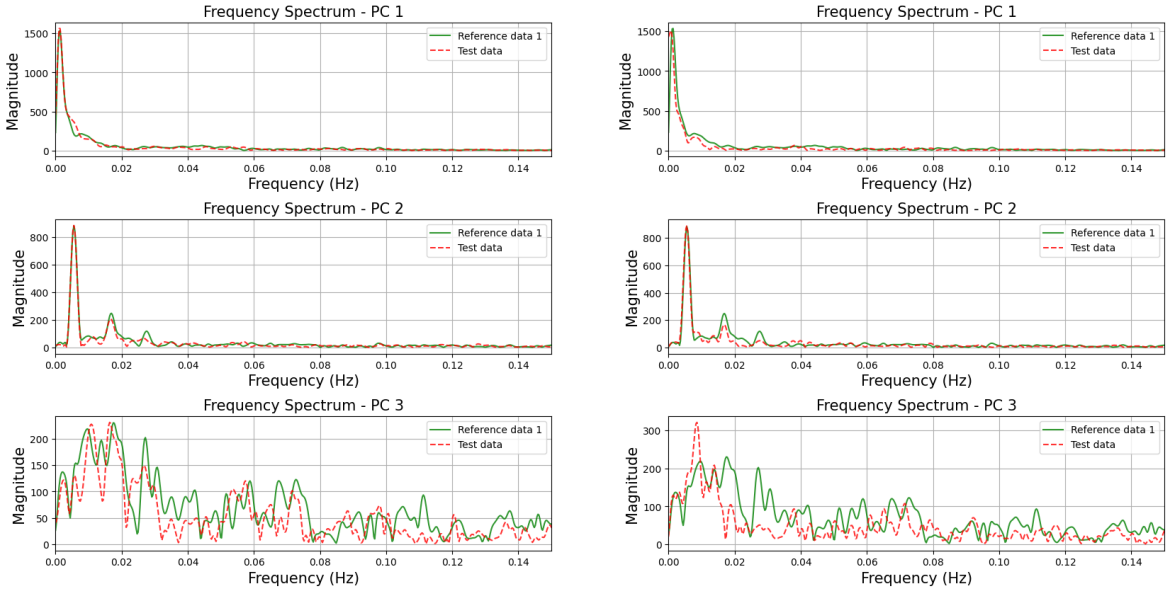

(a) $\Delta V = 0\ l$ (b) $\Delta V = 4\ l$

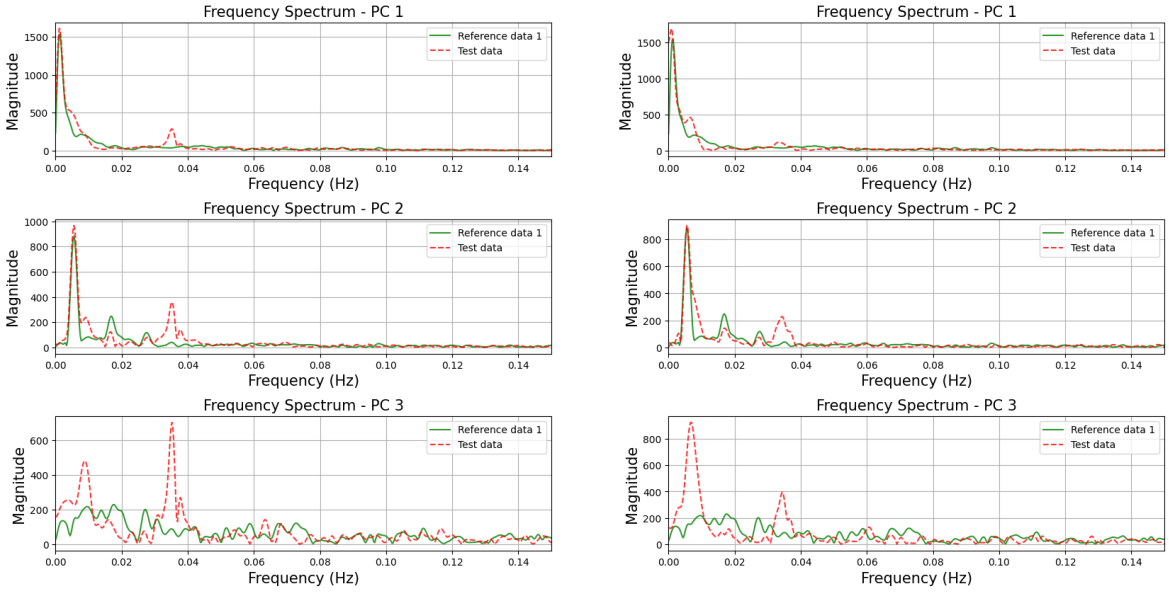

(c) $\Delta V = 8\ l$ (d) $\Delta V = 10\ l$

Figure 30: Plots showing frequency analyses on the three first principal components for $T_i = 5\ s$ for (a) Test 4 in comparison to Reference test 1, (b) Test 5 in comparison to Reference test 1, (c) Test 6 in comparison to Reference test 1, and (d) Test 7 in comparison to Reference test 1.

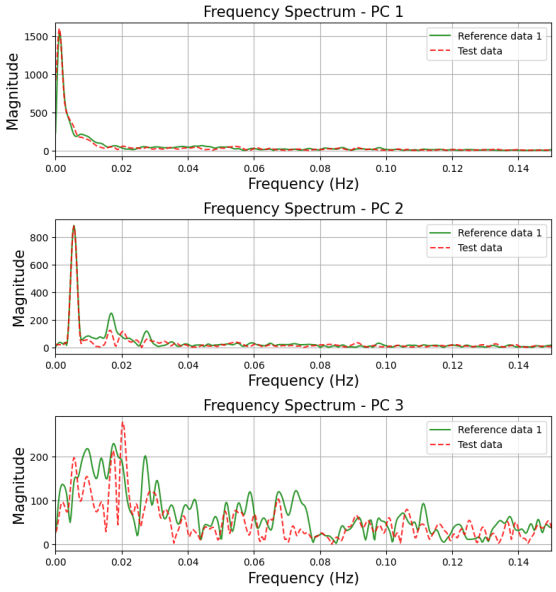

(a) $\Delta V = 0\ l$

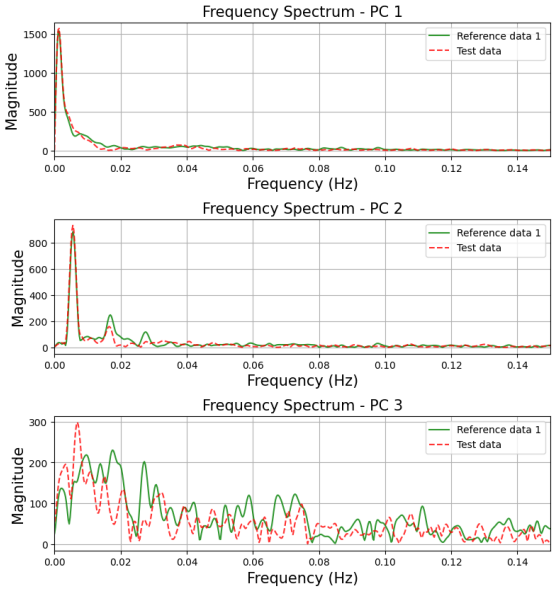

(b) $\Delta V = 4\ l$

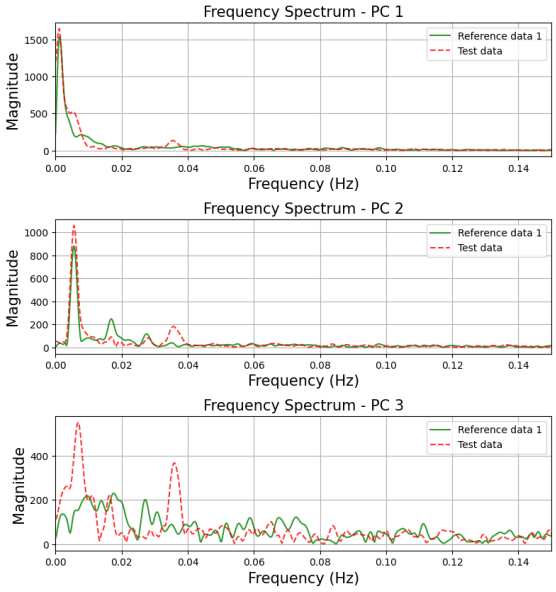

(c) $\Delta V = 8\ l$

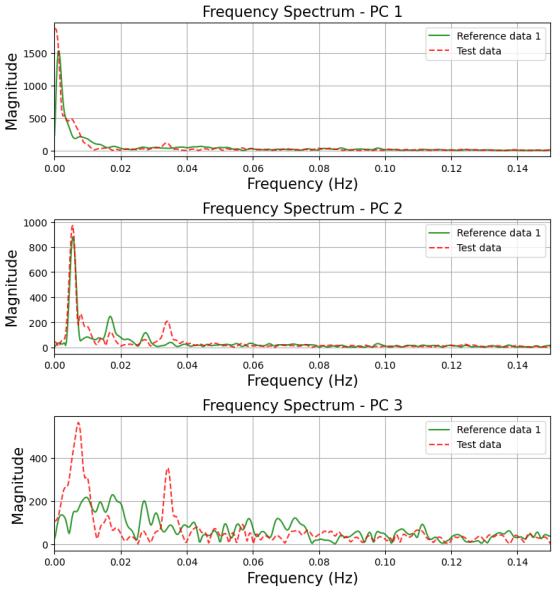

(d) $\Delta V = 10\ l$

Figure 31: Plots showing frequency analyses on the three first principal components for $T_i = 7.5\ s$ for (a) Test 8 in comparison to Reference test 1, (b) Test 9 in comparison to Reference test 1, (c) Test 10 in comparison to Reference test 1, and (d) Test 11 in comparison to Reference test 1.

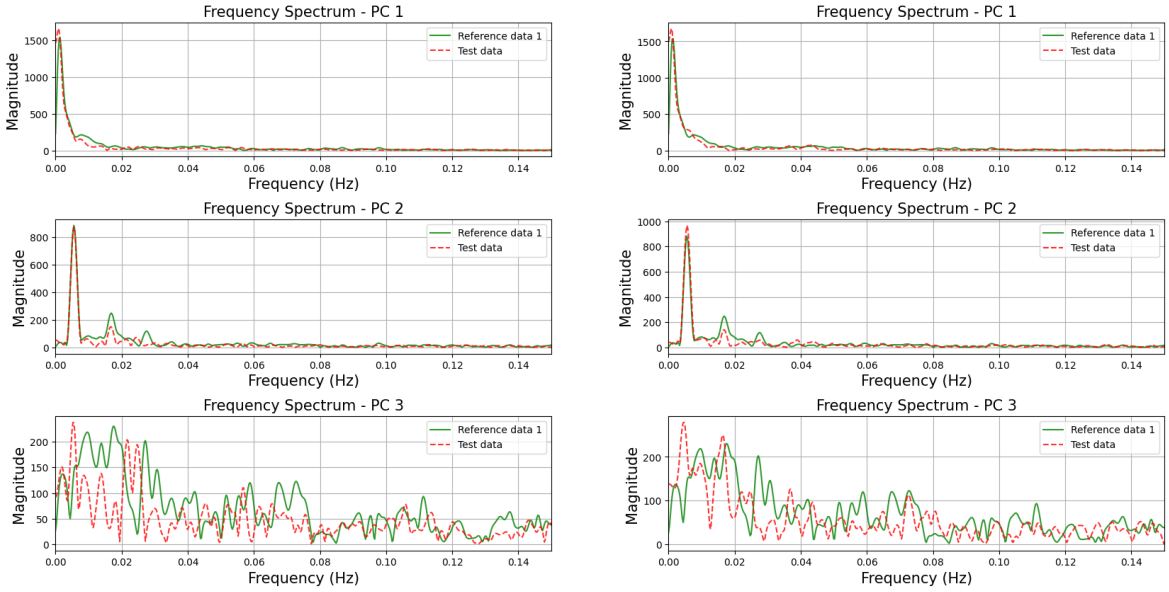

(a) $\Delta V = 0\ l$ (b) $\Delta V = 4\ l$

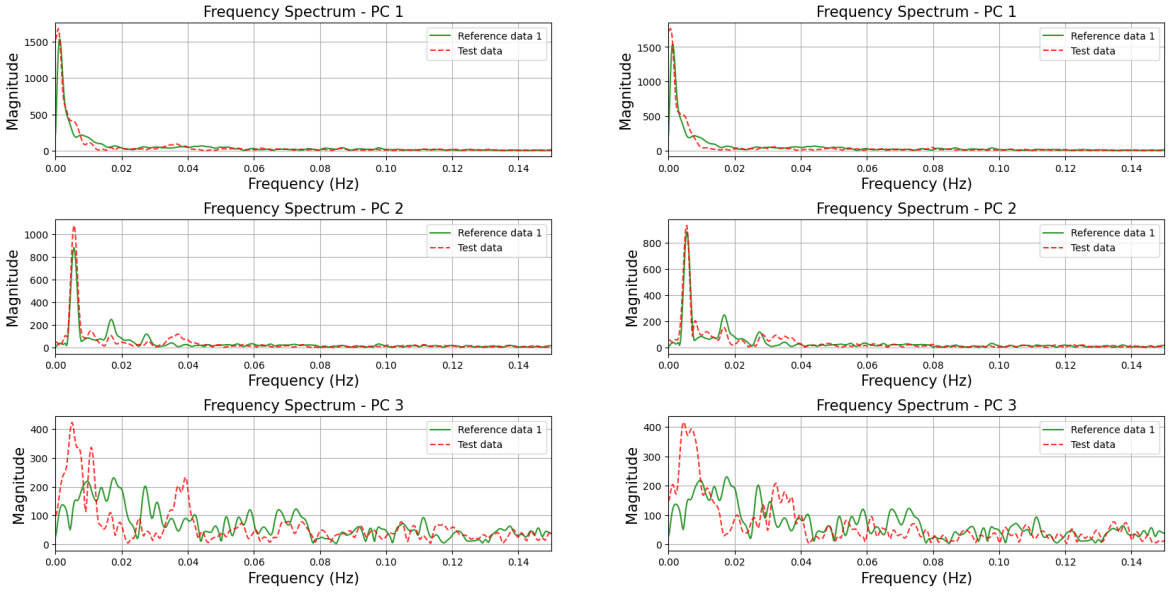

(c) $\Delta V = 8\ l$ (d) $\Delta V = 10\ l$

Figure 32: Plots showing frequency analyses on the three first principal components for $T_i = 10\ s$ for (a) Test 12 in comparison to Reference test 1, (b) Test 13 in comparison to Reference test 1, (c) Test 14 in comparison to Reference test 1, and (d) Test 15 in comparison to Reference test 1.

As expected, the frequency plots all capture a peak in the very beginning of the spectrum, which is due to the slow dynamics in the process. The reference test in Figure 29a does not really reveal any other frequency present, but upon closer examination, another frequency appears consequently in the spectrum plots when there is an introduced volume deviation in the system. Having a closer look at Figure 29b, a small peak is noticeable around 0.037 Hz. Inspecting Figure 29c, which depicts a system that reached instability due to a too large volume deviation and a lack of compensation through an increase in integral time, an interesting pattern is therefore recognized. The same peak is present, and while it is located at the same frequency, the magnitude is significantly larger. This implies that the peak at 0.037 Hz seems to appear as a result of an introduced volume error and that the magnitude of this peak depends on the relative size of the error.

Evaluating the rest of the graphs, this is a recurring pattern. Figure 30a does not show any

indication of a peak present around 0.04 Hz, while there clearly is a peak in Figure 30b, Figure 30c and also in Figure 30d. Although the peak is smaller in 30b, it is still possible to notice it. This is the same for the rest of the plots, where there is a volume deviation of $\Delta V = 4l$, i.e. a peak is present but significantly smaller.

It is also worth mentioning that the frequency peak is most noticeable in the third principal component. In conclusion, since this is a recurring pattern, the frequency is most likely a disturbance from the volume deviation. Figure 29c also confirms this, as the plot clearly shows where the volume deviation is located.

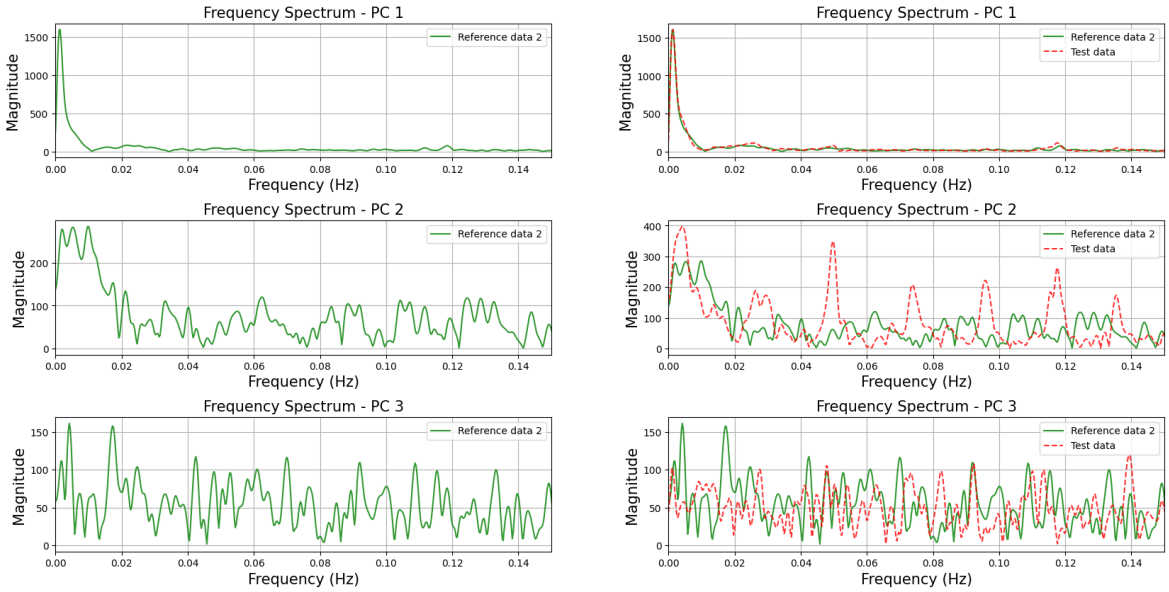

(a) Reference test 2: $\Delta V = 0$ l, $T_i = 3$ s

(b) $\Delta V = 2$ l, $T_i = 5$ s

Figure 33: Plots showing frequency analyses on the three first principal components for (a) Reference test 2 and, (b) Test 2 in comparison to Reference test 2.

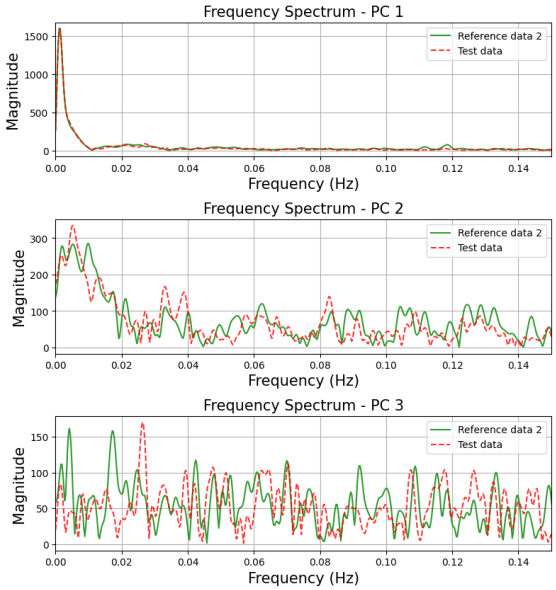

(a) $\Delta V = 0\ l$

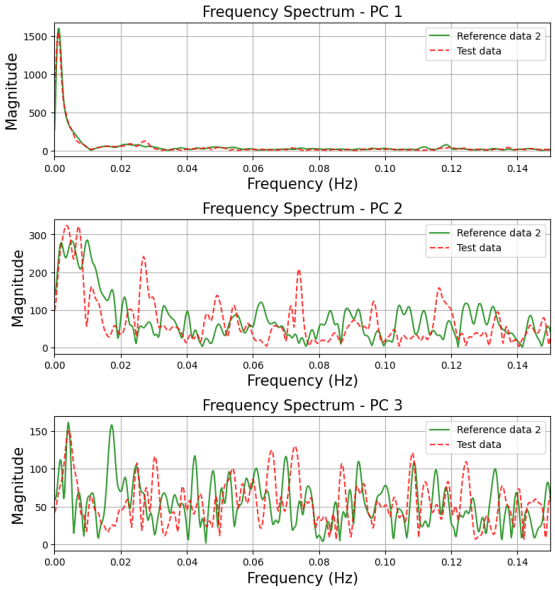

(b) $\Delta V = 2\ l$

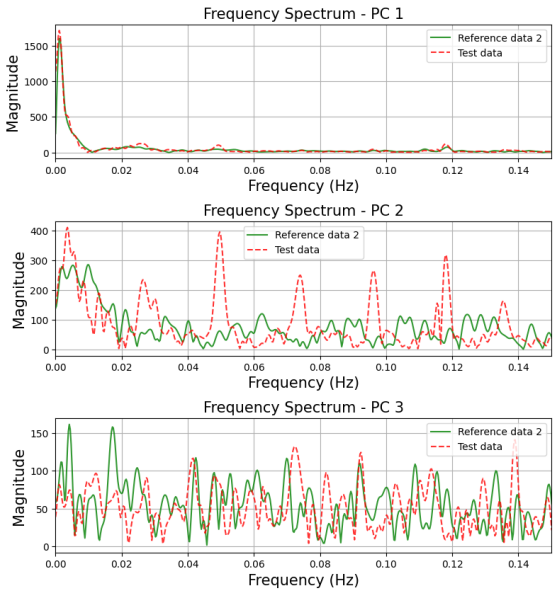

(c) $\Delta V = 4\ l$

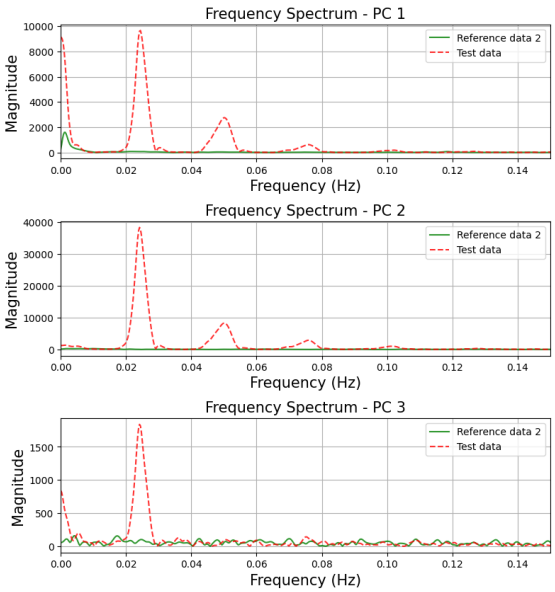

(d) $\Delta V = 6\ l$

Figure 34: Plots showing frequency analyses on the three first principal components for $T_i = 7.5\ s$ for (a) Test 3 in comparison to Reference test 2, (b) Test 4 in comparison to Reference test 2, (c) Test 5 in comparison to Reference test 2, and (d) Test 6 in comparison to Reference test 2. Furthermore, (d) show a system unstable due to a large volume error.

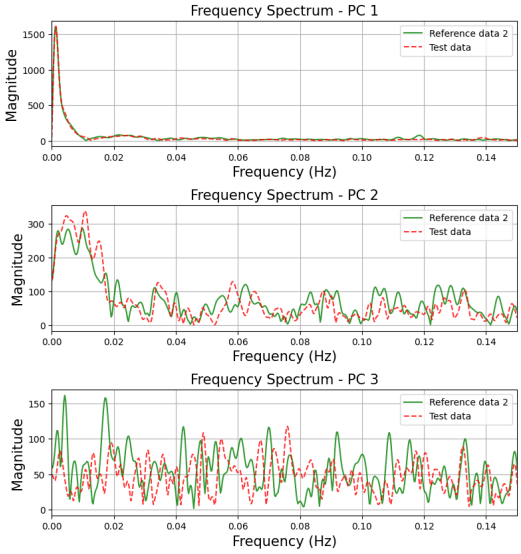

(a) $\Delta V = 0\ l$

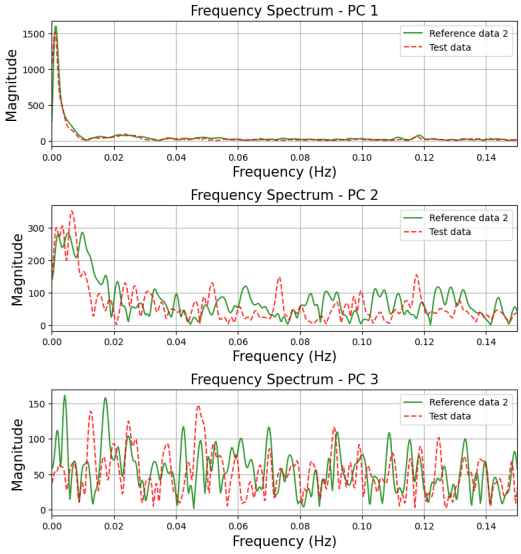

(b) $\Delta V = 2\ l$

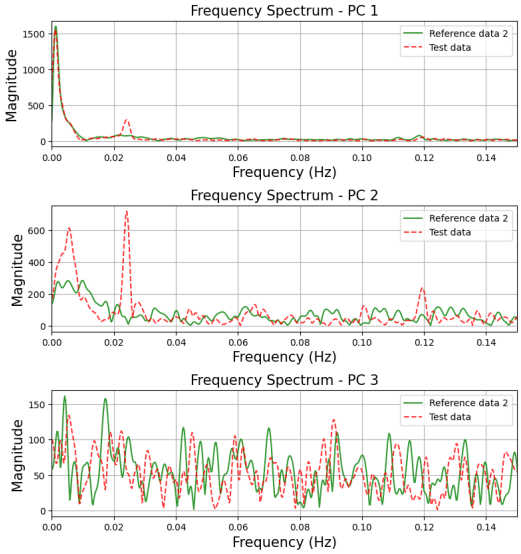

(c) $\Delta V = 4\ l$

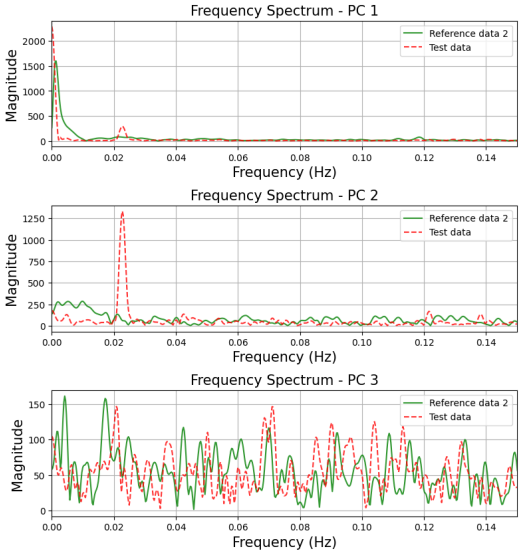

(d) $\Delta V = 6\ l$

Figure 35: Plots showing frequency analyses on the three first principal components for $T_i = 12.5\ s$ for (a) Test 7 in comparison to Reference test 2, (b) Test 8 in comparison to Reference test 2, (c) Test 9 in comparison to Reference test 2, and (d) Test 10 in comparison to Reference test 2. Furthermore, (d) show a system unstable due to a large volume error.

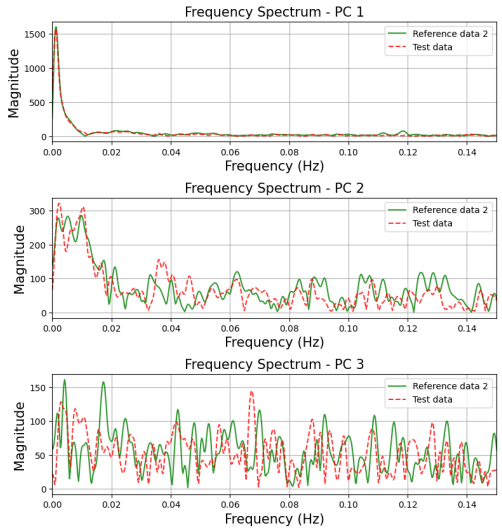

(a) $\Delta V = 0\ l$

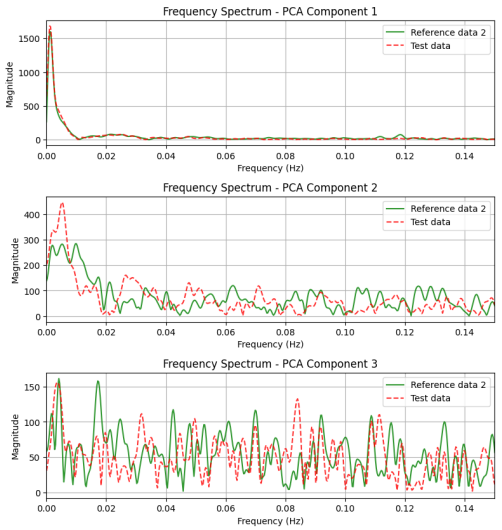

(b) $\Delta V = 2\ l$

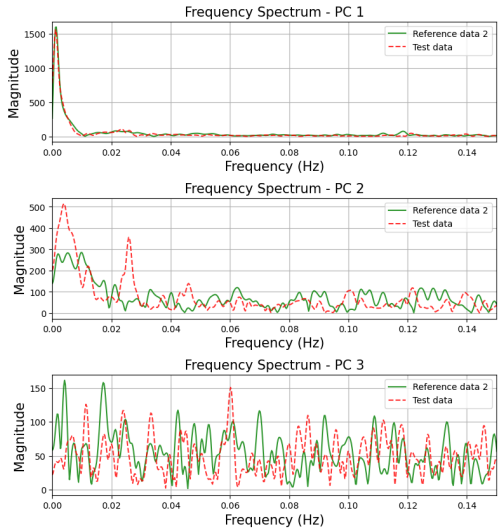

(c) $\Delta V = 4\ l$

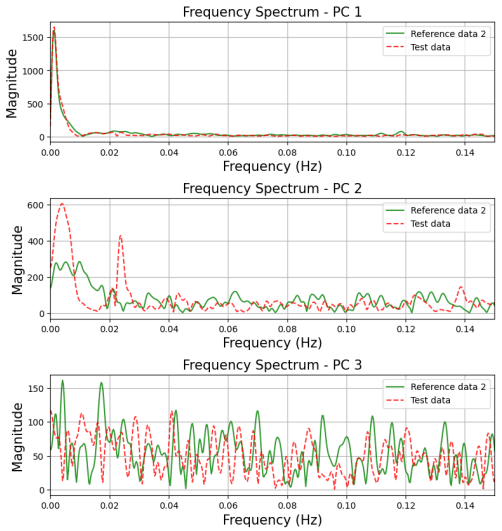

(d) $\Delta V = 6\ l$

Figure 36: Plots showing frequency analyses on the three first principal components for $T_i = 17.5\ s$ for (a) Test 11 in comparison to Reference test 2, (b) Test 12 in comparison to Reference test 2, (c) Test 13 in comparison to Reference test 2 (d) Test 14 in comparison to Reference test 2.

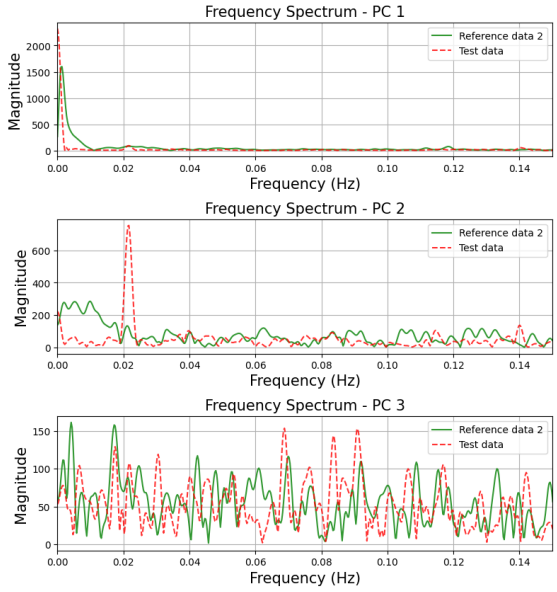

Figure 37: Plots showing frequency analyses on the three first principal components for Test 15 in comparison with Reference test 2. $T_i = 17.5$ $s$and $\Delta V = 8$ l. Furthermore, this plot show an unstable system due to large volume error.

Similarly to the other results, the frequency spectrum plots reveal the same pattern as with Test Matrix 1, however, this time, the disturbance seems to be located around 0.023 Hz and most captured in PC2. Smaller volume deviations are still hard to detect. Lastly, the results from the steady-state operation are presented below.

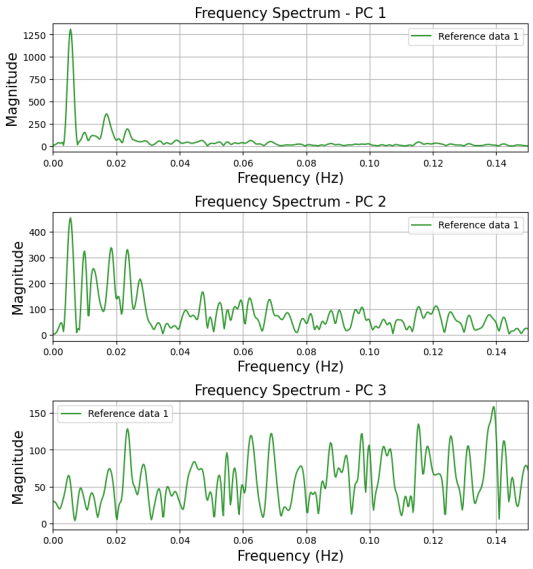

(a) Reference test 1: $\Delta V = 0$ l, $T_i = 3$ s

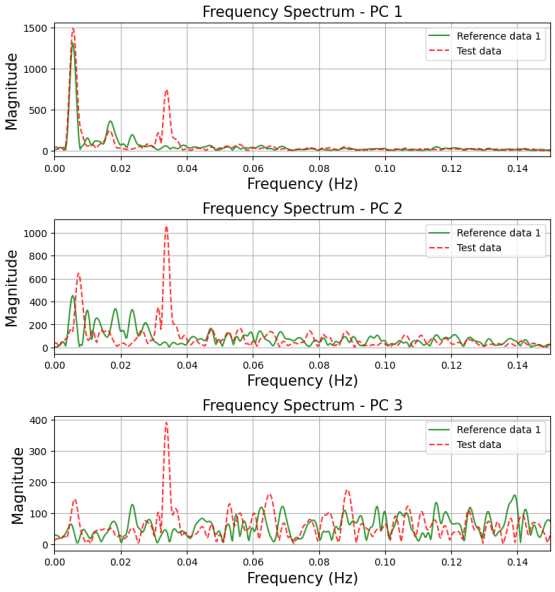

(b) Test 7: $\Delta V = 10$, $T_i = 5$ s

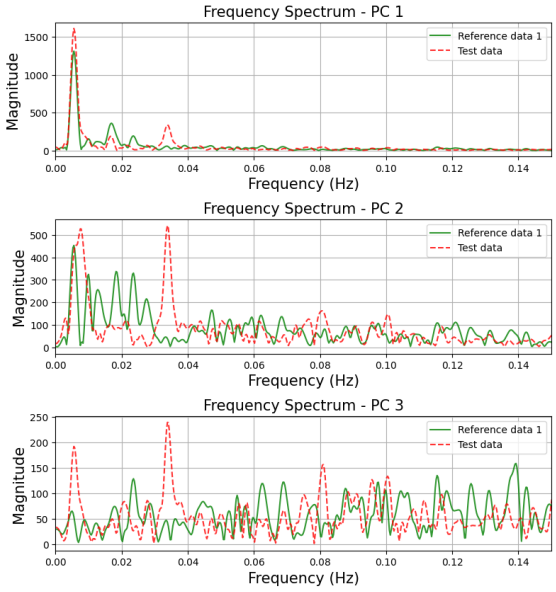

(c) Test 11: $\Delta V = 10$, $T_i = 7.5$ s

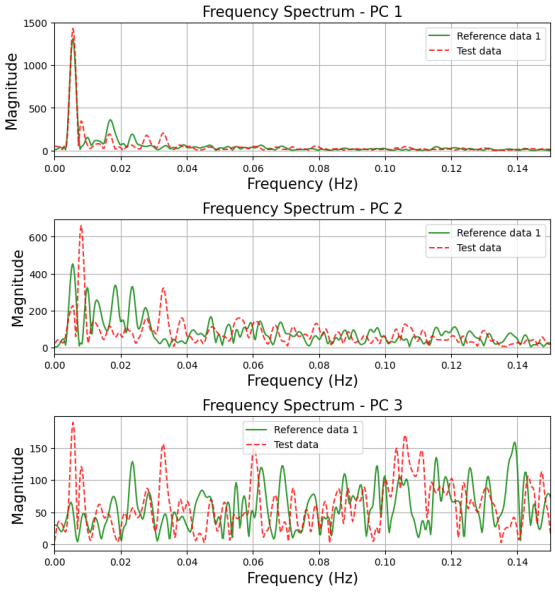

(d) Test 15: $\Delta V = 10$, $T_i = 10$ s

Figure 38: Plots showing frequency analyses on the first three principal components for (a) Reference test 1, (b) Test 7, (c) Test 11 and, (d) Test 15.

From the results, it is clear that even though a setpoint change is absent, the deviation is still present at the same frequency as with a setpoint change.

8 Evaluation of Detection Techniques

This section evaluates the different detection techniques in terms of advantages, limitations, accuracy, validity, and reliability.

8.1 Principal Component Analysis

The Principal Component Analysis succeeded in reducing the dimensionality of the dataset to visualize the variance present in the data. The error that is the target of the identification affects the process by introducing oscillations. These oscillations, when large enough, result in instability. Dynamics such as oscillations will affect the variance of the system, and therefore appear in the score plots. This can be seen in, for example, Figure 14b where an introduced volume error increases the spread of the data points. This trend can generally be identified for both test matrices. The purpose of increasing the integral time is to account for a large volume error to prevent instability. This is a scenario frequently appearing at industrial sites using the TPSU, where the volume error is configured poorly during commissioning, which results in an increased integral time to get a stable system. This increased integral time slows down the dynamics of the system. Figure 16c, which describes a system with a large volume error and considerably high integral time, shows that this increased integral time dampens the spread of the data points marginally while introducing slow process dynamics. These slow process dynamics are seen mainly through the characteristics of the setpoint change, where the process takes longer to stabilize around the new setpoint. Figure 17d displays the same scenario, except with an even higher integral time. In this instance, the system is almost overcompensated, showing little to no spread of data points and extremely slow system process dynamics.

These system dynamics that correlate with the volume error and a corresponding integral time can be distinguished already in PCA-space, at least theoretically. However, implementing an algorithm or a threshold that can identify the volume error in a system that is arbitrarily compensated integral time-wise might prove to be difficult due to limitations. A potential implementation could utilize a predefined "region" where an errorless system would be expected to confine all data points within, while a system with a volume error would have a meaningful portion of the data points lying outside the region. This threshold would resemble an ellipse in an analysis of a steady-state operation. For these datasets, because a setpoint change is included to highlight the behaviors introduced by the volume error, this region would look different and potentially resemble two ellipses depending on what the score plot would look like during optimal operation. To detect the slow process dynamics, another area of focus is the data clusters that "travel" from the first setpoint to the second during the change. The path these data points take is highly dependent on the integral time and stochasticity, since the exact operating point where the setpoint was changed affects where these data points start moving. This can be seen by comparing Figure 21a and Figure 22a where the setpoint probably began at slightly different stages of the process, resulting in different starting points in PCA-space.

To potentially account for the complexity mentioned lastly, a few PCA transformations were done on a dataset without a setpoint change, i.e. a system operating at steady-state. Looking at 23b, it is clear that the volume error can be distinguished due to the spread of the data points in the cluster. In this comparison the test dataset contains a high volume error, and not sufficient compensation in terms of increased integral time, which is not likely to appear in a real-world setting. More likely, the volume error will be compensated for or even overcompensated for, as depicted in 23d. It is easy to see that detecting the volume deviation in this figure is difficult. Although there are data points that could potentially be used for identification, the error is not as easy to identify visually as in the plots containing a dataset with a setpoint change. However, this approach does eliminate the complexity that revolves around the awkward shape of the data clusters when a setpoint change is present.

Another limitation affecting a potential implementation lies in having enough information to establish a baseline that is robust enough to have accurate thresholds. Two different machines at different sites might have different dimensions, which with high likelihood will affect the size and shape of the clusters. The same TPSU during operation with different active recipes will have a similar impact. To account for this, the implementation would have to take into consideration the different setpoints used during operation as well as different dimensions for each and every machine, which might be time consuming to set up every time a new machine has to be evaluated.

When comparing Test Matrix 1 and Test Matrix 2, the behaviors highlighted previously appear to be a general trend. The datasets differ slightly, which results in the PCA-transformation yielding

different components. This explains why the shape and rotation of the data clusters might be different. Inspecting Figures 14a and 18 that show the reference datasets from the two test matrices, it can be seen that the clusters vary in size and orientation. This difference highlights the complexity of the potential general implementation and shows that minor changes in the process might affect the visualization in PCA-space enough to affect the predefined threshold during this potential implementation.

However, it is important to note that the theoretical behavior described in this section can be seen using both the simulations described in test matrix 1 and test matrix 2, which implies that this trend is universal and applicable to a degree in all systems.

With all these factors taken into account, PCA appears to be of better use as a dimensionality reduction technique or for ocular inspection of the process behavior.

8.2 Residuals

As briefly discussed earlier, Hotellings T^2-residual and Q residual exhibit different results. Although Q residuals show a slight potential in identifying volume error, at least when the error is large, Hotellings T^2 performs significantly worse at the same task. Both residuals measure the discrepancies between each sample of the reference datasets and the test datasets and the transformed PCA models. This is a potential limitation to these methods, since these residuals might not exhibit a consistent trend when it comes to exclusively detect the volume error since other process characteristics or disturbances might contribute to a sample not conforming to the PCA-model and therefore result in a high residual. It is therefore easy to assume that these methods will have a high False Positive Rate (FPR) and complexity in establishing a robust threshold.

However, it is worth discussing Q residuals further, as they exhibit a slightly more promising trend. Inspecting Figure 26d, which shows a system with a high volume error and a moderately high integral time, it can be seen that the amplitude during the setpoint change is large. Analyzing the width of the peak corresponding to the setpoint change, it is also clear that a large volume error increases the width in many cases. Comparing the aforementioned figure to Figure 26a showing a system with a smaller volume error and the same integral time, these trends are easy to differentiate. However, these trends are still not consistent, as can be seen in Figure 25b where the reference data without volume error produce a higher residual than the dataset with the introduced volume error. Analyzing the Q residuals in test matrix 2 gives slightly different results. As explained earlier, this dataset differs from the dataset used to adjust the simulation during the tests in test matrix 1. These changes resulted in the system being more prone to instability due to faster process dynamics, which also results in the system reacting more to smaller changes. The Q residuals for these tests show a higher peak during the setpoint change whenever a volume error is present in the system. Looking at Figure 45b, which describes a small volume error and a slight integral time compensation, this is clearly seen. This indicates an inconsistent method that will likely have a large variation in efficiency when the process characteristics change. A system that responds faster to changes will give identifications that are easier to differentiate, which will limit the use of the method in many applications.

Evaluating the simulations performed in steady-state yields similar results. Firstly, a notable difference between the residuals during a setpoint change and during steady-state is that the peak appearing due to the setpoint change disappears. This results in the residuals becoming more uniform as the large-magnitude peak that affected the scale of the graph now does not exist, which seemingly leads to better resolution. However, this improved resolution does not provide any apparent change in how well the residuals detect the volume error. Hotelling's T^2 still behaves unpredictably, providing no reliable trend to distinguish the error. The Q residual performs better, showing slightly elevated peaks when there is a volume error. This can be viewed in Figure 28a where a system with a high volume error is shown. Resembling the results obtained from a residual analysis of the datasets containing a setpoint change, the Q residuals seem to be able to distinguish that the volume error leads to some samples not conforming to the PCA-model, but not consistently reproduce the same result, which is problematic.

A potential implementation involving these residuals could be realized, but there are several limitations that will affect the behavior and applicability. Hotellings T^2 has been concluded, with all results taken into account, to be a poor choice of method to identify this volume error and will not be considered further. The Q residual shows a more promising trend and could be applicable to some extent. There are, as mentioned, limitations that have to be taken into account, such as the efficiency

varying with the process dynamics, resulting in the method being more efficient on systems with faster dynamics.

8.3 Frequency Spectrum Analysis

Already during an initial inspection, frequency spectrum analysis appears to be the more promising method to identify the volume deviation. As explained above, the main characteristic of the volume deviation is an induced oscillation. The presence of this oscillatory behavior strongly indicates that a frequency analysis is efficient. For both test matrices, the general behavior described in Section 7.5 is visible, with some minor differences. The peak at which this oscillation appears is static throughout all simulations for each respective test matrix, but varies in between the matrices. This is likely due to changes in the process dynamics, such as the system responding faster to changes due to some characteristics being altered. For test matrix 2, the flow of raw milk is significantly reduced. This will result in the process reacting faster to changes, and therefore smaller increments of volume errors leading to stronger oscillations. As explained previously, this faster process dynamic leads to the frequency of the oscillation decreasing for all simulations in test matrix 2, which results in the volume error-induced peak appearing at a lower frequency. This can be seen by comparing Figure 29c and Figure 35d where both figures show an unstable system to highlight the placement of the respective oscillatory frequencies.

This requires some knowledge of the process similar to the knowledge described for PCA. However, this amount of knowledge is significantly less and is essentially only the frequency at which the oscillations appear. Inspecting Figure 29b and Figure 31c it is confirmed that the oscillation induced by the volume error appears at the same frequency, independently of the size of the volume error or the chosen integral time. The other required knowledge would be to know the amplitude of the energy content at this frequency for a system without a volume error so this could be compared with the amplitude of the energy content in a system with a volume error.

Evaluating the flexibility of a potential application, the frequency analysis again displays superiority, as the oscillations induced by the volume deviation, in contrast to being more latent in the PCA score plots, are clearly visible during steady-state operation. This implies that detection methods related to frequency analysis might not be limited to a dataset containing a setpoint change and might be applicable in a more flexible manner.

As discussed with respect to PCA, a machine operating in steady-state without the introduction of a setpoint change might hide the elements that are used for detection. For frequency analysis, this is not the case. Inspecting Figures 30d and 38b showing a high volume error without sufficiently compensating integral time and a high volume error in an overcompensated system, respectively, it is clear to see that the frequency peak corresponding to the oscillation appears at the same frequency for both cases. This is promising since it enables the use of frequency analysis in steady-state operation and during setpoint changes. Comparing the aforementioned figures one could even claim that the oscillations are easier to detect during a steady-state operation, which could simplify a potential implementation.

A drawback of this analysis is that the peak corresponding to the oscillation can vary in magnitude. For systems with small volume errors and high integral times, as in 36b, it is difficult to visually compare the peak at around 0.023 Hz with the reference dataset. However, this limitation can be avoided in practice by implementing a detection threshold along with a band-pass filter of appropriate bandwidth. The use of this filter originates from the need to isolate the frequency peak that is the target of detection, which is effectively done with a band-pass filter[20]. This isolation results in an increased validity since frequency peaks appearing due to other deviations will be filtered out and a potential false positive is avoided. This approach still requires extensive knowledge of the exact frequency of the oscillation so that the bandwidths can be chosen both in an efficient and robust manner.

8.4 Accuracy

Detecting process behavior induced by volume error depends on many factors, which have been discussed in the previous sections. This complexity results in the implementation requiring a high accuracy of detection.

Exactly what is defined as a volume error is slightly arbitrary. What size does the volume error have to be to affect the system enough for a detection to be "necessary" to perform? This is an aspect that has to be taken into account when discussing the accuracy of a method, since the volume likely never will be perfectly configured, which results in a small discrepancy almost always being present in any system unless the exact volume is known. Therefore, discussions and conclusions drawn in this section will be comparative between the methods and focus on the theoretical accuracy of the methods at a large scale rather than trying to compare the accuracies of the different methods numerically for different systems.

In all of the methods evaluated, a threshold will be used as a means of detection.

As mentioned earlier, PCA visualizes the behavior induced by the volume error as an increased captured variance. To detect this, a region of appropriate shape could be created to detect when a data point appears too far from the center of the cluster of data points. An implementation utilizing this approach requires the computation of a distance metric such as the Euclidean distance to measure deviations from normal operation [21]. Getting an accurate threshold using PCA is a complex problem, since the size and shape of the cloud will depend on the individual process. To establish a universal region that works for all processes will therefore not give an accurate enough detection, and as concluded earlier, PCA is seemingly a better fit for the purpose of dimensionality reduction and visual analysis of individual process behavior than an accurate method of detection.

The threshold for both residuals would be implemented as a horizontal line that detects unwanted behavior when the amplitude of the residual reaches the threshold. Hotellings T^2 is, as mentioned earlier, not a reliable residual to use and will not give accurate detections. Q residuals are slightly different and can for some systems exhibit an efficient possibility of detecting the error due to a system with faster process dynamics, such as the process at Company B, having residuals with higher amplitudes than processes with slow dynamics, such as the process at Company A. This results in the accuracy of the Q residual becoming situational and highly dependent on the process for which the detection is configured, which lowers the potential accuracy for a universal threshold without individual modifications. Both residuals are, as mentioned formerly, comparing individual samples to the established PCA-model. Residuals such as Hotellings T^2 are highly sensitive to outliers [22], which could lead to an implementation that detects other errors and cannot differentiate between this error and the volume error, resulting in a high false positive rate and lower accuracy.

The frequency spectrum analysis will, in a similar manner as the residuals, utilize a horizontal threshold that is detected whenever the energy content at the frequency of the oscillations induced by the volume error reaches this threshold. For this method, false positives can be avoided by using a band-pass filter. This combination would allow the threshold to only detect threshold-breaches at the desired frequency and therefore lower the risk of false positive detections.

For all of the methods discussed in this section, there is a possibility of missing a detection, i.e. a false negative. The False Negative Rate (FNR) depends on how well the methods can detect smaller volume deviations in highly compensated systems, since these are the scenarios where detection is the most difficult. For PCA this can be compared to Figure 17b which describes an overcompensated system and a small volume error. Inspecting this score plot it is hard to visually detect that the error is present, which implies that a threshold implementation likely would have low possibility of detection for this case.

For the two residuals, the same principle applies. Analyzing Figure 27b, which shows the residuals for the same system, it is clear that a detection of volume error is improbable. Both residuals show no signs of a present error and would contribute with a false negative.

The frequency analysis for the same system is shown in Figure 32b. Analyzing the frequency plot for component 3 knowing that the detection should be done at 0.037 Hz for this system indicates that this method might be slightly superior at detecting volume errors even at more latent sizes since a potential threshold together with a bandpass filter with appropriate bandwidth could be utilized to detect the error. However, the accuracy of the frequency analysis will likely decrease with a decreasing volume error and at some point give false negatives as well.

8.5 Validity

Upon evaluation of the results, it can be concluded that the volume discrepancy, in combination with an increased integral time, influences all statistical analysis measures tested. However, there are some important comments to make. While the PC subspaces demonstrates a larger variance due to

increased deviations, the PCA is only able to conclude that there is a deviation, and not the reason behind a deviation. To make any further assumptions based on a PCA, one needs to have more extensive knowledge about the process. As mentioned before, it is the oscillations in the systems that give rise to a change in the PC subspace, but this oscillation can potentially come from any type of disturbance. An industrial process, such as the TPSU together with the hermetic separator, contains several sources of error and stochastic disturbances, both man-made and machine-made. Therefore, another disturbance might as well result in an oscillation that reflects the same behavior in a PC subspace. More tests need to be conducted to acquire knowledge about different deviations in the PC subspaces. Hence, the validity of the principal component analysis is reduced and it remains uncertain whether it accurately captures the deviation intended to be measured. This holds true even for Hotelling's T^2 and the Q residuals. Both residuals are not selective and will likely exhibit behavior similar to the induced characteristics of the volume error when a different disturbance or error is present. Hotelling's T^2 and the Q residuals are also sensitive to outliers. This creates complexity when the task is to create a robust triggering mechanism, such as a threshold, which greatly decreases the validity of these methods.

The frequency spectrum analysis exhibits a more promising result. As discussed earlier, the deviation seems to appear at the same frequency for all test cases in a test matrix, regardless of the magnitude of the volume discrepancy and integral time. Hence, it is possible to conclude both that there is a deviation and also what type of deviation it is due to its consistent oscillatory behavior. Although the deviation seems to appear at different frequencies for different configurations, the spectrum analysis reveals an enhanced performance of validity, in accurately capturing the targeted deviation. However, it is entirely possible for other errors to cause oscillations at the same frequency as the volume deviation, and thus full validity can be achieved by introducing other sources of error and evaluating the results in the frequency analysis.

8.6 Reliability

For a test result to have high reliability, the results should be the same in consecutive measurements, regardless of the executor. Due to the several different recipe configurations available in the TPSU, reliability is crucial. Extensive conclusions about reliability in this Master's thesis are difficult to draw, since only two different configurations have been tested. However, these two test matrices indicate similar behavior in all the cases. Furthermore, individual tests in the PC subspaces and in the frequency plots exhibit the same pattern in the repeated tests, both with a present and absent setpoint change. Despite exhibiting the same pattern, some differences are evident in the frequency spectrum analysis. The peak of where the frequency of the deviation appears varies from test to test. As can be seen in Figure 30, the peak appears at approximately 0.037 Hz, while in the peak in Figure 29 it seems to be closer to 0.04 Hz. This is likely due to some changed dynamics in the system when increasing the volume discrepancy together with the integral time. But, at least for the simulations because of their somewhat deterministic behavior, the same tests will depict the same results in terms of data collection and sampling for the same configuration. Since the peaks also only vary within a very narrow and limited interval for each different test scenario, it is still somehow repeated and, therefore, still consistent in terms of reliability.

With regard to Hotelling's T^2 and Q residuals, the results are different. As already mentioned earlier, repeated tests do not show a perfectly consistent trend in either of them. There are possibilities to in some cases detect a repeated pattern within Hotelling's T^2 and in the Q residuals, but not with the same certainty as in the PC subspaces and in the frequency spectrum plots. Thus, the reliability of these residuals remains reduced for these statistical evaluations. Hotelling's T^2 is affected by the dimensionality of the data, which results in this residual becoming less reliable for the purpose of fault detection. [23]

While the result of reliability is promising for the simulations, it is worth mentioning that no repeated tests have been executed on the real-world data and, thus, it can not with certainly be said that there is a high reliability generally in the system. A real-world system is of a highly non-deterministic characteristic and the same configurations might yield other data samples and a very different response, due to hidden internal and external disturbances. This is something that needs to be evaluated for future work, but the two test matrices reveal a promising trend.

8.7 Sources of Error

During validation of the accuracy of the simulation, some parameters were adjusted to try to resemble the real-world data acquired from Company A, as best as possible. In the simulation software, only a few trends could be measured, which resulted in a limited view of the attributes of the simulated dataset. However, prior knowledge about the process, acquired from resources at Tetra Pak led to the conclusion that this was not of major importance, since the parameters that were tuned, together with the recipe, change the process dynamics entirely. However, it is worth mentioning that even small differences between the same features in the datasets could have an impact on the PCA space. This could be seen in Section 7.2, when the data clusters from the simulation and the real-world data were separated by a distance. Only being able to visually confirm the tuning of a small portion of the features might result in some characteristics of certain features being overlooked, which can affect the results.

Another source of error worth mentioning is related to data collection. For all tests performed, the sampling frequency is 1 Hz. The process in question is, as mentioned, an industrial process where changes and fluctuations are expected to occur over a longer time span. It is entirely possible that testing lower sample frequencies would result in better results, as more of the process dynamics might be captured if the sampling interval is increased because the system exhibiting relatively slow dynamics. Unfortunately, to make the process of simulation and data gathering efficient and not overly time-consuming, a sampling frequency of 1 Hz was used during these tests.

There are also difficulties in mimicking the exact values and behavior of a system for the variables that were measured and displayed as a trend. Simulation softwares are often simplified in terms of underlying structures such as noise. Industrial processes often exhibit non-linear behaviors that might not be captured to a full extent by a simulation, which might result in differences. Manually tuning parameters to become as similar as possible to a specific value proved to be time consuming. Due to time constraints some minor differences between variables might have been overlooked and could be optimized, but since the simulation sufficiently represented the real-world system dynamics this optimization was not carried out.

In the field of engineering, simulation software is often simplified to provide useful insight to engineers about complex problems[24]. A simplification of the simulation model could lead to a decrease in accuracy. Because the method is based solely on simulations, with some influence from real-world data, the results might be slightly idealized. A simulation is rarely as stochastic and random as a real-world process, even though the simulation software uses the same PLC and control logic, but with some simulated variables. The resulting theory does not take into account any stochastic events that might occur in an industrial setting and focuses solely on the volume deviation.

All the methods used to analyze the datasets focus solely on the detection of a volume deviation. Due to the fact that no other errors are in focus, the effects of external errors are not taken into account. Industrial processes are generally not optimal, and errors and disturbances will be present. Some of the methods utilized in this thesis, such as both Hotellings T^2 and the Q residual, are highly sensitive to the presence of outliers and other deviations from the PCA model on which the residuals are based. This implies that other errors or disturbances might be detected as a false positive, as explained earlier. Since no other errors or disturbances are taken into account, the results gathered from the simulations might not be fully representative of a real-world system, since a simulation is often simplified and lacks some of the disturbances that are commonly present in an industrial process.

9 Potential Implementation

To improve and automate the process, a real-time implementation is beneficial. The implementation would help a machine commissioner, or a machine operator, without sufficient knowledge to tune the settings in the TPSU more accurately and, hence, confine to a smaller margin around the set work point, improving the efficiency and reducing the amount of required resources in dairy milk and cream fat in-line standardization. This section, therefore, presents proposals for a potential future implementation, taking into account the discovered findings and the existing limitations of the system. The section will evaluate potential advantages and drawbacks with different scenarios, and is intended to serve as a guiding framework, rather than a precise solution.

9.1 Choice of Detection Technique

To construct an efficient implementation, a suitable choice of method has to be made. Four different ways of detecting volume errors have been discussed and evaluated, and each method has different strengths and weaknesses. These strengths and weaknesses have been discussed previously and will be used as a theoretical foundation to motivate arguments about which method is the most efficient to implement.

Principal Component Analysis provides a visualization of the behavior induced by the volume error but lacks in other aspects such as accuracy and validity. An implementation utilizing PCA as the means of detection brings complexity, as each implementation must be individually modified for process differences, recipe changes, and potentially real-world process dynamics not perfectly modeled in the simulation. It is therefore, as mentioned above, suggested that PCA is used as a dimensionality reduction technique rather than a fault detection method based on elliptic boundaries around data clusters in scree plots.

Hotelling's T^2 is already, at first glance, easy to dismiss as a method suited for this purpose. In most of the tests performed, the residual exhibits minimal potential to detect the volume error. The method lacks reliability, accuracy, and validity and is due to these factors being considered to be the worst choice out of all methods.

The Q residual is the superior of the two residuals, displaying a more prominent trend when detectability is a possibility. This method exhibits situational accuracy, but lacks validity and reliability.

Frequency Spectrum Analysis is in all cases seemingly superior. Of all the methods, FSA exhibits the most promising characteristics in terms of accuracy, validity, and reliability.

This leads to the method of choice being the FSA. Frequency Spectrum Analysis provides the highest possibility of detecting the volume error while being the most flexible method in terms of applicability. As observed during steady-state tests, FSA can seemingly detect the volume deviation in systems without the presence of a setpoint change. This hypothesis was established in the later stages of the thesis, resulting in a little time invested analyzing steady-state operations. However, the possibility of not needing a setpoint change in an implementation significantly simplifies the problem and should be investigated further. PCA will be used as a dimensionality reduction technique in a manner similar to that used during the tests described in this thesis.

9.2 Limitations in Implementation

Implementing a software to detect volume error brings complexity. All evaluated methods have different limitations and strengths that will affect the performance of the implementation.

9.2.1 Variance Between Processes

The TPSU is applicable in a variety of processes, all with different characteristics. Due to the fact that all the methods evaluated are affected by different process characteristics and different operational setpoints, such as recipes, individual modifications are likely needed to maximize accuracy, reliability, and validity. Comparing the results of test matrix 1 with test matrix 2, where the processes differ only in terms of a small number of variables and a recipe change, it is clear that minor differences affect detection efficiency, regardless of the choice of method. This limitation likely results in the need for a controlled environment where the detection can be run knowing how the system would behave under normal circumstances. However, this invokes the need for additional knowledge regarding the behavior

of the process as well as the detectability of the different methods at different setpoint operations and recipes.

9.2.2 Data Limitations

There are limitations to data collection that must be taken into account. The dataset to be analyzed must be sampled at a rate that conforms to the Nyquist Theorem explained in 21. Another limitation lies in aliasing, which can affect the results of the frequency analysis. This can be avoided by implementing an anti-aliasing filter before computing the DFTs [15]. During the data collection performed in this project, a low-pass filter with a bandwidth lower than the Nyquist frequency is used to avoid aliasing.

9.3 General Implementation

A general implementation includes real-time measurements, which trigger an alarm when the determined threshold is violated. The general implementation would cover all the different recipe configurations, and thus have knowledge about the various appearances of the deviations. The general implementation would also be able to change dynamically in case there is a recipe change while running. A block diagram of the general implementation is seen in Figure 39.

While this implementation yields a more non-static behavior, some disadvantages exist within the confined definition of a general implementation. First and foremost, this scenario would require a thorough investigation of all the different recipe configurations, together with collecting and storing all different PC subplots magnitudes and the frequency where the deviation occurs. These will then be used to individually define unique thresholds for the different recipes.

There is also a risk for false positives to appear while the machine is running, leading to an unnecessary stop in production for tuning attempts. Moreover, the simulation data also deviates in magnitude, as seen in Section 7.2, from the real-world data, further complicating the process of collecting and adjusting the various thresholds. Perhaps already implicitly understood, developing a general implementation algorithm requires significant effort and a huge data acquisition.

Another significant limitation to this method is the fact that the majority of tests conducted in this thesis involve a setpoint change. A general implementation should preferably detect a volume deviation at steady-state, since no setpoint changes likely will be present during operation. Therefore, a crucial prerequisite for this implementation is that Frequency Spectrum Analysis, which is the detection technique that displays the most flexibility and accuracy, can detect a volume deviation at steady-state operation. For this to be evaluated, further analysis must be performed, which is explained in Section 10.2.

The question also arises, if a general implementation is needed, as the volume configuration generally appears as a one-time occurrence during commissioning. Therefore, this seems like a redundant implementation since there will most likely not appear any volume deviation within a running process, and will solely be a costly alternative for an implementation.

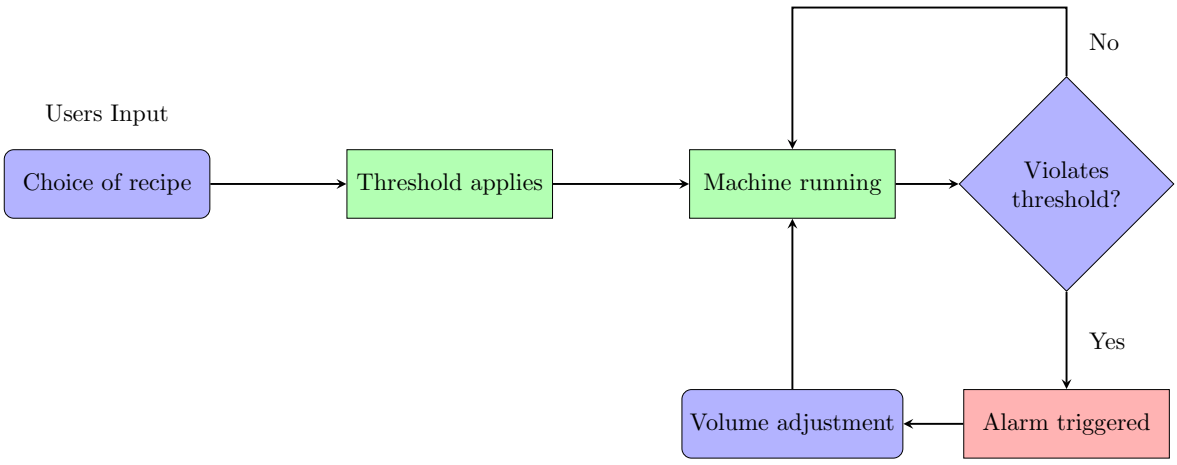

Figure 39: Block diagram of a General Implementation

9.4 Test Case Implementation

As explained earlier, the complexity that arises from the fact that the system behaves differently at different setpoints, using different recipes and using different machines is problematic and requires extensive knowledge of different scenarios of different machines. A proposed solution for this complexity is to implement a test case. This test case will be run during commissioning in a controlled environment where the volume error is detected in an efficient manner. The analysis performed on data from Company A and Company B is essentially representative of a specific recipe and a specific setpoint change for each matrix. Creating a controlled environment where the frequency of the oscillation induced by the volume error is known drastically improves the chances of detection. A controlled environment essentially means that the test case implementation should have a preset recipe that works universally for all machines. This implementation structure is recommended because it significantly reduces the amount of knowledge required to detect volume errors. Due to the fact that the origin of the volume error is solely poor configuration during commissioning, running a test case implementation once in a controlled environment is sufficient. This test implementation should also be executed after all sorts of maintenance that might affect the actual volume that contributes to the volume error, such as changing the dimensions of the pipe transporting the cream. Process setups often have predesigned characteristics, such as a tolerance interval of raw milk mass flow, which affects the process dynamics. Looking at the FSAs performed in this thesis, the process dynamics between the process in Company A and the process in Company B differ significantly in terms of this mass flow. This drastically affects how much the volume error affects the system, as well as the frequency at which the oscillation occurs.

This solution operates under the assumption that the system the implementation is created for resembles one of the systems used in the test matrices and therefore that the simulation accurately enough represents the real-world process, where the frequency at which the oscillation occurs is known and can be assumed to have a similar location for the new system being commissioned. This solution also operates under the assumption that the simulation adequately represents the real-world process. This validation requires some additional research and is described further in Section 10.2 and Appendix C.

The proposed solution is described in a block diagram, seen in Figure 40.

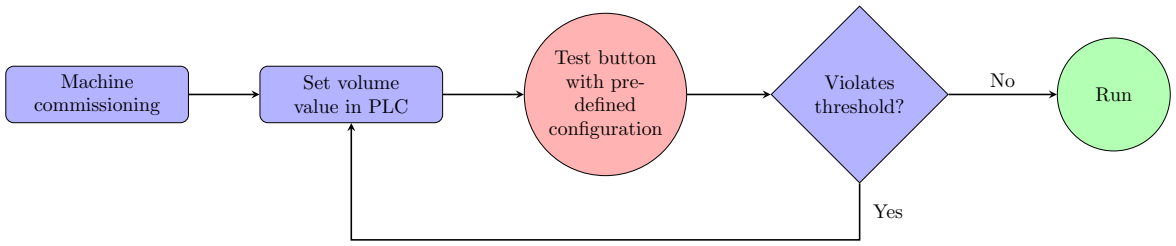

Figure 40: Block diagram of Test Case Alternative 1

However, it is strongly recommended to validate the location of the frequency of the oscillation induced by the volume error for the two systems evaluated in this thesis. As explained in Section 8.7, it is difficult to adjust the simulation to perfectly resemble the real-world process, which might result in some differences in the PCA space and lead to the frequency of the oscillation being slightly different for the two real systems than the frequency of the oscillation for their simulated counterparts. Therefore, to take this into account, it might be beneficial to validate these claims using the secondary method presented below.

If the system in question does not resemble one of the systems used in this project, due to factors such as the system being designed for conditions that differ much from the conditions present in the two systems analyzed in this project, a second solution is presented, where the sole difference is that for these systems a significant volume error is introduced in order to locate the frequency of the oscillation before commencing the test sequence. The second solution is presented in the block schematic, seen in Figure 41.

The additional step introduced in Figure 41 marked yellow, is described in the block diagram in Figure 42.

The determination of which of these methods to be used during the commissioning of a new system depends on how much the system resembles the two processes evaluated in this project. This similarity

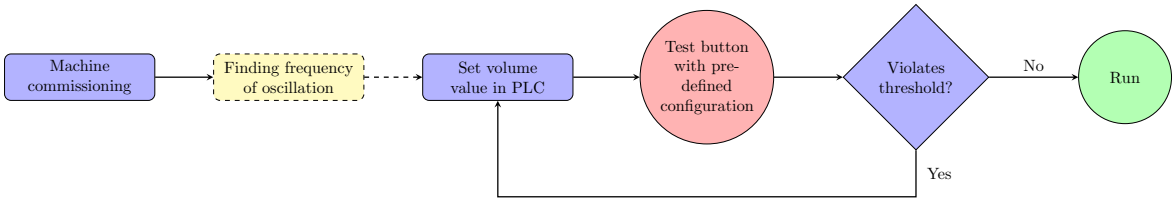

Figure 41: Block diagram of Test Case Alternative 2

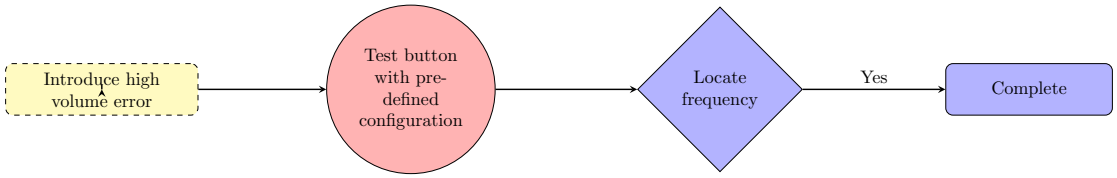

Figure 42: Block diagram describing the additional step added in Test Case Alternative 2 to locate the frequency at which the oscillations induced by the volume occur.

is dependent on the process dynamics of each system, and determining whether the system resembles the commissioned system sufficiently is left to a professional possessing advanced knowledge of the process. However, to potentially maximize accuracy and simplify the detection process in future machines identical to the one being commissioned, the second test case solution is superior. Using the second solution is also advantageous in a long-term application, since every execution gathers new information regarding the location of the oscillation for a different system.

Knowing the rough location of the peak of the oscillation is crucial for detection and will optimally be combined with a band-pass filter of appropriate bandwidth so that efficient isolation of this peak can be acquired.

Furthermore, determining the exact thresholds that should be used from case to case is a different question and comes with complexity. The degree to which the oscillations induced by the volume deviations stand out in a dataset collected from a real-world process has yet to be determined and will have to be evaluated on a new set of data. However, it is likely that the amplitude of the peak of the error-induced oscillation is mainly affected by the size of the volume error rather than by differences in process dynamics. The data needed is explained in more detail in Appendix C.

9.5 Implementation in PLC or HMI

This section will briefly describe the suggested implementation in terms of the general structure and where this structure could be implemented. Implementing these proposed solutions is similar in terms of where the implementation would be constructed. Both solutions require a surveillance system and a system that performs the analysis and collects the data. The analysis might require a large portion of computer memory and should therefore be implemented on the HMI-computer. The surveillance system must be implemented in the PLC to enable the possibility of canceling the analysis if an unforeseen event occurs. Implementing this system in the PLC also helps taking scheduled events into account, such as a separator cleaning that occurs at a preset interval and heavily disrupts the process.

The general implementation is as mentioned more complex than the test case scenario, and would require more knowledge about the process as well as experience from the operator. The analysis must collect data without the influence of the aforementioned occurrences, which requires that the operator has sufficient knowledge about these events and can determine when the analysis should be run.

The test case scenario is less complex and can be implemented in a more simple manner. The PLC should preferably be used to program a state machine of a test sequence of a preset interval. Figure 40 describes the sequence that the operator would use. The red circle describing the test button would be the main activator of the analysis and is pressed by the operator. Pressing this button should activate a pre-programmed sequence in the PLC with a preset recipe, sampling interval, and sampling frequency. After the sampling period has ended, the analysis is performed on the HMI computer. Technical aspects such as data retrieval will not be discussed further than mentioning that it would be performed similar to how it was performed during this project. The rest of the blocks in this diagram

are done by the operator, such as manually setting the volume value before executing the analysis and reconfiguring the volume value if the test results show a volume error.

Figure 41 describes the second proposed test case implementation which includes an additional step in the form of introduction of a high volume error to identify the frequency of the oscillation. This introduction of a high volume error could be preprogrammed in the PLC and executed with the press of a button by the operator in the HMI in a manner similar to activation of the main analysis test sequence described above.

For both of these sequences, it is crucial that no external disturbances or scheduled events affect the analysis. Therefore, when these sequences are active, the PLC should cancel the analysis and notify when an unforeseen disturbance occurs, such as sensor failure or circulation in the process. The PLC should also notify the operator if the operator tries to execute the test sequence with an event such as a separator shoot, which is a periodic event that heavily impacts the process conditions, scheduled during the time allocated for the test sequence.

In summary, the test case implementation would consist of two different sequences, one of which is the main analysis of the system to identify the potential presence of a volume error. This sequence should have a preset time allocated for data retrieval and to analyze the data after the interval ends. The analysis should be performed on the HMI computer. This sequence is the only run sequence on systems where the frequency of the oscillation induced by the volume error is known. The second sequence is inherently the same as the first sequence, but with an additional step. This step is an introduction of a high enough volume error to identify the frequency at which the oscillation appears. The analysis part of the sequence is identical to the main test sequence, with the exception of that the time span when data is collected can be shorter and still give a visible volume error if it is configured high enough. This sequence should be run separately before the main test sequence on new machines where a similar test has not yet been performed to gain knowledge of the position of the volume-induced frequency oscillation.

As a final note, it could be beneficial to always run the second implementation presented in Figure 41 because the known location of the frequency of the oscillation might be slightly affected by non-ideal simulation adjustments. This would simply imply that running the sequence to determine the frequency of the oscillation is beneficial to increasing the validity of the detection for all systems.

9.6 Choice of Implementation Method

Two different implementations have been proposed in this thesis. The general implementation is dynamic and operates in real time during production. If unlimited access to data and the ability to construct an optimal implementation were possible, the general implementation would be superior, since it would detect the volume deviation in real time during production, with the possibility of being extended to take into account different recipes and processes with different capacities. This dynamic model could even be extended to cover other disturbances if these are detectable using the same method. However, this implementation is both costly and time inefficient if the sole purpose of the implementation is to identify only the volume deviation. Complexity arises because the non-static conditions a general implementation would require to enable analysis in real time during operation together with a static detection method like PCA complicates the distinction between false positives detected during operation and the actual detection target [25]. Because of this, the implementation is heavily based on the frequency spectrum analysis being able to detect the volume deviation in steady-state operation, which limits the flexibility of the method.

The test case implementation is designed as a test sequence, where the detection is performed in a controlled environment under conditions more optimal for the purpose of detecting the volume deviation. This implementation does not rely on FSA being able to operate on a steady-state production, since a setpoint change can be included in this test sequence. This implementation also requires additional information and data, but the extent of these is significantly smaller. Since the volume deviation essentially only requires to be corrected once, unless any physical change is done to a process, a test sequence like the one proposed is optimal. This implementation also removes some complexity regarding real-time identification, since the test sequence is executed, and afterwards the data collected during a preset sampling interval is analyzed. This methodology removes the need of constantly accessing new data and re-executing the detection technique.

As mentioned earlier, the test sequence implementation would consist of two implemented sequences, one detecting the volume error in a system and one using the same analysis to identify the

location at which the oscillation induced by the volume error appears. These implementations require a small amount of process knowledge from the operator, rely on preset settings to conduct the analysis, and are easily executed through the HMI by the operator.

Taking everything into account, it is concluded that the test case implementation is superior in terms of flexibility, required data resources, and time efficiency. In high probability, it is preferable to opt for the second test case implementation described in Figures 41 and 42 since this increases detection accuracy in general.

10 Conclusions and Future Work

10.1 Conclusions

To preface this conclusion, prior to this Master's thesis, no similar, or statistical research on the data from the TPSU had previously been carried out. Beginning this Master's Thesis without preceding foundations, investigations of the data had to be done. The multivariate data analysis yielded promising results, as a moderate correlation between variables was proven, both in real-world data and in simulation data. Furthermore, this indicates that the data obtained from the TPSU is well suited for the application of a principal component analysis. Therefore, it can be concluded that the collected data is suitable for further principal component analyzes by Tetra Pak, if there is a need for it.

Principal component analysis is common in industrial applications, but in many cases it is not enough to locate what is wrong in the process. Therefore, a complementary frequency spectrum analysis was carried out, together with a Hotelling's T^2 and a Q residual analysis. The different statistical analyzes yielded different results, and the different advantages along with the disadvantages have been rigorously discussed in the above sections. Reaching a conclusion from the preceding discussions, Hotelling's T^2 and the Q residuals are not much of a help when trying to detect an implicit volume deviation. Although the Q residuals are slightly better than Hotelling's T^2, there are no advantages in proceeding with these strategies.

Instead, the best findings lie in the principal component score plots and in the frequency spectrum analysis. The PC subspaces depicted a great response to different volume and integral time changes. However, it is still unclear whether other faults can result in a similar pattern and there is no way to tell different faults apart in a PC subspace. Therefore, the frequency spectrum analysis yields superior results when one has to pick a single advantageous method. The frequency spectrum analysis managed to locate the deviation at a certain frequency very precisely, which minimizes the risk of confusing different disturbances. Although this seems to be the single best choice to opt for, this Master's Thesis arrives at the conclusion that the best choice probably is to combine the PC subspaces, together with the frequency component analysis, to increase the chance of the detecting the fault, and to minimize the risk of false positives.

Proceeding with the statistical methods of choice, the preferable method of implementation is the test case alternative, which remains superior in terms of cost, data, and time efficiency. The general implementation requires a relatively high workload of data collection and implementation, in relation to its advantages. Also, because volume deviations are most likely to appear during the commissioning phase, this further motivates the lack of necessity of a general implementation. The best option to implement the test case alternative is furthermore a pre-programmed test sequence in the PLC, combined with analysis executed in the HMI. Finally, a foundation has been established in order to improve the efficiency of the TPSU, but more needs to be done to manage a successful implementation. Hence, the research that needs to continue this Master's thesis will be described below.

10.2 Future Work

This study provides insight in whether the detection techniques analyzed can detect the volume deviation, as well as the feasibility for a future implementation. However, to fully accomplish this, this topic requires further research. This section briefly discusses complexities that must be further tested to validate and improve the theoretical findings of this study. To perform these tests, multiple specific datasets must be collected. Information regarding this data collection and how the tests should be performed, is left for Tetra Pak personnel in Appendix C.

Due to the fact that all tests performed are based solely on simulations, after assuming that the simulation represents a real-world system sufficiently, there is a need to validate this assumption. Because no data describing a system with exact knowledge of both the presence and size of a volume error exist, this validation has to be performed in the near future, after collecting the required data. To effectively compare a real-world system with the simulation and validate the theory in which these tests resulted, similar test matrices should be constructed on data acquired from a real process. This will require a controlled environment where volume errors and integral times can be manually adjusted to resemble the different tests described in Table 6 and Table 7.

As mentioned in previous sections, to structure a general implementation that is applicable in real time during process operation, it is optimal that no setpoint change is required to detect the volume

deviation, since no setpoint changes will be present at steady-state operation. FSA shows potential to accomplish this, but needs further evaluation to establish certainty.

A source of error that was mentioned previously is that no other errors than the volume error have been analyzed. To improve the accuracy of the detection, knowledge regarding commonly occurring errors and disturbances should be analyzed using the same methods, so that the implementation can differentiate between the two and give more reliable detections. There is also a possibility that different errors or disturbances can induce process behavior similar to the volume error, which might limit the use of some methods discussed.

References

References

[1] Tetra Pak, "Who we are – company overview," 2025, accessed: 2025-05-23. [Online]. Available: https://www.tetrapak.com/about-tetra-pak/who-we-are/company

[2] ——, "Tetra Pak® Standardization Unit," 2025, accessed: 2025-05-23. [Online]. Available: https://www.tetrapak.com/solutions/integrated-solutions-equipment/processing-equipment/standardization/tetra-pak-standardization-unit

[3] ——, *Dairy Processing Handbook*, 4th ed. Lund, Sweden: Tetra Pak Processing Systems AB, 2025, accessed: May 23, 2025. [Online]. Available: https://dairyprocessinghandbook.tetrapak.com/

[4] C. M. Bishop, *Pattern Recognition and Machine Learning*. New York, NY, USA: Springer, 2006.

[5] J. Jackson, *A User's Guide to Principal Components*. New York, NY, USA: John Wiley Sons inc, 1991.

[6] L. Mujica, J. Rodellar, A. Güemes, and J. López-Diez, "PCA based measures: Q-statistic and T^2-statistic for assessing damages in structures," *Structural Health Monitoring*, vol. 10, no. 5, pp. 539–553, 2008. [Online]. Available: https://journals.sagepub.com/doi/10.1177/1475921710388972

[7] I. T. Jolliffe, *Principal Component Analysis*, 2nd ed. New York, NY, USA: Springer, 2002.

[8] B. G. Tabachnick and L. S. Fidell, *Using Multivariate Statistics*, 7th ed. Boston, MA, USA: Pearson, 2019.

[9] R. Bedre, "Principal component analysis (PCA) and visualization using python (detailed guide with example)," https://www.reneshbedre.com/blog/principal-component-analysis.html, 2025, accessed: May 23, 2025.

[10] P. Nomikos and J. F. MacGregor, "Monitoring batch processes using multiway principal component analysis," *AIChE Journal*, vol. 40, no. 8, pp. 1361–1375, 1994.

[11] B. M. Wise and N. B. Gallagher, "The pls_toolbox: Guide to multivariate data analysis in matlab," Eigenvector Research, Inc., Tech. Rep., 1996, User Manual.

[12] J. G. Proakis and D. G. Manolakis, *Digital Signal Processing: Principles, Algorithms and Applications*, 4th ed. Upper Saddle River, NJ, USA: Pearson Prentice Hall, 2006.

[13] C. Rauscher, V. Janssen, and R. Minihold, "Fundamentals of spectrum analysis," https://sites.science.oregonstate.edu/~hetheriw/astro/rt/info/instruments/Fundamentals_of_spectrum_analysis_Rauscher.pdf, 2001, accessed: May 26, 2025.

[14] G. Olsson and C. Rosén, *Industrial Automation, Application, Structures and Systems*. Lund, Skåne, Sweden: IEA, Lund University (LTH), 2005, kompendium.

[15] G. Ellis, "Chapter 9 - Filters in control systems," in *Control System Design Guide (Fourth Edition)*, fourth edition ed., G. Ellis, Ed. Boston, MA, USA: Butterworth-Heinemann, 2012, pp. 165–183. [Online]. Available: https://www.sciencedirect.com/science/article/pii/B9780123859204000096

[16] International Electrotechnical Commission, "IEC 60601-1: Medical electrical equipment – Part 1: General requirements for basic safety and essential performance," https://webstore.iec.ch/en/publication/4552, 2005, accessed: 2025-06-12.

[17] Siemens AG, "Totally integrated automation portal," https://www.siemens.com/global/en/products/automation/industry-software/automation-software/tia-portal.html, 2025, accessed: May 23, 2025.

[18] AVEVA Group PLC, "AVEVA InTouch HMI," https://www.aveva.com/en/products/intouch-hmi/, 2025, accessed: May 23, 2025.

[19] R. G. Brereton, "Negative impact of noise on the principal component analysis of nmr data," *Chemometrics and Intelligent Laboratory Systems*, vol. 81, no. 2, pp. 242–248, 2006. [Online]. Available: https://www.sciencedirect.com/science/article/pii/S1090780705002958

[20] S. Paul, A. Saikia, V. Majhi, and V. K. Pandey, "Chapter 3 - Transducers and amplifiers," in *Introduction to Biomedical Instrumentation and Its Applications*, S. Paul, A. Saikia, V. Majhi, and V. K. Pandey, Eds. London, UK: Academic Press, 2022, pp. 87–167. [Online]. Available: https://www.sciencedirect.com/science/article/pii/B9780128216743000085

[21] A. Ghosh and S. Barman, "Application of euclidean distance measurement and principal component analysis for gene identification," *Gene*, vol. 583, no. 2, pp. 112–120, 2016. [Online]. Available: https://www.sciencedirect.com/science/article/pii/S0378111916300683

[22] G. Willems, G. Pison, P. J. Rousseeuw, and S. V. Aelst, "A robust hotelling test," *Metrika*, vol. 55, no. 1, pp. 125–138, Apr. 2002. [Online]. Available: https://doi.org/10.1007/s001840200192

[23] B. Mnassri, E. M. E. Adel, B. Ananou, and M. Ouladsine, "Fault detection and diagnosis based on PCA and a new contribution plot," *IFAC Proceedings Volumes*, vol. 42, no. 8, pp. 834–839, 2009, 7th IFAC Symposium on Fault Detection, Supervision and Safety of Technical Processes. [Online]. Available: https://www.sciencedirect.com/science/article/pii/S1474667016358803

[24] D.-J. van der Zee, "Model simplification in manufacturing simulation – review and framework," *Computers Industrial Engineering*, vol. 127, pp. 1056–1067, 2019. [Online]. Available: https://www.sciencedirect.com/science/article/pii/S0360835218305783

[25] H. A. N. Søndergaard, H. R. Shaker, and B. Nørregaard Jørgensen, "Enhanced fault detection in energy systems using individual contextual forgetting factors in recursive principal component analysis," *Energy and Buildings*, vol. 324, p. 114851, 2024. [Online]. Available: https://www.sciencedirect.com/science/article/pii/S0378778824009678

A Appendix

For the code described below, the dataset on which the model is based is denoted as correct. This is during the validation of the simulation the real-world data from Company A, and for the tests performed in this study the two Reference tests. The dataset denoted as error in the code is the simulated dataset that is compared to the above.

```
import pandas as pd
import numpy as np
import matplotlib.pyplot as plt
import seaborn as sns
from sklearn.decomposition import PCA
from sklearn.preprocessing import StandardScaler
from scipy.fft import fft, fftfreq
from scipy.signal import windows, butter, filtfilt
from scipy import signal

def mean_square_error(data1, data2):
    mse = np.mean(np.square(data1 - data2))
    return mse

# Load and preprocess the reference data
# General file location
df_correct = pd.read_csv(r"FILE_LOCATION\DOCUMENT_NAME...", delimiter=';')
df_correct = df_correct.applymap(lambda x: x.strip() if isinstance(x, str) else x)
scaler = StandardScaler()
scaled_data_correct = scaler.fit_transform(df_correct)

# Load and preprocess the test data
# General file location
df_error = pd.read_csv(r"FILE_LOCATION\DOCUMENT_NAME...", delimiter=';')
df_error = df_error.applymap(lambda x: x.strip() if isinstance(x, str) else x)
scaled_data_error = scaler.transform(df_error)

# Perform PCA
n_components = 4
pca = PCA(n_components=n_components)
pca.fit(scaled_data_correct)
T_correct = pca.transform(scaled_data_correct)
Q_correct = scaled_data_correct - T_correct.dot(pca.components_)

T_error = pca.transform(scaled_data_error)
Q_error = scaled_data_error - T_error.dot(pca.components_)

# Scree plot
plt.figure(figsize=(8, 6))
plt.plot(range(1, len(pca.explained_variance_ratio_) + 1), pca.explained_variance_ratio_,
marker='o', label='Explained Variance')
plt.title('Explained Variance Ratio by Principal Component')
plt.xlabel('Principal Component')
plt.ylabel('Variance Explained')
plt.legend()
plt.grid(True)
plt.show()

# Scores Plots
fig, axes = plt.subplots(1, 3, figsize=(18, 6))
```

```
axes[0].scatter(T_correct[:, 0], T_correct[:, 1], alpha=0.7, label='Reference Data 1')
axes[0].scatter(T_error[:, 0], T_error[:, 1], alpha=0.7, label='Test Data', marker='x')
axes[0].set_xlabel('PC1')
axes[0].set_ylabel('PC2')
axes[0].set_title('PC1 vs PC2')
axes[0].legend()
axes[0].grid(True)

axes[1].scatter(T_correct[:, 1], T_correct[:, 2], alpha=0.7, label='Reference Data 1')
axes[1].scatter(T_error[:, 1], T_error[:, 2], alpha=0.7, label='Test Data', marker='x')
axes[1].set_xlabel('PC2')
axes[1].set_ylabel('PC3')
axes[1].set_title('PC2 vs PC3')
axes[1].legend()
axes[1].grid(True)

axes[2].scatter(T_correct[:, 2], T_correct[:, 0], alpha=0.7, label='Reference Data 1')
axes[2].scatter(T_error[:, 2], T_error[:, 0], alpha=0.7, label='Test Data', marker='x')
axes[2].set_xlabel('PC3')
axes[2].set_ylabel('PC1')
axes[2].set_title('PC3 vs PC1')
axes[2].legend()
axes[2].grid(True)

plt.tight_layout()
plt.show()

# Calculate correlation matrix
correlation_matrix = df_correct.corr()
rows, columns = correlation_matrix.shape
print(f"The matrix has {rows} rows and {columns} columns.")

# Heatmap of correlation matrix
plt.figure(figsize=(12, 8))
sns.heatmap(correlation_matrix, annot=True, cmap='coolwarm', fmt='.2f', cbar=True)
plt.title('Correlation Matrix Heatmap')
plt.show()
threshold = 0.7
high_correlation_count = ((correlation_matrix > threshold) | (correlation_matrix
< -threshold)).sum().sum()

# Remove the diagonal (correlation of a variable with itself) from the count
high_correlation_count -= len(correlation_matrix)
print(f"Number of correlations above 0.7 or below -0.7: {high_correlation_count}")

# Hotelling's T
mean_correct = np.mean(T_correct, axis=0)
cov_correct = np.cov(T_correct, rowvar=False)
inv_cov_correct = np.linalg.inv(cov_correct)
T2_correct = np.array([np.dot(np.dot((x - mean_correct), inv_cov_correct),
(x - mean_correct).T) for x in T_correct])

mean_error = np.mean(T_error, axis=0)
cov_error = np.cov(T_error, rowvar=False)
inv_cov_error = np.linalg.inv(cov_error)
T2_error = np.array([np.dot(np.dot((x - mean_error), inv_cov_error),
```

```
(x - mean_error).T) for x in T_error])

# Q Residuals
Q_squared_correct = np.sum(Q_correct**2, axis=1)
Q_squared_error = np.sum(Q_error**2, axis=1)
q_threshold = np.percentile(Q_squared_correct, 95)

fig, axs = plt.subplots(1, 2, figsize=(16, 6))

# Plot T²
axs[0].plot(T2_correct, marker='o', linestyle='--', color='green', label='Reference Data 1')
axs[0].plot(T2_error, marker='x', linestyle='--', color='red', label='Test Data')
axs[0].set_title("Hotelling's T2 Statistic")
axs[0].set_xlabel('Sample Index')
axs[0].set_ylabel("T2 Value")
axs[0].legend()
axs[0].grid(True)

# Plot Q Residuals
axs[1].plot(Q_squared_correct, marker='o', linestyle='--', color='green', label='Reference Data 1')
axs[1].plot(Q_squared_error, marker='x', linestyle='--', color='red', label='Test Data')
axs[1].axhline(y=q_threshold, color='blue', linestyle='--', label='Threshold (95%)')
axs[1].set_title('Squared Prediction Error (Q Residuals)')
axs[1].set_xlabel('Sample Index')
axs[1].set_ylabel('Q Residual')
axs[1].legend()
axs[1].grid(True)

plt.tight_layout()
plt.show()

# Low-pass filter
def lowpass_filter(data, cutoff_freq, fs, order=4):
    nyquist = 0.5 * fs
    normal_cutoff = cutoff_freq / nyquist
    b, a = butter(order, normal_cutoff, btype='low', analog=False)
    return filtfilt(b, a, data)

# FFT
def plot_fft_first_3_pca(T_correct, T_error, fs=1.0, padding_factor=4, cutoff_freq=0.2):
    N = T_correct.shape[0]
    padded_length = padding_factor * N
    f = fftfreq(padded_length, d=1/fs)[:padded_length//2]
    num_to_plot = min(3, T_correct.shape[1])

    plt.figure(figsize=(8, 8.5))

    for i in range(num_to_plot):
        windowed_correct = T_correct[:, i] * windows.hann(N)
        windowed_error = T_error[:, i] * windows.hann(N)

        filtered_correct = lowpass_filter(windowed_correct, cutoff_freq, fs)
        filtered_error = lowpass_filter(windowed_error, cutoff_freq, fs)

        zero_padded_correct = np.pad(filtered_correct, (0, padded_length - N), mode='constant')
        zero_padded_error = np.pad(filtered_error, (0, padded_length - N), mode='constant')
```

```
        fft_correct = fft(zero_padded_correct)
        fft_error = fft(zero_padded_error)

        plt.subplot(3, 1, i + 1)
        plt.plot(f, np.abs(fft_correct[:padded_length//2]), label='Reference data', color='green',
        alpha=0.8)
        plt.plot(f, np.abs(fft_error[:padded_length//2]), label='Test data', color='green',
        linestyle='--', alpha=0.8)
        plt.title(f'Frequency Spectrum - PCA Component {i + 1}')
        plt.xlabel('Frequency (Hz)')
        plt.ylabel('Magnitude')
        plt.grid(True)
        plt.legend()
        plt.xlim([0, 0.15])

    plt.tight_layout()
    plt.show()

plot_fft_first_3_pca(T_correct, T_error, fs=1.0, padding_factor=4, cutoff_freq=0.2)
```

B Appendix

Table 8: List of parameters in the dataset for Company A

H40_Cream_Density_Value	H40_Cream_Fat_Value	H40_Cream_Flow_Value
H40_Cream_MassFlow_Value	H40_Cream_Prot_Value	H40_Cream_SNF_Value
H40_Cream_Temp_Value	H40_Cream_TS_Value	H40_CreamFT_Fat_Value
H40_CreamRemix_Density_Value	H40_CreamRemix_Fat_Value	H40_CreamRemix_Flow_Value
H40_CreamRemix_Flow_ValueUS	H40_CreamRemix_MassFlow_Value	H40_CreamRemix_Prot_Value
H40_CreamRemix_SNF_Value	H40_CreamRemix_Temp_Value	H40_CreamRemix_TS_Value
H40_CreamSurplus_Density_Value	H40_CreamSurplus_Fat_Value	H40_CreamSurplus_Flow_Value
H40_CreamSurplus_MassFlow_Value	H40_CreamSurplus_Prot_Value	H40_CreamSurplus_SNF_Value
H40_CreamSurplus_Temp_Value	H40_CreamSurplus_TS_Value	H40_Product_Density_Value
H40_Product_Fat_Value	H40_Product_MassFlow_Value	H40_Product_Prot_Value
H40_Product_SNF_Value	H40_Product_Temp_Value	H40_Product_TS_Value
H40_ProductFT_Fat_Value	H40_Rawmilk_Density_Value	H40_Rawmilk_Fat_Value
H40_Rawmilk_Flow_Value	H40_Rawmilk_Flow_ValueUS	H40_Rawmilk_MassFlow_Value
H40_Skimmilk_Density_Value	H40_Skimmilk_Flow_Value	H40_Skimmilk_MassFlow_Value
H40_Skimmilk_Temp_Value	H40W00BF011_Value	H40W00BF020_D_Value
H40W00BF020_FC_ManValueCV	H40W00BF020_FC_PV	H40W00BF020_M_Value
H40W00BT022_Value	H40W00Q0021_Value	H40W10BF031_FC_ManValueCV
H40W10BF031_FC_ManValueSP	H40W10BF031_FC_PV	H40W10BF031_Value
H40W10Q0050_Value	H40W00Q0023_SW	H40_Product_Flow_Value

Table 9: List of parameters in the dataset for Company B

H40W00BF020_D_Value	H40_Cream_Fat_Value	H40W00BF020_M_Value
H40_Cream_Prot_Value	H40_Cream_SNF_Value	H40W00BT022_Value
H40_Cream_TS_Value	H40_Cream_FatFT_Value	H40_Group0_PID_PV
H40_Product_Fat_Value	H40_Product_MassFlow_Value	H40_Product_FatFT_Value
H40_Rawmilk_Fat_Value	H40_Rawmilk_Flow_Value	H40_Rawmilk_MassFlow_Value
H40W00BF010_D_Value	H40_Skimmilk_Flow_Value	H40_Skimmilk_MassFlow_Value
H40W00BT012_Value	H40_Skimmilk_Flow_Value	H40W00BF020_D_Value
H40_Cream_PID_ManValueCV	H40_Cream_PID_PV	H40W00BF020_M_Value
H40W00BT022_Value	H40W00Q0021_AO_Value	H40_Group0_PID_ManValueCV
H40_Group0_PID_ManModeSP	H40_Group0_PID_PV	H40W10BF031_Value
H40W10Q0050_AO_Value	H40_Product_Flow_Value	

C Appendix

To collect all the data needed to perform the evaluations described in Section 10.2 in an efficient manner, a certain methodology is suggested. Manually tuning the volume in the PLC and the integral time in the HMI enables quick and efficient test structuring. For the first three data collections, the test matrices are the proposed structure of tests, since this methodology simplifies comparisons between datasets.

Firstly, it is crucial that the theory accumulated in this thesis is validated. This will be done through a comparison, which will validate that the macroscopical behavior of the system with and without a volume error present is representable by the simulations and that the behavior seen during the tests based on simulation is visible in a real-world process. Therefore, collecting data from a system that possesses perfectly identical characteristics as the real-world process is not strictly needed, as long as it resembles the settings used in the test matrices sufficiently. The real-world should include a setpoint change of the same size as the one used in the simulations. The comparison originating from these collected datasets should be used to validate that the theory acquired from simulations is applicable in a real-world process. As mentioned before, the proposed test matrix structure should optimally be followed, since this simplifies the validating comparison between the simulation and the real-world behavior.

Frequency spectrum analysis is the obvious choice for a detection technique, but it needs to be further evaluated. As mentioned earlier, there are indications that the FSA can detect a volume deviation in systems without the presence of a setpoint change. Since this drastically simplifies the complexity of a potential implementation, it needs to be evaluated. To further investigate, real-world data that do not include any setpoint changes should be collected. Furthermore, data collection should be done analogously to the data collection mentioned earlier in this section and follow the same structure. Establishing that the FSA is efficient in detecting a volume deviation during steady-state operation greatly simplifies a future implementation.

Data that include commonly occurring errors and disturbances should also be collected, preferably using the same methodology and system described above. The purpose of this data collection is to analyze how the different methods evaluated in this thesis are affected by other deviations from a fully functional process. To structure the collection of data, a professional with knowledge about the process and common process deviations is needed to be sure that no obvious errors are missed or ignored, as well as that the errors introduced are of relevance for the process.

To gain knowledge of the behavior of the system at different sites, where different process setups display different process dynamics, data should be collected from these different sites. The goal of the data collection is to gain an understanding of how the frequency where the oscillatory peak lies changes depending on process dynamics and different process designs, so that a mapping of the behaviors can be made. This data collection is a more prolonged collection process, in which data is collected during the commissioning of new units. Moreover, this method used to collect data is not as rigid as for the other scenarios, and the data collection will be a part of the proposed implementation rather than a test to be performed before implementation to validate the theory.

The suggested data collection is listed below.

1. Data validating the simulation.
2. Data assessing the potential of FSA on steady-state operation.
3. Data containing other errors.
4. Data giving knowledge about the effect of different process dynamics on the detection. The collection is performed as part of the test sequence.

To efficiently gather these data, the same structure as used in the thesis is suggested. For the first datasets mentioned above, the system should optimally have sufficiently similar settings and process dynamics, and use the same recipe changes during the setpoint change. The process from which the data are collected must have some known characteristics, such as the actual volume of the process, so that the volume deviation can be manually changed. For the second datasets, the data collection should be done analogously to the first datasets, except the fact that no setpoint change should be introduced. However, it is still recommended that the structure of tests follow the same matrix methodology so

that comparison between the first and second datasets can be done in an easy manner, determining the potential of FSA in steady-state. It is also worth mentioning that these two collections of data will be the foundation for the test case implementation, which is the suggested detection technique. Preferably, the settings used during these tests, optimally the same settings used for either of the matrices in this thesis, should be the settings used during the test case implementation, unless different settings are deemed to be more efficient during testing or due to the process being commissioned not resembling the system used in the test matrices enough. These tests will therefore also potentially explore the threshold of the test case implementation, since different volume errors and different integral times will be evaluated. These comparisons will give an idea of how the threshold should be implemented for these systems, depending on the size of the volume error that is the target of detection. This idea is assumed to be sufficiently translatable between processes and is applicable in systems with different process characteristics as long as the differences are not major. This assumption is done due to the two systems simulated in this thesis displaying moderate, if not large differences in process dynamics, with high differences in parameters such as raw milk mass flow, but seemingly displaying similar amplitudes in compensated systems with present volume errors. This can be seen in Figure 31d and Figure 36d. Note that the volume errors are not equal and that the compensation is not equal in magnitude. However, this is expected since these systems have different process dynamics, which results in smaller volume deviations affecting the system more for the second figure. However, analyzing this from a wider angle and identifying that both systems are compensated and do not show signs of a present volume error, it can be concluded that a latent volume error in a compensated system, regardless of process dynamics, will have similar amplitudes of the oscillations. Although, if the process as mentioned earlier can not be tuned to remotely resemble one of the evaluated process dynamics, new data should be collected for the sole purpose of analyzing this specific system.

The third dataset should preferably be collected last, since successful validations from the aforementioned datasets result in flexibility for these tests. Should the second comparison described indicate that FSA works equally well or potentially better for steady-state operations, these datasets should optimally be performed on datasets with no setpoint errors. If the opposite is true, and FSA displays higher detection accuracy during a setpoint change, these tests should be structured with a setpoint change instead. Lastly, this section will not describe what errors should be included during these tests, since this is knowledge not currently available. These decisions should be made by a Tetra Pak professionals with sufficient knowledge about the TPSU and common process deviations.

The fourth data collection is slightly different and will be a more prolonged test. The purpose of this analysis is to determine at what frequency the oscillation occurs for different systems. As mentioned in earlier sections, this data gathering might not be needed for all systems, unless the system dynamics is significantly different from the two systems evaluated in the test matrices. However, the process will be explained for the cases where it is necessary. Since data collections 1 and 2 in C will evaluate the potential threshold for the test case implementation, the only remaining degree of freedom is the frequency at which oscillations occur. This frequency might vary with different process dynamics and will need to be analyzed. This procedure should be performed during the commissioning of new units, where the detection should be used on the machine with a high volume error and insufficient compensation in terms of integral time. This result gives a clear indication of at which frequency the oscillation will occur, which simplifies the analysis of the future test case implementation for the unit in question. This data collection is the reason for the creation of the second test case implementation shown in Figure 41. This data collection is, as mentioned, a more prolonged collection, where different frequencies for different systems are collected and mapped. The data collection does not have to be done pre-implementation to validate any theory like the other comparisons mentioned in this section. However, this is still discussed in this paragraph because it involves data collection that must be performed in the future for the implementation to work optimally even though the collection is an important part of the proposed test sequence. For this to be valid, it is important that the third comparison mentioned previously, which accounts for different types of errors and disturbances, is performed in a thorough manner so that it is certain that the volume deviation is the origin of the measured oscillation and not another unrelated disturbance for the system being analyzed. This must be done to avoid losing validity during the execution of the test case implementation that locates the frequency of the oscillation induced by the volume error.

D Appendix

The results obtained from Test Matrix 2 for the residuals are presented below.

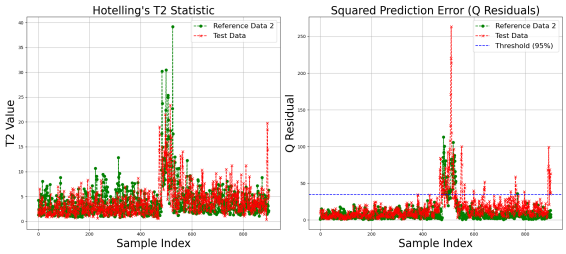

Figure 43: Figures showing Hotellings T^2 (left) and Q residuals (right) for Test 2 in comparison with Reference test 2. $\Delta V = 2$ l, $T_i = 5$ s

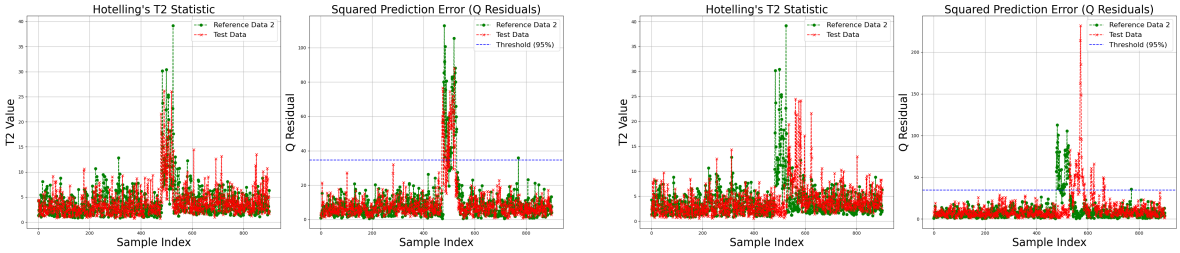

(a) $\Delta V = 0$ l

(b) $\Delta V = 2$ l

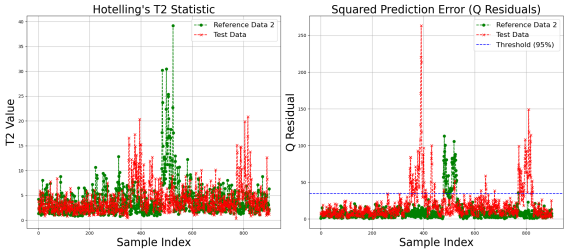

(c) $\Delta V = 4$ l

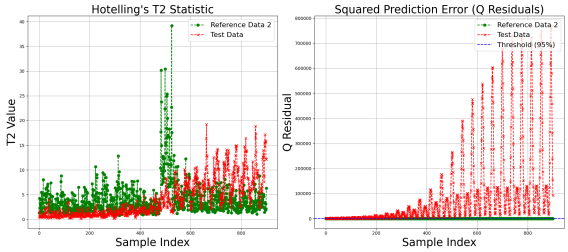

(d) $\Delta V = 6$ l

Figure 44: Figures showing Hotellings T^2 (left) and Q residuals (right) for $T_i = 7.5$ s for (a) Test 3 in comparison with Reference test 2, (b) Test 4 in comparison with Reference test 2, (c) Test 5 in comparison with Reference test 2 and, (d) Test 6 in comparison with Reference test 2. Furthermore, (d) shows a system unstable due to a large volume deviation.

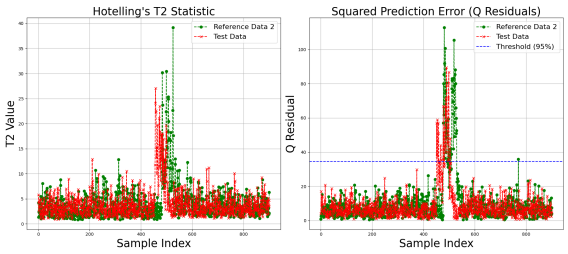

(a) $\Delta V = 0\ l$

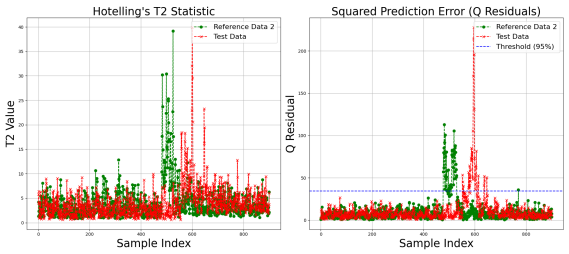

(b) $\Delta V = 2\ l$

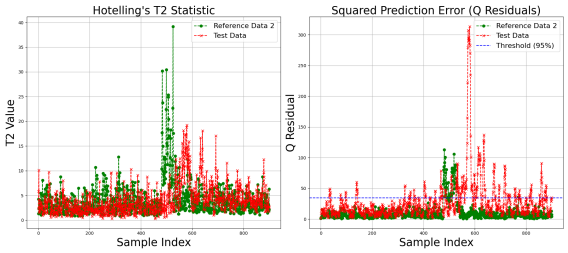

(c) $\Delta V = 4\ l$

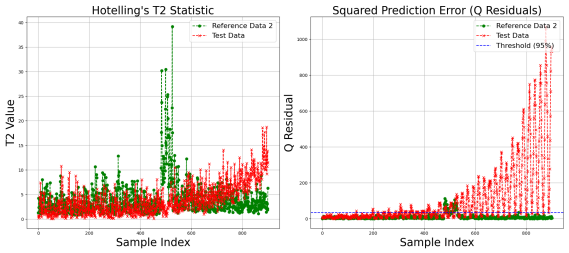

(d) $\Delta V = 6\ l$

Figure 45: Figures showing Hotellings T^2 (left) and Q residuals (right) for $T_i = 12.5\ s$ for (a) Test 7 in comparison with Reference test 2, (b) Test 8 in comparison with Reference test 2, (c) Test 9 in comparison with Reference test 2 and, (d) Test 10 in comparison with Reference test 2. Furthermore, (d) shows a system unstable due to a large volume deviation.

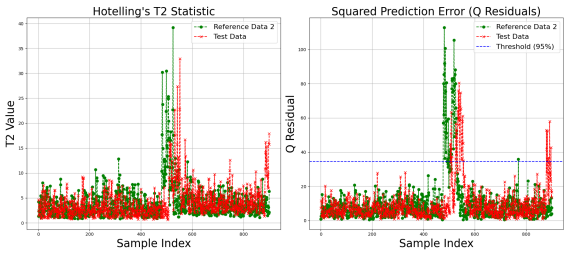

(a) $\Delta V = 0\ l$

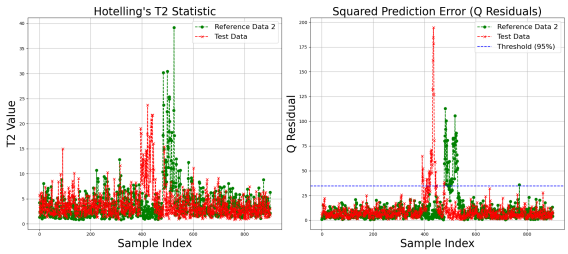

(b) $\Delta V = 2\ l$

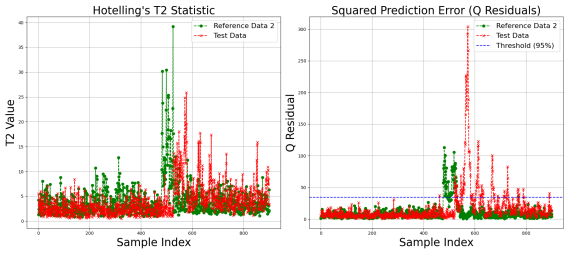

(c) $\Delta V = 4\ l$

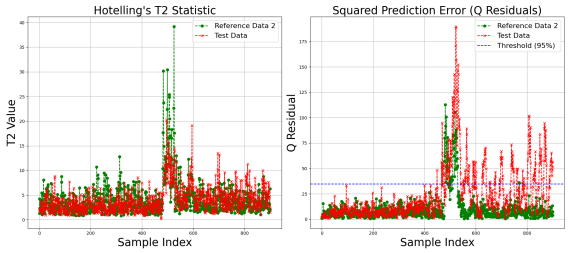

(d) $\Delta V = 6\ l$

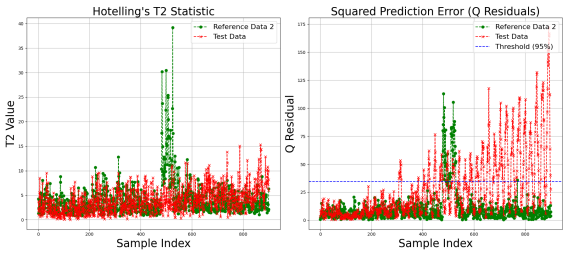

(e) $\Delta V = 8\ l$

Figure 46: Figures showing Hotellings T^2 (left) and Q residuals (right) for (a) Test 11 in comparison with Reference test 2, (b) Test 12 in comparison with Reference test 2, (c) Test 13 in comparison with Reference test 2 and, (d) Test 14 in comparison with Reference test 2, and (e) Test 15 in comparison with Reference test 2. Furthermore, (e) shows a system unstable due to a large volume deviation. $T_i = 17.5$ s